Universität Hamburg

DER FORSCHUNG | DER LEHRE | DER BILDUNG

The Bidirectional Crosstalk between CD4$^+$ T Cells and Cholangiocytes in a Patient-Derived Organoid Model

Dissertation

to obtain the degree

Doctor rerum naturalium (Dr. rer. nat.)

at the Faculty of Mathematics, Informatics and Natural Sciences
of the University of Hamburg

submitted by
Nicola Iuso

Hamburg, October 2025

REFEREES:

Prof. Dr. med. Christoph Schramm
I. Department of Medicine and Martin Zeitz Center for Rare Diseases
University Medical Center Hamburg-Eppendorf
Martinistraße 52
20251 Hamburg

Prof. Dr. Tim-Wolf Gilberger
Department of Cellular Parasitology
Bernhard Nocht Institute for Tropical Medicine
Bernhard Nocht Straße 74
20359 Hamburg

Date of oral defence: 18.03.2026

And I'm still a believer, but I don't know why
I've never been a natural, all I do is try, try, try
I'm still on that trapeze
I'm still trying everything to keep you looking at me

— Taylor Swift, *"mirrorball", Folklore (2020)*

AKNOWLEDGEMENTS

In this chapter, I won't talk about cells, genes, or graphs, but about what my PhD has taught me beyond science. These years have been about learning to navigate uncertainty, to fall and start again, and to find meaning even in unfinished stories.

Effort is not something to hide; there is honesty in showing how much you care about what you do. In science, we are often taught that confidence means appearing unbothered, as if wanting something deeply were a sign of weakness. But I have come to understand that there is grace in trying — whether the effort leads to success or to failure. There were moments when perfectionism felt like a hefty weight, when the fear of making mistakes overshadowed curiosity itself. Yet, over time, I learned to let go of that pressure — to see that science, like life, is built on trial, imperfection, and patience. The courage to keep showing up, to stay curious, to ask one more question, to repeat an experiment that failed ten times before — that is where progress truly begins.

Progress rarely follows a straight line; it often comes disguised as failure, and growth as the quiet consequence of persistence. The beauty of research lies not only in the answers we find, but in the questions we keep asking, even when the answers don't come easily.

Mistakes are never the opposite of success — they are an essential part of it. Every wrong turn, every failed experiment, and every unexpected result carried a lesson that shaped both my work and my perspective. The moments of rejection and self-doubt, when things felt bigger than myself, were as defining as the breakthroughs. Letting go does not always mean losing; sometimes it means creating space for something better to take shape.

Moving from Italy to Germany was one of those defining experiences. It forced me to confront change in all its forms — cultural, linguistic, and personal — while building a life and identity far from what was familiar. It made me realise that courage is not the absence of fear, but the willingness to act despite it.

A PhD can indeed be heavy, especially when you try to carry it all at once. But thanks to Doro, Christoph, Pia, Victor, Cornelia, Jonas, Gela, everyone on top of the Zahnklinik, Jeason, Sophie, Ruth, The Book Club, Lorenzo, Lorenza, Maria, and all those who crossed my path — everything became lighter. You turned long days into shared victories and setbacks into moments of laughter. This journey would not have been the same without you.

Hey, thank you for this lovely bouquet!
Nico

SUMMARY

DECLARATION ON OATH

I hereby declare and affirm that this doctoral dissertation is my own work and that I have not used any aids or sources other than those indicated. If electronic resources based on generative artificial intelligence (gAI) were used in the course of writing this dissertation, I confirm that my own work was the main and value-adding contribution and that complete documentation of all resources used is available in accordance with good scientific practice. In this context, gAI tools were used solely for language refinement. I am responsible for any erroneous or distorted content, incorrect references, violations of data protection and copyright law, or plagiarism that may have been generated by the gAI.

EIDESSTATTLICHE VERSICHERUNG

Hiermit versichere ich an Eides statt, die vorliegende Dissertationsschrift selbst verfasst und keine anderen als die angegebenen Hilfsmittel und Quellen benutzt zu haben. Sofern im Zuge der Erstellung der vorliegenden Dissertationsschrift generative Künstliche Intelligenz (gKI) basierte elektronische Hilfsmittel verwendet wurden, versichere ich, dass meine eigene Leistung im Vordergrund stand und dass eine vollständige Dokumentation aller verwendeten Hilfsmittel gemäß der Guten wissenschaftlichen Praxis vorliegt. In diesem Zusammenhang wurden gKI-Werkzeuge ausschließlich zur sprachlichen Überarbeitung eingesetzt. Ich trage die Verantwortung für eventuell durch die gKI generierte fehlerhafte oder verzerrte Inhalte, fehlerhafte Referenzen, Verstöße gegen das Datenschutz- und Urheberrecht oder Plagiate.

Hamburg, den 30/10/2025 Unterschrift

PUBLICATIONS

1. **Poch T, Bahn J, Casar C, Krause J, Evangelakos I, Gilladi H, Kunzmann LK, Laschtowitz A, Iuso N, Schäfer AM, Liebig LA, Steinmann S, Sebode M, Folseraas T, Engesæter LK, Karlsen TH, Franke A, Hubner N, Schlein C, Galun E, Huber S, Lohse AW, Gagliani N, Schwinge D, Schramm C.** *Intergenic risk variant rs56258221 skews the fate of naive CD4⁺ T cells via miR4464-BACH2 interplay in primary sclerosing cholangitis*. Cell Rep Med. 2024 Jul 16;5(7):101620. doi: 10.1016/j.xcrm.2024.101620. Epub 2024 Jun 19. PMID: 38901430; PMCID: PMC11293351.

CONFERENCE PARTICIPATIONS

1. **Young investigator workshop on basic science and translation immunology in PSC 2023.** Participation with a poster: "The bidirectional regulatory network of immune cells and cholangiocytes in Primary Sclerosing Cholangitis (PSC)" Iuso N., Haas V., Grafen V., Steinmann S., Sebode M., Schramm C., Schwinge D.

2. **International PSC Study Group Biennial Meeting 2024**. Participation with a poster: "The bidirectional regulatory network of immune cells and cholangiocytes in Primary Sclerosing Cholangitis (PSC)" Iuso N., Haas V., Grafen V., Steinmann S., Sebode M., Schramm C., Schwinge D.

GENES AND PROTEINS ABBREVIATIONS

ALB: Albumin

APBB1IP: APBB1-interacting protein 1 (RIAM)

AQP1: Aquaporin-1

ARL6: ADP-ribosylation factor-like 6

BCL2: B-cell lymphoma 2

BRCA1: Breast cancer type 1 susceptibility protein

C3: Complement component 3

CA13: Carbonic anhydrase 13

CADPS: Calcium-dependent activator protein for secretion

CASP7: Caspase-7

CCL20/28: C-C motif chemokine ligand 20/28

CCR6: C-C chemokine receptor 6

CD25: Interleukin-2 receptor alpha (IL2RA)

CD133 / PROM1: Prominin-1

CD137 / 4-1BB / TNFRSF9: 4-1BB

CD137L / 4-1BBL / TNFSF9: 4-1BB ligand

CFTR: Cystic fibrosis transmembrane conductance regulator

CHAC1: ChaC glutathione-specific γ-glutamylcyclotransferase 1

CNKSR1: Connector enhancer of kinase suppressor of Ras 1

CNTNAP3: Contactin-associated protein-like 3

CXCL1–5: C-X-C motif chemokine ligands 1-5

DEFB4A / DEFB4B: Beta-defensin 4A / 4B

DUOX2: Dual oxidase 2

ELOVL4: Elongation of very long chain fatty acids protein 4

EPCAM: Epithelial cell adhesion molecule

FAM133B: Family with sequence similarity 133 member B

FASL / FASLG: Fas ligand

FOS: Proto-oncogene c-Fos

G2E3: G2/M phase-specific E3 ubiquitin-protein ligase

GJC1: Gap junction gamma-1 (Connexin-45)

GPBAR1 (TGR5): G-protein-coupled bile acid receptor 1

HLA-DR: Major histocompatibility complex, class II, DR

HPRT: Hypoxanthine-guanine phosphoribosyltransferase

ICAM1: Intercellular adhesion molecule 1

ICOS: Inducible T-cell co-stimulator

IFI6: Interferon alpha-inducible protein 6

IFI16: Interferon gamma-inducible protein 16

IL1B: Interleukin-1 beta

IL6: Interleukin-6

IL-17A: Interleukin-17

KRT7: Keratin 7

KRT13: Keratin 13

KRT19: Keratin 19

LAG-3: Lymphocyte activation gene 3 protein

LGR5: Leucine-rich repeat-containing G-protein-coupled receptor 5

MCL1: Myeloid cell leukemia sequence 1

MND1: Meiotic nuclear divisions 1

MUC6: Mucin 6

NFKBIZ: Nuclear factor of kappa light polypeptide gene enhancer in B-cells inhibitor zeta

OX40 / TNFRSF4: OX40, a member of the tumor necrosis factor receptor family

OX40L / TNFSF4: OX40 ligand

PD-1 / PDCD1: Programmed cell death protein 1

PD-L1 / CD274: Programmed death-ligand 1

PDZK1IP1: PDZK1-interacting protein 1 (MAP17)

PIGR: Polymeric immunoglobulin receptor

PLXDC2: Plexin domain containing 2

PTPRR: Protein tyrosine phosphatase receptor type R

RGS5: Regulator of G-protein signaling 5

ROBO1: Roundabout guidance receptor 1

SAA1 / SAA2: Serum amyloid A1 / A2

SLIT3: Slit guidance ligand 3

SLC44A5: Solute carrier family 44 member 5

SOX9: SRY-box transcription factor 9

SORBS3: Sorbin and SH3 domain containing 3

SPRR2A / SPRR2B / SPRR2D: Small proline-rich proteins 2A, 2B and 2D

TERF1: Telomeric repeat binding factor 1

TIM-3 / HAVCR2: T-cell immunoglobulin and mucin domain containing 3

TMEM200A / TMEM220 / TMEM45A: Transmembrane proteins 200A, 220, 45A

TNF: Tumor necrosis factor

TXK: TXK tyrosine kinase

UGT2B7 / UGT2B11 / UGT2B10: UDP-glucuronosyltransferases 2B7, 2B11 and 2B10

USP34: Ubiquitin specific peptidase 34

WDR76: WD repeat domain 76

ZC3H12A: Zinc finger CCCH-type containing 12A (Regnase-1)

ZKSCAN7: Zinc finger with KRAB and SCAN domains 7

ABSTRACT

Primary sclerosing cholangitis (PSC) is a rare disease characterised by long-standing periductal inflammation directed against cholangiocytes, the epithelial lining cells of the bile ducts. Over time, chronic inflammation leads to fibrosis and progressive destruction of the biliary tree. The aetiology of PSC remains only partly understood, but immune dysregulation is thought to be a key driver. Cholangiocytes are now recognised not as passive bystanders of tissue injury, but as active participants capable of releasing cytokines, expressing adhesion molecules and, under certain conditions, presenting antigens, thereby shaping the immune milieu. In contrast, alcohol-associated liver disease (ALD) arises from toxic and metabolic injury due to sustained alcohol intake. Here, inflammation and ductular reaction are also prominent, but the underlying mechanisms differ fundamentally from immune-mediated cholangiopathies. Comparing cholangiocytes from PSC and ALD therefore provides an opportunity to distinguish disease-specific features from general responses to chronic injury. In this work, patient-derived cholangiocyte organoids were used as a three-dimensional model to explore how these cells contribute to inflammation and immune regulation. Two main questions were addressed: whether PSC- and ALD-derived organoids differ at baseline and under inflammatory stimulation, and how cholangiocytes interact with $CD4^+$ T cells in co-culture, with attention to activation, regulation and survival pathways. Transcriptomic analysis revealed subtle but consistent differences in PSC-derived organoids at baseline. Our observations suggest that PSC cholangiocytes retain a plastic, immune-ready state, likely imprinted through epigenetic mechanisms that persist outside their native tissue. Upon IL-17A stimulation, organoids from both PSC and ALD donors activated a broad inflammatory transcriptional programme. Chemokines, cytokines, defensins and acute-phase markers were upregulated, and pathway analysis confirmed engagement of IL-17, TNF and NF-κB signalling. Despite this strong and consistent response, only a limited number of transcripts remained differentially expressed between PSC and ALD, indicating convergence of acute responses, while a small number of disease-specific traits were preserved. $CD4^+$ T cells were brought into co-culture with organoids under optimised conditions that preserved epithelial integrity and enabled physical interaction. Exposure to T cell-derived supernatants alone induced a pro-inflammatory response, but direct contact resulted in broader activation of cholangiocytes, highlighting the importance of cell–cell interaction. In parallel, $CD4^+$ T cells displayed changes in both activation and regulatory pathways, with a clear involvement of the PD-1/PD-L1 axis. This suggests that cholangiocytes are able not only to stimulate T cells, but also to engage inhibitory checkpoint mechanisms. Overall, PSC- and ALD-derived organoids were more similar than different, reflecting a tendency towards phenotypic convergence *in vitro*, which facilitates expansion but can obscure tissue-specific signatures. Nevertheless, key disease-associated features were

retained. These findings underscore both the strengths and limitations of organoid models: while they effectively recapitulate essential epithelial functions, they cannot fully reproduce the complexity and fidelity of the disease environment.

ZUSAMMENFASSUNG

Primär sklerosierende Cholangitis (PSC) ist eine seltene Erkrankung, die durch eine langanhaltende periduktale Entzündung gekennzeichnet ist, die sich gegen Cholangiocyten, also die Epithelzellen der Gallengänge, richtet. Im Verlauf führt diese chronische Entzündung zu Fibrose und progressiver Zerstörung der Gallengänge. Die Ätiologie der PSC ist bisher nur teilweise verstanden, jedoch wird eine Fehlregulation des Immunsystems als zentraler Mechanismus angesehen. Cholangiocyten, die Epithelzellen, die den Gallenbaum auskleiden, werden in Cholangiopathien nicht mehr als passive Zuschauer des Leberschadens betrachtet, sondern als aktive Akteure. Sie sind in der Lage, Zytokine freizusetzen, Adhäsionsmoleküle zu exprimieren und unter bestimmten Bedingungen sogar Antigene zu präsentieren und somit das immunologische Milieu aktiv zu beeinflussen. Im Gegensatz zur PSC entsteht die alkoholassoziierte Lebererkrankung (ALD) durch toxische und metabolische Schädigung infolge eines anhaltenden Alkoholkonsums. Auch hier spielen Entzündung und ductuläre Reaktion eine wichtige Rolle, jedoch unterscheiden sich die zugrunde liegenden Mechanismen grundlegend von den immunvermittelten Cholangiopathien. Der Vergleich von Cholangiocyten aus PSC- und ALD-Gewebe bietet daher die Möglichkeit, krankheitsspezifische Merkmale von allgemeinen Reaktionen auf chronische Schädigung zu unterscheiden. In der vorliegenden Arbeit wurden patientenabgeleitete Cholangiocyten-Organoide als dreidimensionales Modell verwendet, um zu untersuchen, wie diese Zellen zur Entzündung und Immunregulation beitragen. Zwei zentrale Fragestellungen wurden behandelt: ob sich PSC- und ALD-abgeleitete Organoide in ihrem Ausgangszustand und unter entzündlicher Stimulation unterscheiden, und wie Cholangiocyten mit $CD4^+$-T-Zellen in Kokultur interagieren – insbesondere im Hinblick auf Aktivierungs-, Regulations- und Überlebensmechanismen. Die Transkriptomanalyse zeigte, dass PSC-abgeleitete Organoide im Ausgangszustand subtile, aber konsistente Unterschiede im Vergleich zu ALD aufwiesen. Unsere Beobachtungen deuten darauf hin, dass PSC-Cholangiocyten in einem plastischen, immunologisch „bereiten“ Zustand verbleiben, der wahrscheinlich durch epigenetische Mechanismen geprägt und auch außerhalb des nativen Gewebes erhalten bleibt. Nach Stimulation mit IL-17A aktivierten Organoide beider Gruppen (PSC und ALD) ein breites Spektrum entzündlicher Gene. Chemokine, Zytokine, Defensine und Akutphasenmarker waren hochreguliert, und die Pfadanalyse bestätigte die Aktivierung der IL-17-, TNF- und NF-κB-Signalwege. Trotz einer starken und konsistenten Reaktion auf IL-17A blieben nur wenige Transkripte unterschiedlich exprimiert, wenn PSC- und ALD-Organoide direkt verglichen wurden, was darauf hinweist, dass akute Reaktionen weitgehend konvergieren, während nur wenige krankheitsspezifische Merkmale unter Basalbedingungen bestehen bleiben

INTRODUCTION

1. CHOLANGIOCYTE MORPHOLOGY AND HETEROGENEITY WITHIN THE BILIARY TREE

The metabolism of lipids and carbohydrates is certainly what the liver is best known for, but its functions extend far beyond this. Positioned at the interface between the intestine and the systemic circulation, it receives approximately 1.5 L of blood per minute from the portal vein, carrying not only nutrients but also bacteria, toxins, and antigens from the diet[1–3]. This constant exposure forces the organ to act as a biological filter: most incoming molecules must be tolerated, while potentially harmful ones must trigger an appropriate immune response. Achieving this balance is not trivial, and it is one of the reasons why the liver has long been regarded as both an immunologically active and a highly tolerogenic organ[1,2,4]. Hepatocytes constitute the majority of liver parenchymal cells and are organised in plates within the lobular structure that radiates from the terminal branches of the hepatic veins. Adjacent plates are separated from the bloodstream by liver sinusoidal endothelial cells (LSECs), characterised by fenestrations and the absence of a basement membrane, which enable the direct exchange of antigens and other molecules, facilitating immediate immune recognition. The narrow space of Disse, which separates hepatocytes from the sinusoidal endothelium, provides a niche for hepatic stellate cells (HSCs). Under physiological conditions, these cells primarily store vitamin A; however, when the liver is injured, they undergo activation and contribute to extracellular matrix deposition and fibrosis[5]. Kupffer cells (KCs) constitute another essential component of the hepatic immune defence. Residing within the sinusoids, they represent the largest population of resident macrophages in the human body and continuously clear microbes and cellular debris from the bloodstream, while secreting cytokines that shape and modulate adaptive immune responses[2,4] (Fig.1 A-C).

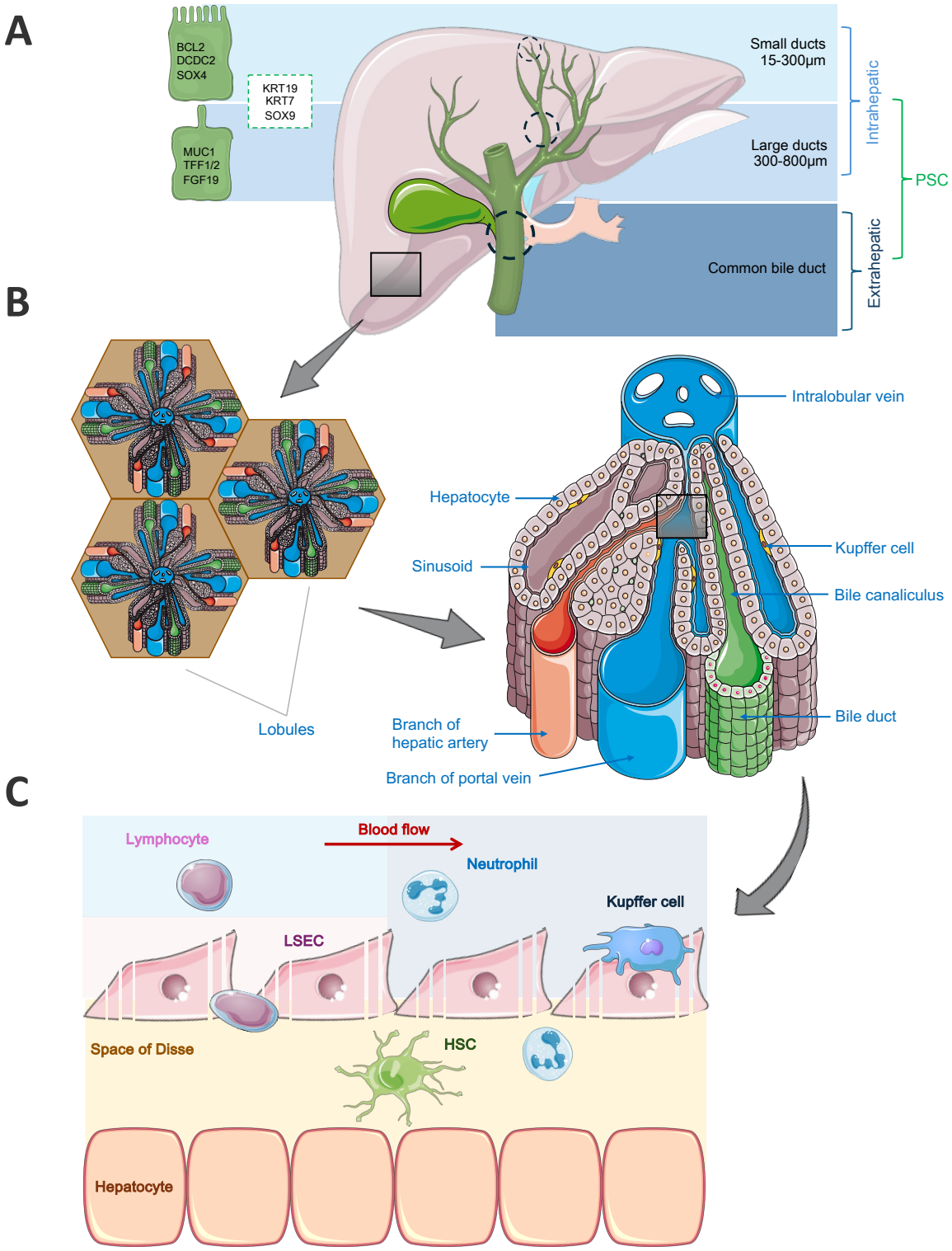

Figure 1. Morphological and functional organisation of the liver and biliary tree.
A) Schematic representation of intrahepatic and extrahepatic bile ducts. Small ducts (15–300 µm) express BCL2, DCDC2, and SOX4, whereas large ducts (300–800 µm) express MUC1, TFF2, and FGF19. Both share

epithelial markers KRT19, KRT7, and SOX9. (B) The hepatic lobule is organized around the central vein, with hepatocyte plates bordered by sinusoids that receive blood from the portal vein and hepatic artery. (C) Sinusoids are lined by LSECs and Kupffer cells, while the space of Disse hosts hepatic stellate cells. Together, these components regulate metabolism, immune surveillance, and tissue remodelling. *Adapted from Banales et al., 2019 and Boyer, 2013. Adapted from Servier Medical Art (https://smart.servier.com), licensed under CC BY 4.0 (https://creativecommons.org/licenses/by/4.0/).*

Bile is produced by hepatocytes and transported from the liver to the duodenum through the biliary tree, a complex, tree-like system of branching ducts[6]. Starting from the canals of Hering (CoH), bile flows towards the intestine through intrahepatic and then extrahepatic bile ducts which, together with the cystic duct of the gallbladder, unite to form the common bile duct (choledochus)[7–9]. Within the liver, intrahepatic ducts are organised according to their diameter, ranging from the smallest bile ducts (<15 μm) to the right and left hepatic ducts that exceed 800 μm[9]. The smaller ducts are lined by approximately 4–5 cuboidal cholangiocytes measuring 8–10 μm in diameter, whereas larger ducts contain 8 to 15 taller columnar cholangiocytes of approximately 15 μm[10]. Although they represent only a very small proportion of the hepatic cell population, cholangiocytes form a selective barrier specialised in the transport and modification of bile[11,12]. All cholangiocytes possess microvilli on their apical membrane, but only the larger cells carry a single primary cilium that acts as a mechanosensor and chemosensor of bile flow and composition[13]. The secretory and proliferative capacities of cholangiocytes vary depending on duct size and anatomical location. In smaller ducts, cholangiocytes display generally reduced synthetic and secretory activity, yet they still contribute to biliary regeneration in the event of injury[9,14–16]. Notably, while there are no major qualitative differences in organelle composition between small and large cholangiocytes, both the number and size of organelles tend to be greater in large cholangiocytes, consistent with their more active role in bile modification, including bicarbonate and water secretion in response to hormonal stimulation[10,17,18].

2. DIVERSITY, PLASTICITY, AND SECRETORY FUNCTION OF CHOLANGIOCYTES

The cells that constitute the biliary epithelium display significant heterogeneity. This is reflected in the distinct transcriptomic profiles observed along different regions of the biliary tree. Stemness markers such as SOX9 and HNF1β are expressed by cells of the ductal plate, distinguishing them from hepatocytes. These cells subsequently differentiate to form mature biliary tissue. As the small and large ducts develop, cholangiocytes acquire distinct gene expression profiles[19,20], yet despite differences in

several key functional proteins, they continue to share the same epithelial markers, including keratins 7 and 19 and EpCAM. Large cholangiocytes exclusively express the secretin receptor (SR), the cystic fibrosis transmembrane conductance regulator (CFTR) chloride channel, and the anion exchanger 2 (AE2). Together, these proteins form a cAMP-dependent secretory pathway[17,21]. When secretin, a peptide hormone produced in the duodenum, binds to its basolateral receptor, intracellular cAMP levels rise, resulting in CFTR-mediated chloride secretion and chloride/bicarbonate exchange via AE2. This leads to bile alkalinisation[22] and creates the so-called "bicarbonate umbrella", a protective microenvironment that shields the biliary epithelium from the detergent properties of protonated bile acids[23,24]. By modifying bile primarily formed by hepatocytes, cholangiocytes contribute up to 40% of the final bile volume in humans[25]. In doing so, they play a role not only in regulating bile volume, but also in responding dynamically to its composition. Bile acids regulate cholangiocyte activity through receptors such as the nuclear farnesoid X receptor (FXR) and the membrane receptor TGR5, enabling cholangiocytes to detect bile acid concentration. Through feedback mechanisms, cholangiocytes modulate transporter expression and secretory rates, helping maintain bile flow and composition during physiological fluctuations, for example after meals[26,27]. Cholangiocyte secretion is also modulated by a wide range of hormones and paracrine mediators. Glucagon and vasoactive intestinal peptide (VIP) mimic the effects of secretin by increasing cAMP levels and promoting bicarbonate secretion, whereas somatostatin and endothelin exert opposing effects[25,26]. In addition, ATP and UTP released from nerves or from cholangiocytes themselves act on P2Y receptors, raising intracellular calcium and altering chloride channel function. This makes small cholangiocytes responsive to purinergic signalling via the IP_3 pathway, resulting in calcium-dependent chloride secretion through TMEM16A[28,29]. This alternative secretory pathway is especially important when the function of large ducts is compromised[11]. Small cholangiocytes lack SR, CFTR and AE2 expression and therefore do not rely on the cAMP pathway, instead depending on calcium-mediated mechanisms. These anatomical and functional differences between small and large cholangiocytes not only define their secretory capacities but also underlie their distinct responses to apoptotic and proliferative signals. For instance, following selective injury to large ducts using acute carbon tetrachloride (CCl_4) administration in murine models, small cholangiocytes, which are normally mitotically quiescent, begin to proliferate and newly express SR. Secretin binding then promotes not only bicarbonate secretion but also morphological and functional adaptations that facilitate bile duct repair[17,30,31]. This plasticity reflects a hierarchical organisation within the biliary epithelium, in which small cholangiocytes can serve as progenitor or reserve cells. The increased number of progenitor cells observed in the canals of Hering and in peribiliary glands during chronic liver injury further supports this concept[32–34].

Injury can also be triggered in murine models using cholestatic toxins such as 3,5-diethoxycarbonyl-1,4-dihydrocollidine (DDC), where small cholangiocytes similarly contribute to biliary regeneration and remodelling[35]. However, following ligation of the large bile ducts (BDL), only large cholangiocytes showed robust proliferation[36]. It is important to emphasise that small cholangiocytes are not entirely inactive, but rather exhibit a lower basal proliferative rate. Moreover, in experimental liver injury models they have been shown to acquire hepatocyte-like features[37] (Fig. 2).

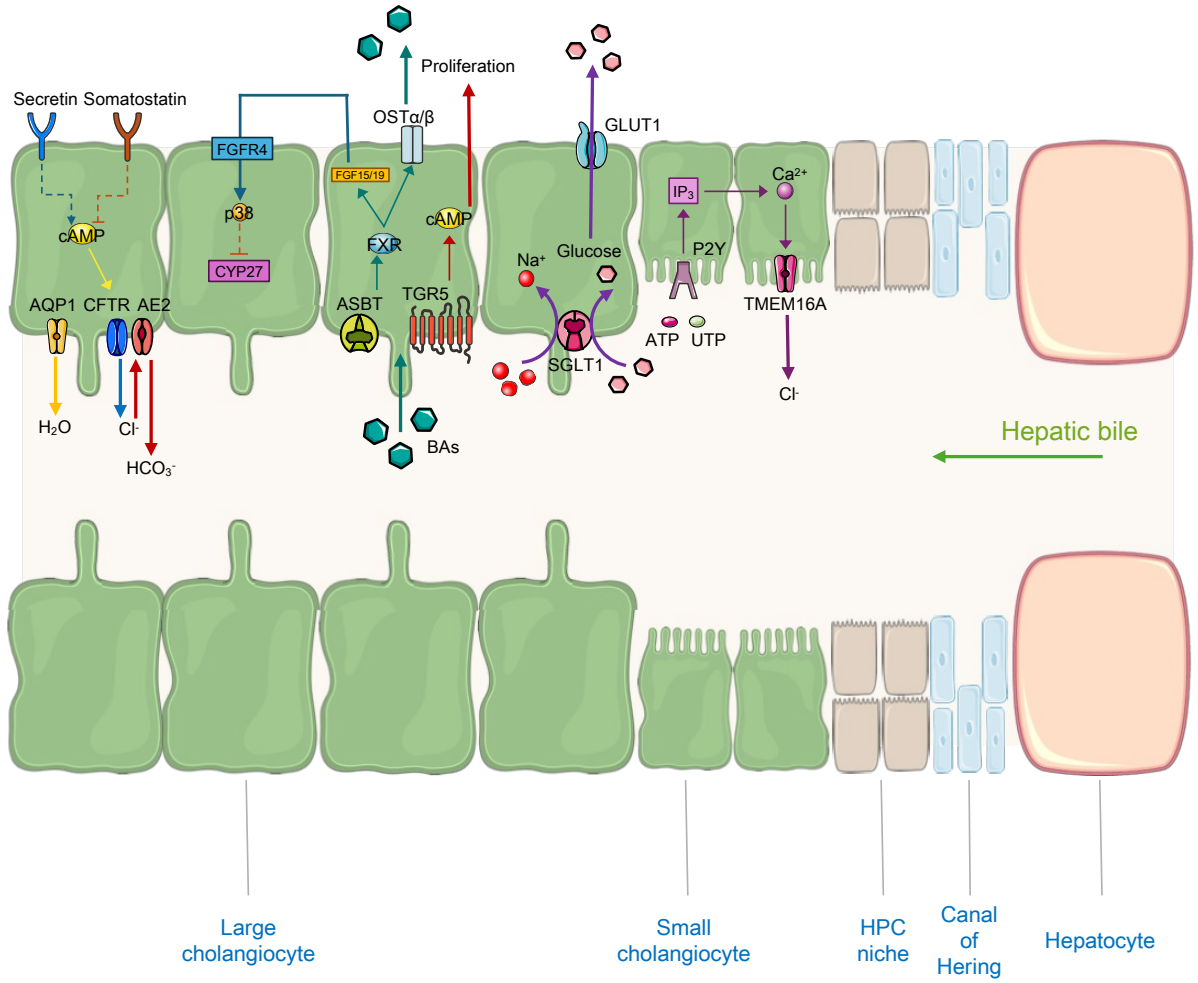

Figure 2. Transport and signalling pathways in cholangiocytes.
Hepatic progenitor cells (HPCs) in the canals of Hering differentiate into cholangiocytes forming the biliary epithelium. Large cholangiocytes express the secretin receptor (SR), which activates cAMP-dependent CFTR and AE2, promoting chloride and bicarbonate secretion and bile alkalinisation. Aquaporin-1 (AQP1) facilitates water movement. FXR and TGR5 receptors regulate bile acid transport and enhance secretion and proliferation. Small cholangiocytes lack SR, CFTR, and AE2, relying instead on calcium-dependent purinergic signaling: ATP/UTP activate P2Y receptors, raising intracellular Ca^{2+} and stimulating TMEM16A-mediated secretion. Cholangiocytes also sustain the cholehepatic shunt through glucose transporters SGLT1 and GLUT1, supported by Na^+/K^+-ATPase activity. *Adapted from Banales et al., 2019 and Alpini et al., 2002. Adapted from Servier Medical Art (https://smart.servier.com), licensed under CC BY 4.0 (https://creativecommons.org/licenses/by/4.0/).*

On top of their regenerative and secretory functions, cholangiocytes help to maintain essential homeostatic processes within the liver. To do so, they express a range of transporters involved in the uptake and efflux of different solutes. The sodium-dependent bile acid transporter ASBT (SLC10A2) and the sodium–glucose co-transporter SGLT1 (SLC5A1) are located on the apical membrane. Conversely, the basolateral membrane features the organic solute transporters α and β (OSTα/OSTβ), which mediate bile acid efflux, as well as the glucose transporter 1 (GLUT1/SLC2A1) for glucose reabsorption[26,38]. Together, these transporters allow cholehepatic shunting, the process by which bile acids are reabsorbed by cholangiocytes and returned to the liver via the portal circulation. In addition, cholangiocytes express a wide range of specialised carriers that facilitate the bidirectional movement of solutes such as amino acids, peptides, and both organic and inorganic ions. Members of the multidrug resistance protein family also contribute to these transport processes, thereby supporting biliary homeostasis and detoxification[25].

3. IMMUNOBIOLOGY OF CHOLANGIOCYTES

The bile ducts are anatomically connected to the intestine through the enterohepatic circulation, meaning that cholangiocytes are continuously exposed to microbe-derived molecules. As a result, they function as sentinels of the biliary tree and contribute to the recognition and clearance of microbial products[39]. In PSC and PBC, increased exposure or heightened sensitivity to pathogen-associated molecular patterns (PAMPs), such as bacterial lipopolysaccharide (LPS), has been reported. This is not thought to reflect the direct entry of bacteria into the ducts, but rather alterations in bile flow, dysbiosis, or changes in immune surveillance mechanisms[40]. Cholangiocytes respond strongly to LPS via Toll-like receptor signalling pathways, which is essential for antimicrobial defence but, when sustained, can contribute to chronic inflammatory injury of the bile ducts[41]. To cope with microbial threats, cholangiocytes employ a series of pattern recognition receptors (PRRs) that detect bacteria, viruses, and other pathogens. These include Toll-like receptors (TLRs) and NOD-like receptors (NLRs). Human cholangiocytes constitutively express TLR1–4 and additional PRRs not only on the cell surface but also within endocytic vesicles[40,42]. Activation of these receptors leads to the release of pro-inflammatory cytokines and chemokines through pathways such as NF-κB and MAPK[43]. A typical example is the recognition of LPS via TLR4. With the involvement of MD-2 and CD14, TLR4 triggers MyD88-dependent signalling, resulting in NF-κB activation and the production of cytokines such as TNF-α, IL-1β, IL-6, IL-8, and MCP-1[40,42,44]. MCP-1 contributes to monocyte recruitment into the portal tract, while IL-8 similarly attracts neutrophils. IL-6 and TNF-α also act on Kupffer cells and support activation of the

adaptive immune system[43]. Although NF-κB is central to this response, MAPK pathways including ERK1/2, JNK, and p38 also participate, together shaping the inflammatory response and contributing to the ductular reaction[42]. Cholangiocytes also express NLRP3 and other NOD-like receptors that sense cellular stress signals. For example, the presence of bile acid crystals can activate these receptors, promoting the release of IL-1β and IL-18 and thereby amplifying the inflammatory response[45,46]. In addition, cholangiocytes communicate directly with immune cells through adhesion molecules and co-stimulatory proteins. In response to cytokines such as IFN-γ, TNF-α, or IL-1β, cholangiocytes upregulate ICAM-1 and VCAM-1 on their surface. These changes enhance lymphocyte adhesion via LFA-1 and neutrophil adhesion via Mac-1. In PSC and PBC, however, ICAM-1 is often aberrantly or persistently expressed, contributing to the accumulation of immune cells along the biliary epithelium and within the periductal tissue, rather than allowing their physiological resolution[47,48]. VCAM-1 plays a different role, as it helps Th17 and $CD8^+$ T cells migrate into the ducts[49]. Additionally, cholangiocytes can produce LFA-3, which binds to CD2 on cytotoxic T cells and NK cells, strengthening adhesion and enhancing cytotoxic activity[50,51]. Furthermore, one study suggests that T cells can interact with CD40 expressed by cholangiocytes, thereby increasing local cytotoxic responses and inducing IL-12 production. While interaction with LFA-2 on T cells stimulates CD40L expression, IFN-γ further enhances CD40 expression[52]. The antigen-presenting capacity of cholangiocytes is relatively limited. Conventional co-stimulatory molecules such as CD80 and CD86, which are required for efficient priming of naïve $CD4^+$ T cells, are generally absent, although HLA class I and class II (HLA-DR) molecules can be induced by IFN-γ[50,53,54]. Consequently, class II expression is often regarded as an epiphenomenon of inflammatory activation rather than evidence of professional antigen presentation[50]. Nonetheless, cholangiocytes may engage alternative co-stimulatory pathways, such as through CD40, or present antigen to memory or already primed T cells[52]. In addition, during microbial challenge, cholangiocytes can interact with unconventional T cells, including MAIT and NKT cells, which recognise non-peptide antigens via MR1 and CD1d, respectively, leading to cytokine secretion and biliary inflammation[55–57]. Under homeostatic conditions, PD-L1 expression on cholangiocytes is low, but it is markedly upregulated in response to TNF-α and IFN-γ. Through PD-1 engagement on activated T cells, cholangiocytes can therefore exert co-inhibitory effects[58,59]. In recent experimental models of cholangitis, Stein et al. (2021) reported that IL-17A further enhances PD-L1 expression in cholangiocytes, establishing a negative feedback loop that limits $CD8^+$ T-cell-mediated bile duct injury[60] (Fig. 3).

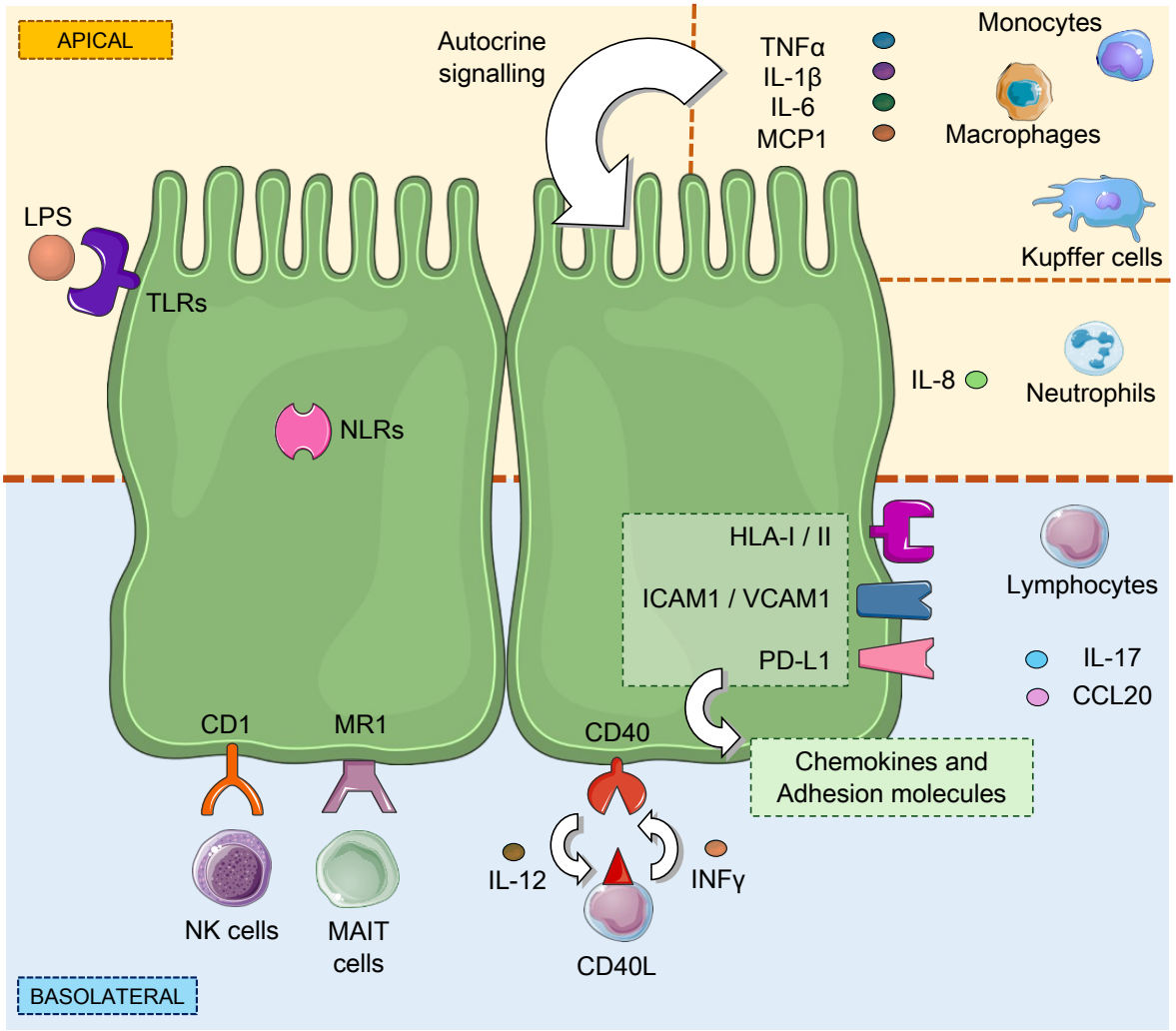

Figure 3. Cholangiocyte–immune cell crosstalk

Cholangiocytes act as immune sentinels of the biliary tree, detecting microbial and inflammatory signals. Apical TLRs sense LPS and activate NF-κB/MAPK pathways, inducing cytokines such as TNF-α, IL-1β, IL-6, and IL-8 that recruit immune cells and activate Kupffer cells. NLRs detect bile acid crystals, amplifying IL-1β release. Basolateral ICAM-1, VCAM-1, and HLA molecules mediate lymphocyte interactions, while IFN-γ–induced CD40 and IL-12 promote Th1 responses. Cholangiocytes also present antigens via MR1 and CD1, and upregulate PD-L1 in response to cytokines and IL-17A, providing feedback inhibition of T cell activity. *Adapted from Banales et al., 2019. Adapted from Servier Medical Art (https://smart.servier.com), licensed under CC BY 4.0 (https://creativecommons.org/licenses/by/4.0/).*

4. CHOLANGIOCYTES AND CHOLANGIOPATHIES: FOCUS ON PRIMARY SCLEROSING CHOLANGITIS (PSC)

The term “cholangiopathies” refers to a group of chronic diseases that damage both intrahepatic and extrahepatic bile ducts. Their aetiology ranges from genetic alterations to viral infections and toxic insults, and in some cases remains idiopathic; however, regardless of cause, the immune system consistently targets cholangiocytes driving uncontrolled inflammation[61–63]. As a result, cholangiocytes become reactive and proliferative while releasing pro-inflammatory cytokines and chemokines such as IL-8, TNF-α and IL-6. These mediators act not only on surrounding cells but also feed back onto cholangiocytes themselves, thereby perpetuating the inflammatory cycle. If this vicious cycle is not interrupted, inflammation progressively involves the extracellular matrix. Step by step, this leads to periportal fibrosis, cholestasis and ultimately cirrhosis, resulting in liver failure and the need for liver transplantation. The list of cholangiopathies is extensive, including PSC, PBC, biliary atresia, cystic fibrosis-related liver disease, Alagille syndrome and cholangiocarcinoma, although the pathogenesis of PSC remains particularly complex. Current evidence suggests that multiple factors contribute to disease onset. An abnormal response to environmental triggers, such as antigens derived from the gut microbiota, may initiate disease in genetically predisposed subjects[64–66]. This leads to chronic inflammation and scarring that remodels the hepatic architecture. Far from being passive targets, cholangiocytes play an active role in this process. Under persistent epithelial injury, they may enter a senescent state and develop a senescence-associated secretory phenotype (SASP), characterised by the release of pro-fibrogenic cytokines and growth factors that intensify local inflammation and promote a pro-fibrotic milieu[67]. These mediators activate hepatic stellate cells and portal fibroblasts, resulting in excessive extracellular matrix deposition and the characteristic “onion-skin” fibrosis observed in PSC[68–70]. Over time, this fibrotic remodelling culminates in ductopenia, biliary cirrhosis and liver failure[64,71,72]. Approximately 60% of people affected by PSC are young to middle-aged men, presenting clinically with fatigue, pruritus and recurrent episodes of cholangitis[72,73]. Notably, up to 70% of people with PSC also develop inflammatory bowel disease (IBD), most commonly ulcerative colitis, highlighting the contribution of the gut–liver axis to disease pathogenesis[73,74]. Microbial translocation and dysbiosis may activate cholangiocytes through Toll-like receptors, particularly TLR4, and promote chronic inflammation via NF-κB signalling[40,65,66]. In addition, epithelial barrier defects in PSC cholangiocytes, including reduced expression of tight junction proteins such as ZO-1, may exacerbate bile leakage into portal areas, further amplifying immune activation and fibrosis[75]. The biliary epithelium in PSC exhibits clear immunological activation. Increased expression of adhesion molecules (ICAM-1, VCAM-1), MHC class I/II, and secretion of chemokines such as CCL20 recruit lymphocytes into the portal tracts[76–79]. $CD4^+$ and $CD8^+$ T cells, together with

macrophages, neutrophils, NK cells and γδ T cells, accumulate in peribiliary areas and sustain chronic inflammation[80–82]. Th17 cells are particularly enriched and may contribute directly to fibroinflammatory progression, especially since regulatory T cells (Tregs) appear to be numerically or functionally impaired in PSC[78,79]. Importantly, people with PSC have a significantly increased risk of malignancy, particularly cholangiocarcinoma and gallbladder cancer[83–85]. Despite progress in understanding PSC pathogenesis, no effective pharmacological therapy is currently available. Although ursodeoxycholic acid (UDCA) may offer some benefit, it does not significantly improve survival or halt disease progression[86]. Liver transplantation remains the only curative option, although recurrent disease can occur post-transplantation[87].

5. CHOLANGIOCYTES IN ALCOHOL-ASSOCIATED LIVER DISEASE (ALD)

Alcohol-associated liver disease (ALD) remains the leading cause of chronic liver disease worldwide. In Europe, more than 40% of cirrhosis-related deaths are related to alcohol intake, representing a significant impact on liver disease worldwide[88]. Alcohol metabolism varies between people and particularly between Asia and Western countries, due to polymorphisms in the ADH and ALDH2 genes, which influence acetaldehyde production and thereby the pathogenesis of ALD. In particular, ALDH2 variants, common in Asia, are associated with increased inflammation and fibrosis[89,90]. The picture is further complicated by a clear sex disparity. Likely due to hormonal and metabolic differences[91], women are more susceptible than men to alcohol-induced liver injury at lower levels of consumption. Although more men are diagnosed with ALD overall, women often experience more severe disease and worse outcomes[92,93]. Alcohol-associated hepatitis (AH), cirrhosis, hepatocellular carcinoma (HCC) and simple steatosis all fall within the clinical and histological spectrum of ALD[94]. The progression from early-stage steatosis to cirrhosis and hepatocellular carcinoma (HCC) is a gradual process driven by chronic inflammation and ongoing cellular injury. Cirrhosis and HCC resulting from ALD account for nearly 20% of liver cancer deaths worldwide, underscoring the severity of ALD[95,96]. Sustained high-level alcohol consumption suppresses immune function, increasing susceptibility to bacterial and viral infections[97], while compromising the integrity of the gut barrier[98]. Long-term alcohol consumption is also closely linked to intestinal dysbiosis and small intestinal bacterial overgrowth[99,100]. Progressive hepatocyte loss due to alcohol-induced injury and increased intestinal permeability leads to robust recruitment of immune cells to the liver. This includes infiltrating neutrophils and macrophages, as well as the activation of Kupffer cells, the liver's resident macrophages[95]. These cells release reactive oxygen species (ROS) and proteases that support antimicrobial defence and regeneration[98,101,102], but, when

persistent, cause oxidative hepatocyte damage. Neutrophils can also form neutrophil extracellular traps (NETs), web-like structures composed of DNA and antimicrobial proteins which, in alcoholic hepatitis, may further exacerbate inflammation and contribute to tissue injury[101]. Other lymphocyte subsets participate in the inflammatory milieu. In addition to NKT cells, Th17 cells and mucosa-associated invariant T cells, infiltration of $CD8^+$ T lymphocytes is commonly observed, although their precise role remains incompletely understood[95,103]. B cells also play a direct role; in severe alcoholic hepatitis (SAH) they promote inflammation through antibody secretion and activation of the complement cascade[104]. In advanced disease stages, the ductular reaction becomes a key feature of ALD progression. In people with sAH, Dubuquoy et al. identified $CK7^+$ or $CK19^+$ cells, suggesting that the ductular reaction originates primarily from cholangiocytes or progenitor cells rather than hepatocytes. More recent work has shown that neutrophils associated with the ductular reaction (DRAN) actively promote biliary remodelling by stimulating cholangiocyte proliferation and fibrosis[105]. Inflammatory infiltration and extracellular matrix deposition are frequently observed during cholangiocyte and hepatic progenitor cell expansion[37]. Altered NF-κB signalling and mTOR activation in cholangiocytes have been identified as major drivers of the ductular reaction in humans[106–109]. However, because these pathways are difficult to target selectively, effective therapies remain lacking, therfore ductular reaction is associated with poorer outcomes in ALD. Genetics play a substantial role in ALD progression. Variants in PNPLA3 (rs738409 C>G) and TM6SF2 (rs58542926 C>T), both involved in lipid handling, influence not only the risk of cirrhosis but also the likelihood of progression to HCC[110,111]. Conversely, variants in genes such as HSD17B13 and MARC appear protective, reducing the risk of cirrhosis[112,113]. Other variants, including in MBOAT7, NCAN or WNT3A–WNT9A, promote disease progression and hepatocarcinogenesis[114–116]. Despite extensive research, there are still no FDA-approved drugs for ALD. Corticosteroids are used in severe alcoholic hepatitis but provide only short-term benefit[117]. For this reason, therapeutic strategies have focused more on modulating the immune response. For instance, in animal models, treatment with cenicriviroc, a dual CCR2/CCR5 antagonist, reduced macrophage infiltration and fibrosis, making it a promising potential therapeutic approach[118].

6. DEVELOPMENT AND OPTIMIZATION OF CHOLANGIOCYTE ORGANOID CULTURE FOR DISEASE MODELLING AND REGENERATIVE THERAPY

In advanced liver diseases, when treatment options are limited, the liver's intrinsic regenerative capacity is often insufficient[119]. This highlights the urgent need for new strategies that can either enhance the natural repair potential of liver cells or replace damaged tissue through cell-based therapies and tissue engineering[119–122]. Three-dimensional cell technologies have emerged as a promising approach in this context. Organoids are three-dimensional structures that mimic the architecture and function of the original tissue, in which progenitor cells self-organise and differentiate into functional cell types[123]. Numerous strategies have been developed to support organoid growth, proliferation and maturation, enabling the study of both disease pathogenesis and potential pharmacological interventions, thereby showing strong promise for personalised medicine[124]. In the context of cholangiopathies, organoids have been successfully established using different culture strategies, providing disease-relevant models for both basic and translational research[125]. However, cholangiocyte organoids do not fully resemble adult biliary cells. They typically show reduced expression of mature markers such as HNF1B, CK7, CK19 and CFTR, while maintaining higher levels of genes associated with progenitor or foetal states, including LGR5, PROM1 (CD133) and TBX3[126,127]. Nevertheless, organoids display several key characteristics of differentiated cholangiocytes, including MDR1-mediated bile salt export and responsiveness to physiological stimuli such as secretin, somatostatin and VEGF. These responses are mediated through transporters and receptors such as CFTR, ASBT, SCTR and SSTR2, which are also present in mature biliary tissue. Thus, despite their comparatively less mature transcriptional profile, cholangiocyte organoids retain a physiologically meaningful and relevant phenotype[128]. Embedding cholangiocytes within an extracellular matrix (ECM) is crucial for the morphological and functional development of organoids, since ECM components such as laminin, collagen IV and associated growth factors provide both mechanical support and biochemical cues necessary for cell polarisation and appropriate three-dimensional organisation[129–132]. When embedded in matrix, cholangiocytes self-organise into organoids characterised by an "inside-out" epithelial polarity, where the apical membrane faces the inner lumen and the basal surface interfaces with the surrounding ECM[133]. Just as ECM composition is essential for organoid expansion and maturation, so too is the culture medium. Huch et al. (2015) developed one of the earliest protocols, combining mitogens such as EGF, HGF and FGF10 with inhibition of TGF-β signalling via A83-01 and activation of the canonical Wnt/β-catenin pathway through R-spondin1[123]. According to Francis et al. (2004), forskolin is also used to increase cAMP signalling, promoting lumen expansion and

secretory activity. Nicotinamide supports cellular stability and stress resistance, while supplements such as B27, N2 and gastrin provide metabolic and hormonal support[134]. The essential components of cholangiocyte organoid culture media are listed in the table below:

Component	Main Role / Function	Phase of Use	Ref.
EGF	Promotes cholangiocyte maturation, transdifferentiation, and biliary marker expression (e.g., CFTR, CK19). Enhances Wnt/β-catenin signaling and upregulates biliary progenitor genes (NOTCH2, LGR5). Critical for 3D organoid morphology and functional maturation.	Expansion / maintenance	[135]
RSPO	Potentiates Wnt signaling by binding LGR4/5/6 and ZNRF3/RNF43. Maintains stemness and progenitor identity ($LGR5^+$ cells). Essential for long-term organoid expansion.	Expansion / maintenance	[136]
Wnt (Wnt3a CM)	Activates β-catenin-dependent Wnt signaling. Maintains progenitor cell identity and supports early organoid formation.	Initial phase / expansion	[135,137]
FGF10	Drives biliary specification from hepatoblasts. Promotes cholangiocyte progenitor formation and ductal morphogenesis.	Expansion / maintenance	[126]
HGF	Supports cell motility, proliferation, and morphogenesis via c-MET signaling.	Expansion / maintenance	[138]
Nicotinamide	Protects against cellular stress; supports NAD^+ metabolism and genomic stability.	Expansion / maintenance	[139]
A83-01	Inhibits ALK5/TGF-β signaling; prevents premature differentiation and senescence.	Expansion / maintenance	[140]
Forskolin (FSK)	Increases intracellular cAMP; enhances apical secretion, lumen expansion, and epithelial polarization.	Expansion / maintenance	[141]
N-Acetylcysteine	Antioxidant; improves cell viability and proliferation.	Expansion / maintenance	[142]
N2 supplement	Provides insulin, transferrin, selenium, etc.; supports growth under serum-free conditions.	Expansion / maintenance	[143]
B27 supplement	Supplies vitamins, antioxidants, fatty acids; enhances epithelial survival and maturation.	Expansion / maintenance	[143]
Gastrin	Gastrointestinal hormone; stimulate pro-proliferative pathways.	Expansion / maintenance	[144]

Refinements in these culture protocols have enabled the generation of cholangiocyte organoids from different anatomical regions. Intrahepatic cholangiocyte organoids (ICOs) arise from $LGR5^+$ progenitor cells and require canonical Wnt signalling to sustain proliferation and maintain stemness[123]. Extrahepatic cholangiocyte organoids (ECOs), on the other hand, grow more efficiently under conditions favouring non-canonical Wnt signalling, such as planar cell polarity pathways, which support functional duct formation and more advanced differentiation. Cholangiocyte organoids derived from bile or extrahepatic tissue under non-canonical conditions, for example in the presence of DKK1, show higher expression of CFTR, AQP1 and other mature functional markers, while retaining hormonal responsiveness such as secretin sensitivity, as demonstrated by studies from Sampaziotis et al. (2015) and Roos et al. (2021)[126,128]. Applications of patient-derived cholangiocyte organoids now span multiple research areas, including PSC, PBC, cystic fibrosis, cholangiocarcinoma and emerging clinical uses. Notably, cholangiocyte organoids derived from people with cystic fibrosis are used to model disease-associated pro-inflammatory features[145] and to perform drug screening via forskolin-induced swelling assays. In genetic disease research, cholangiocyte organoids are valuable tools because CRISPR-mediated correction of CFTR mutations can be directly evaluated in these cultures, facilitating personalised therapeutic strategies[128,145]. In cholangiocarcinoma research, organoid models enable preclinical assessment of tumour-specific drug sensitivity and regenerative capacity in a patient-specific manner[125]. With regard to regeneration, Sampaziotis et al. (2021) transplanted cholangiocyte organoids into damaged bile ducts in human livers maintained under normothermic perfusion ex vivo[121]. The transplanted organoids successfully repopulated the injured ducts and restored both structure and function. These findings open the way for cell-based therapies that could potentially repair biliary injury without requiring full liver transplantation.

AIM OF THE STUDY

Cholangiocytes are directly exposed to immune attack in chronic liver diseases such as primary sclerosing cholangitis (PSC) and alcohol-associated liver disease (ALD), which are characterised by fibrosis, epithelial damage and ultimately progressive loss of liver function due to excessive inflammation around the bile ducts. Rather than being passive targets, cholangiocytes actively shape the local immune environment. They release cytokines and express adhesion molecules, and under prolonged stress can acquire a senescence-associated secretory phenotype (SASP), which sustains inflammation in a feedback loop. Cholangiocytes can also express MHC class II molecules, which are involved in antigen recognition, although the extent of their antigen-presenting capacity and how this may contribute to the overall immune response in liver diseases remains unclear.

Based on these observations, we hypothesised that the bidirectional interaction between immune cells and cholangiocytes determines biliary inflammation and thereby contributes to the pathogenesis of cholangiopathies. Using our newly developed and optimised cholangiocyte organoid co-culture system, we first aimed to investigate transcriptional and functional changes in cholangiocytes, highlighting disease-associated alterations that may explain differences in epithelial regulation between immune-mediated (PSC) and non-immune-mediated (ALD) liver diseases. Secondly, we examined the interaction between cholangiocytes and $CD4^+$ T cells under both HLA-matched and HLA-mismatched conditions, to assess whether the immune response in PSC could be attributed to disease-related autoimmune mechanisms. In this context, we analysed how cholangiocytes influenced T cell activation, and, conversely, how T cells impacted cholangiocyte phenotype. This approach also enabled us to evaluate the suitability of the organoid co-culture model for studying such bidirectional interactions in vitro and to identify mechanisms that may contribute to disease progression.

RESULTS

Primary sclerosing cholangitis is a rare liver disease of still uncertain origin. A distinguishing feature is the accumulation of immune cells around the bile ducts, accompanied by a gradual loss of epithelial integrity. In this setting, cholangiocytes are not merely passive targets; they release cytokines, express adhesion molecules and might even present antigens. Yet, how they communicate with immune cells remains incompletely understood. In this work, we used patient-derived cholangiocyte organoids as a three-dimensional model to investigate these interactions. Organoids provide a physiologically relevant system, as they reproduce key features of native tissue, including epithelial polarity, expression of differentiation markers and essential functional properties. To this end, we combined organoid culture with immune cells and applied a range of approaches, including flow cytometry, gene expression profiling and imaging-based analyses, to characterise both cholangiocyte identity and their response to immune-derived stimuli. We anticipated that these data would establish cholangiocyte organoids as a robust model for studying epithelial–immune interactions in PSC, providing new insights into the role of cholangiocytes in sustaining or modulating chronic inflammation.

1. GENERATION OF CHOLANGIOCYTE ORGANOIDS FROM LIVER TRANSPLANT TISSUE

Cholangiocyte organoids are an innovative three-dimensional model system for studying liver disease. Derived from progenitors of the biliary epithelium, these organoids replicate many of the functional and structural properties of *in vivo* cholangiocytes. However, how well they mirror the molecular and functional features of the specific pathology or the donor largely depends on the culture conditions applied in each laboratory. In this study, we generated cholangiocyte organoids according to the protocol described by Broutier *et al.*[125]

We found that the generation of intrahepatic cholangiocyte organoids from people with PSC was less efficient than from those with ALD. Among the 42 liver samples processed (PSC, n = 26; ALD, n = 16), 13 samples from people with ALD successfully gave rise to cholangiocyte organoids, corresponding to an overall success rate of 81.2%. In contrast, organoids were obtained from only nine out of 26 PSC-derived liver samples,

corresponding to a markedly lower success rate of 34.6%. These results suggest that the derivation of cholangiocyte organoids from PSC tissue is more complex, possibly reflecting underlying disease-related alterations in cholangiocyte physiology.

Diagnosis	Organoids Generated from Patients	Total Patients	Success Rate (%)
Alcoholic Liver Disease (ALD)	13	16	81,2
Primary Sclerosing Cholangitis (PSC)	9	26	34,6

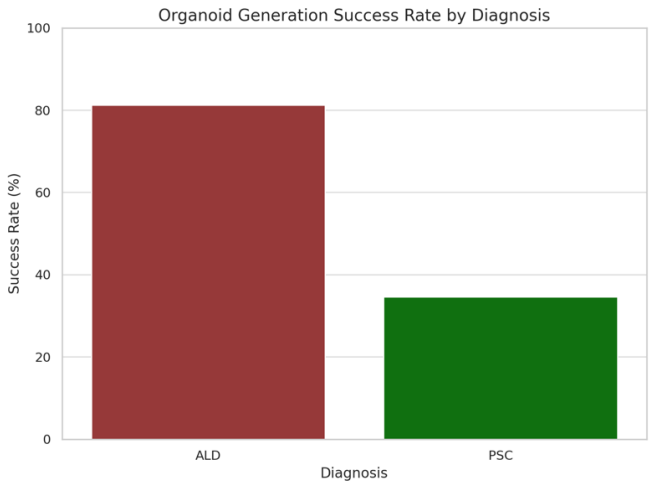

Figure 4. Comparison of cholangiocyte organoid generation success rates from liver samples derived from people diagnosed with Alcoholic Liver Disease (ALD) and Primary Sclerosing Cholangitis (PSC).

2. CHARACTERIZATION OF CHOLANGIOCYTE ORGANOID MODELS: TRANSCRIPTOMIC ANALYSIS

Since methods for the isolation and cultivation of organoids are not yet fully standardised, we next aimed to characterise the cholangiocyte organoids we established in detail to ensure their reliability. To this end, we performed a comparative transcriptomic analysis of cholangiocyte organoids derived from people with PSC and ALD, using the Clariom S Human microarray platform. The table below summarises the clinical details of the cohort included in the study.

Pseudonym	Age	Sex	Disease	Histopathology
ALD-01	60	male	ALD	Cirrhosis with low-to-mid grade chronic periportal inflammation, low-grade hepatocellular siderosis, low-grade cholestasis, and chronic cholecystitis
ALD-02	63	male	ALD	Low grade steatosis (<5%), swollen hepatocytes, ischemic remodelling, cirrhosis
ALD-03	60	male	ALD	Cholestasis, low grade steatosis (ca. 10%), cirrhosis, chronic cholecystitis
PSC-01	66	male	PSC	Chronic sclerosing cholangitis with severe cholestasis, hepatocellular siderosis, bile infarctions, and cirrhosis
PSC-02	37	male	PSC	Bile duct dilatations with 40% steatosis, chronic sclerosing and ulcerative cholangitis, coagulative necrosis (90%), several bile infarctions, cirrhosis, and low-grade chronic cholecystitis.
PSC-03	56	male	PSC	Chronic sclerosing cholangitis with canalicular and hepatocellular cholestasis, fibro-obliterative degeneration of bile ducts, loss of bile ducts (over 50% of portal fields), cirrhotic remodelling, low-grade siderosis, bile stones in the liver hilus, chronic cholecystitis, cholecystolithiasis, and bile ducts with ulcerative and necrotic inflammation plus purulent inflammation.

2.1. TRANSCRIPTOMIC PROFILING OF BASELINE PSC AND ALD ORGANOIDS USING MICROARRAY ANALYSIS

Transcriptomic analysis (Fig. 5A) of organoids in a basal quiescent state revealed modest but significant differences between PSC- and ALD-derived samples. In PSC-derived cholangiocyte organoids, we detected higher expression levels of PLXDC2, a molecule implicated in angiogenesis and cell orientation, and PROM1 (CD133), a marker of epithelial progenitor cells. Upregulation of INSL4 was also observed, which, although classically linked to placental growth and development, may also be involved in morphogenesis and apoptosis. Among the genes involved in extracellular matrix deposition, we identified SLIT3, which interacts with ROBO receptors to regulate tissue organization, along with ROBO1 itself. Further differences were detected in the expression of TXK, a tyrosine kinase associated with oxidative stress responses, and MUC6, a mucin important for epithelial protection. PSC-derived organoids also showed

higher levels of IFI6 associated with innate immunity, as well as the transcriptional regulator ZKSCAN7, and the adhesion molecule CNTNAP3. Collectively, the enrichment of PLXDC2, PROM1, and SLIT3/ROBO1 suggests that PSC-derived cholangiocyte organoids display transcriptional features related to tissue growth, structural organisation and progenitor cell activity, while also engaging immune- and stress-associated pathways even when maintained in a resting state. In contrast, cholangiocyte organoids derived from people with ALD showed higher expression of CADPS, a calcium-dependent activator of vesicle exocytosis, PTPRR, a tyrosine phosphatase that modulates MAPK signalling and cell differentiation, and TMEM200A, a poorly characterised transmembrane protein potentially linked to epithelial integrity. Further upregulation was observed in SLC44A5, which encodes a choline transporter, and GJC1, which encodes a connexin family protein forming gap junction channels. The upregulation of these genes indicates that ALD-derived organoids preserve a cohesive and functionally stable epithelial architecture, with a pronounced focus on metabolic regulation. To explore the functional significance of these molecular differences, KEGG pathway enrichment analysis was performed on genes upregulated in PSC-derived organoids. At a less stringent cut-off ($p < 0.2$), the axon guidance pathway emerged, in line with the increased expression of ROBO1 and SLIT3 (Fig. 5B). Gene Ontology analysis of genes enriched in PSC-derived organoids further pointed to cytokine- and chemokine-mediated responses (Fig. 5C). Even under basal conditions, PSC-derived organoids display a molecular signature enriched in immune-related pathways, suggesting they are primed to respond to immune stimuli. Although the overall expression patterns of PSC- and ALD-derived organoids remain substantially similar in the absence of stimulation, the presence of these disease-specific signatures suggests a degree of transcriptional imprinting derived from the tissue of origin.

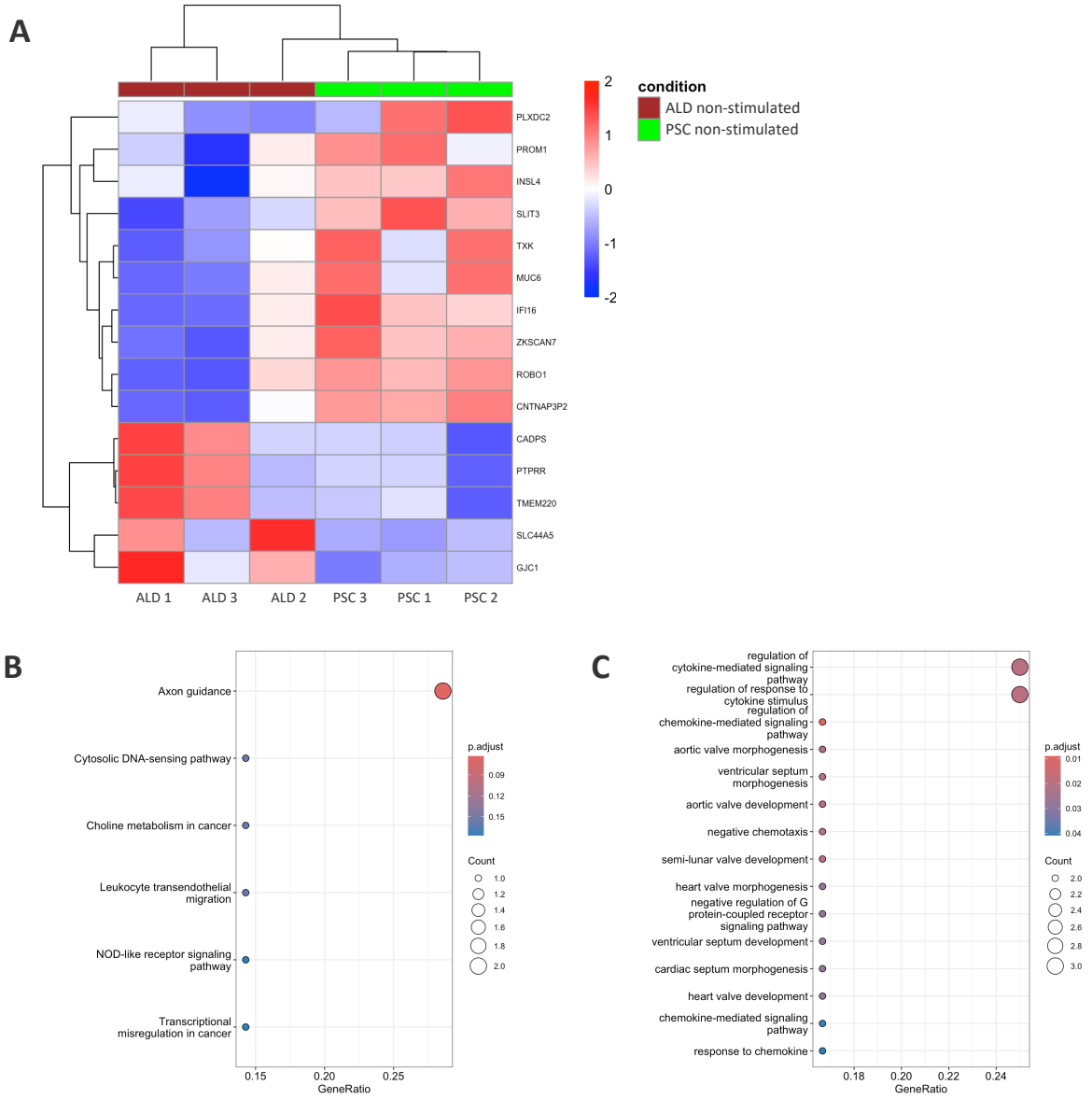

Figure 5. Transcriptomic comparison between unstimulated cholangiocyte organoids derived from people with ALD and PSC.

(A) Heatmap showing hierarchical clustering of the top differentially expressed genes ($p < 0.05$, $|log2FC| > 1$) between unstimulated cholangiocyte organoids derived from people with ALD and PSC. Z-score normalized expression values are shown. (B) KEGG pathway enrichment analysis performed on genes upregulated in PSC-derived cholangiocyte organoids compared to ALD (cutoff: p-value < 0.2). The Axon guidance pathway was identified as enriched. (C) GO enrichment analysis (Biological Process) performed on genes upregulated in PSC organoids compared to ALD. Significant enrichment was observed in cytokine-mediated signalling and chemokine-related pathways.

2.2. MOLECULAR RESPONSE OF PSC- AND ALD-DERIVED CHOLANGIOCYTE ORGANOIDS TO IL-17A STIMULATION

Three-dimensional cell culture provides a powerful model to reproduce disease-specific features, including cellular responses to inflammatory stimuli. In this study, we established cholangiocyte organoids from people with two chronic inflammatory diseases (PSC and ALD) characterized by persistent cytokine imbalance.Cholangiocyte organoids were analysed both under basal conditions, in the absence of external stimuli, and after 24 hours of stimulation with IL-17A, a pro-inflammatory cytokine known to be involved in biliary tract injury. The aim was to evaluate the ability of the cholangiocyte organoids to mirror the inflammatory responses observed *in vivo* in PSC and ALD, in order to confirm the suitability of the model for studying disease mechanisms.

2.2.1. TRANSCRIPTOMIC ANALYSIS OF PSC-DERIVED CHOLANGIOCYTE ORGANOIDS STIMULATED WITH IL-17A

The heatmap shows a clear separation between upregulated and downregulated differentially expressed genes in PSC-derived cholangiocyte organoids stimulated with IL-17A, compared with non-stimulated ones after 24 hours (Fig. 6A). In the control group, we observed higher expression of genes associated with epithelial differentiation and homeostasis. These include CCDC66, associated with cytoskeletal organisation, CPA4, a secreted carboxypeptidase that modifies extracellular peptides and contributes to tissue remodeling, and MND1, which participates in meiotic recombination processes. In addition, ELOVL4, involved in lipid biosynthesis, and KRT13, a marker of epithelial differentiation, were also found to be more highly expressed. Following IL-17A stimulation, cholangiocyte organoids expressed a broad set of genes related to inflammation and the recruitment of neutrophils and lymphocytes, including CXCL1–5 and CCL20. Pro-inflammatory cytokines IL1B, together with its mRNA regulator ZC3H12A, were also upregulated, alongside the antimicrobial genes DEFB4A and DEFB4B, and the acute-phase proteins SAA1 and SAA2. Genes involved in cytokine signalling, such as ZC3H12A and NFKBIZ, were increased, together with PDZK1IP1, which is associated with membrane transport and signal transduction, and PIGR, responsible for mucosal immunity. KEGG pathway enrichment analysis of the upregulated genes confirmed a significant overrepresentation of inflammatory and immune-related pathways, including TNF and NF-κB signalling (Fig. 6B). Gene Ontology analysis further highlighted biological processes such as neutrophil migration, granulocyte chemotaxis, antimicrobial activity and cytokine-mediated signalling, all of which are linked to epithelial defence and leukocyte recruitment (Fig. 6C).

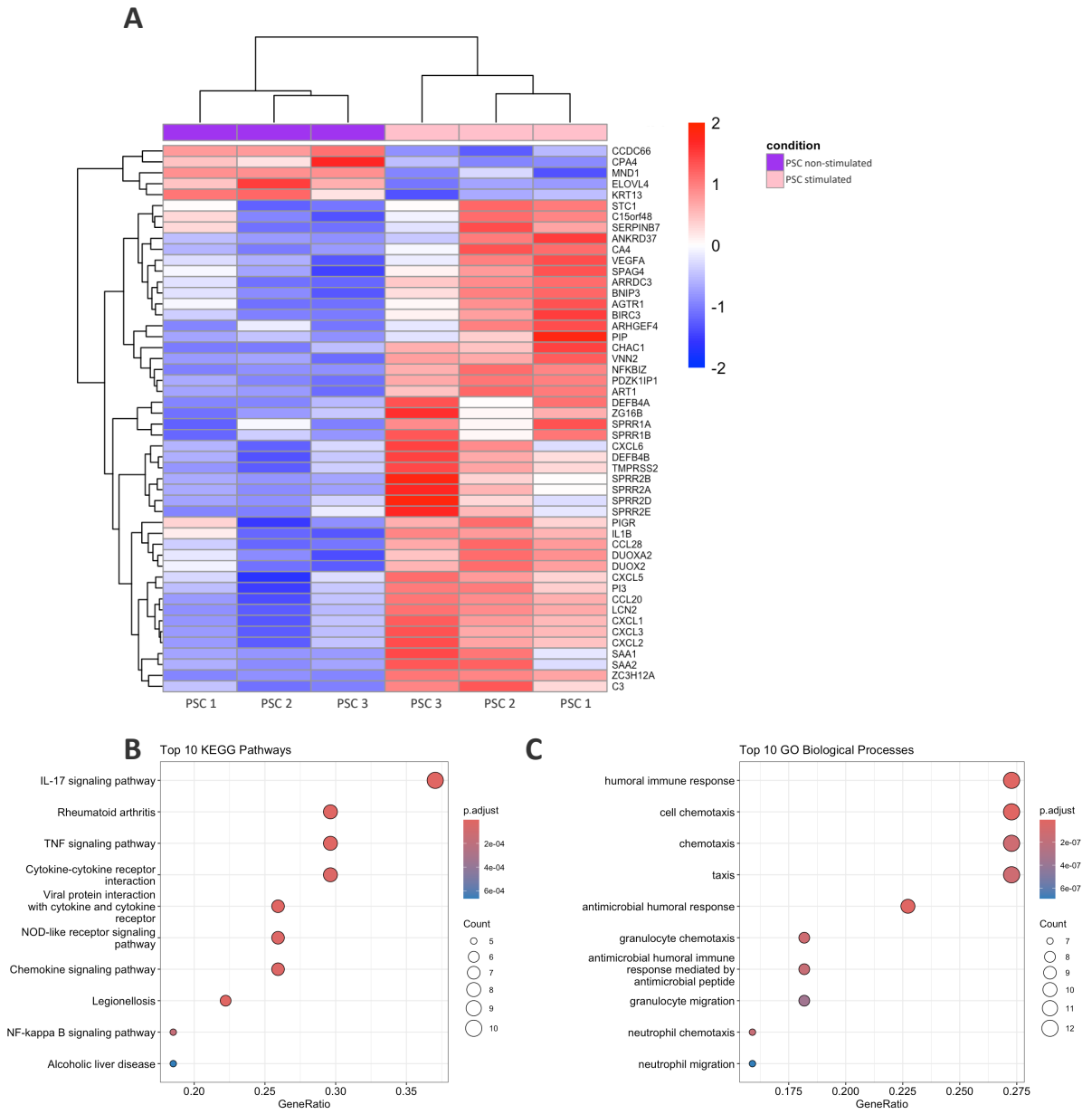

Figure 6. Comparative analysis of gene expression and enriched pathways between PSC non-stimulated and PSC stimulated samples.

(A) Heatmap showing the expression levels of differentially expressed genes (|log2FC| > 1, p < 0.05) between PSC non-stimulated and PSC stimulated cholangiocyte organoids. Blue represents downregulated genes, and red represents upregulated genes. (B) Top 10 KEGG pathways enriched among the differentially expressed genes, identified via functional enrichment analysis. Dot size corresponds to the number of genes in each pathway, and the colour gradient indicates the adjusted p-value (p.adjust). (C) Top 10 GO Biological Processes associated with the differentially expressed genes. Similar to (B), dot size reflects the number of genes involved, and the colour gradient represents the adjusted p-value (p.adjust).

2.2.2. TRANSCRIPTOMIC ANALYSIS OF ALD-DERIVED CHOLANGIOCYTE ORGANOIDS STIMULATED WITH IL-17A

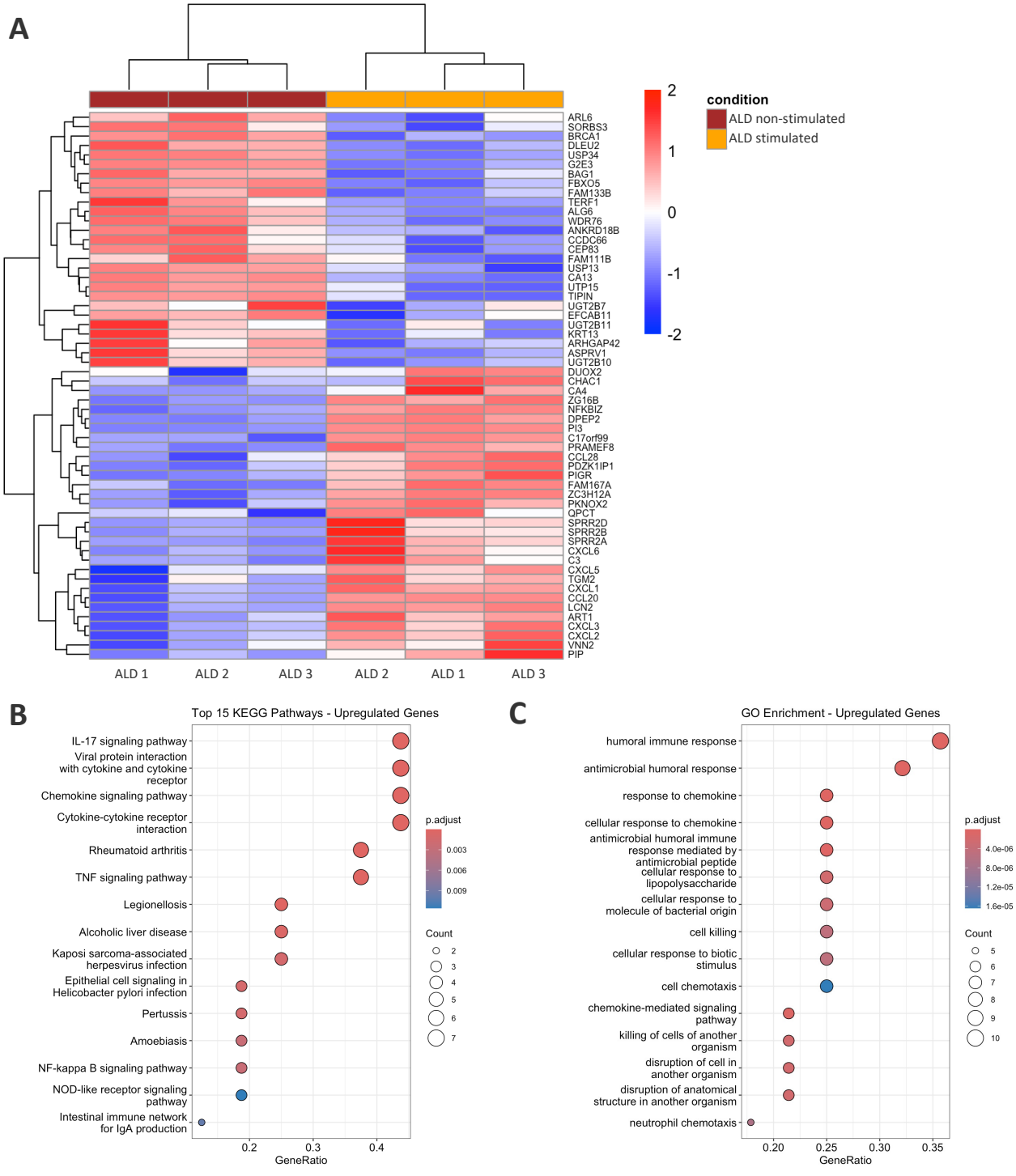

Figure 7. Comparative analysis of gene expression and enriched pathways between ALD non-stimulated and ALD stimulated samples.
Heatmap displaying the expression levels of differentially expressed genes (|log2FC| > 1, p < 0.05) between ALD non-stimulated and ALD stimulated cholangiocyte organoids. Blue represents downregulated genes, and red represents upregulated genes. (B) Top 10 KEGG pathways enriched among the differentially expressed genes, identified via functional enrichment analysis. Dot size indicates the number of genes involved in each pathway, and the colour gradient represents the adjusted p-value (p.adjust). (C) Top 10 GO Biological Processes associated with the differentially expressed genes. Dot size reflects the number of genes, and the colour gradient corresponds to the adjusted p-value (p.adjust).

ALD-derived cholangiocyte organoids showed marked transcriptional changes after 24 hours of IL-17A stimulation compared to the non-stimulated condition, as expected. The heatmap (Fig. 7A) illustrates that in the absence of stimulation, ALD-derived cholangiocyte organoids predominantly expressed genes linked to epithelial differentiation and integrity, including USP34, TERF1, G2E3, BRCA1, WDR76, and KRT13. Genes related to metabolism and detoxification, such as UGT2B7, UGT2B11, UGT2B10, and FAM133B, were also enriched. Additional transcripts associated with cytoskeletal organisation and cellular transport included CA13, ARL6, and SORBS3. In contrast, ALD-derived cholangiocyte organoids stimulated with IL-17A showed a strong induction of inflammatory and antimicrobial genes, similar to PSC-derived organoids. These included the chemokines CXCL1–5, CCL20 and CCL28, as well as NFKBIZ and DUOX2. Further upregulated transcripts comprised ZC3H12A, PDZK1IP1, CHAC1, and members of the SPRR family (SPRR2A/B/D), all of which are linked to cytokine-mediated signalling, glutathione metabolism and epithelial barrier repair. To assess the functional significance of these changes, KEGG and GO enrichment analyses were performed on the upregulated gene set. KEGG analysis highlighted a clear dominance of immune- and epithelium-related signalling pathways (Fig. 7B). The IL-17 signalling pathway was the most strongly enriched, alongside chemokine, TNF, cytokine–cytokine receptor interaction, and NF-κB signalling. Additional enriched pathways included NOD-like receptor signalling, the intestinal immune network for IgA production, and antimicrobial defence pathways. GO enrichment analysis (Fig. 7C) confirmed the activation of innate immune and epithelial defence processes. The top enriched terms included neutrophil chemotaxis, granulocyte migration, antimicrobial humoral response, response to chemokines, and cell killing. Processes reflecting epithelial interaction with immune cells, such as cytokine-mediated signalling and structural responses to inflammation, were also prominent. Together, these results demonstrate that, while ALD-derived organoids retain a stable epithelial and metabolic programme in a quiescent state, IL-17A stimulation activates a broad immune-related transcriptional response characterised by chemokine release, antimicrobial peptide production and epithelial immune signalling.

2.2.3. TRANSCRIPTOMIC ANALYSIS OF IL-17A STIMULATED CHOLANGIOCYTE ORGANOIDS REVEALS SHARED AND DISEASE-SPECIFIC RESPONSES

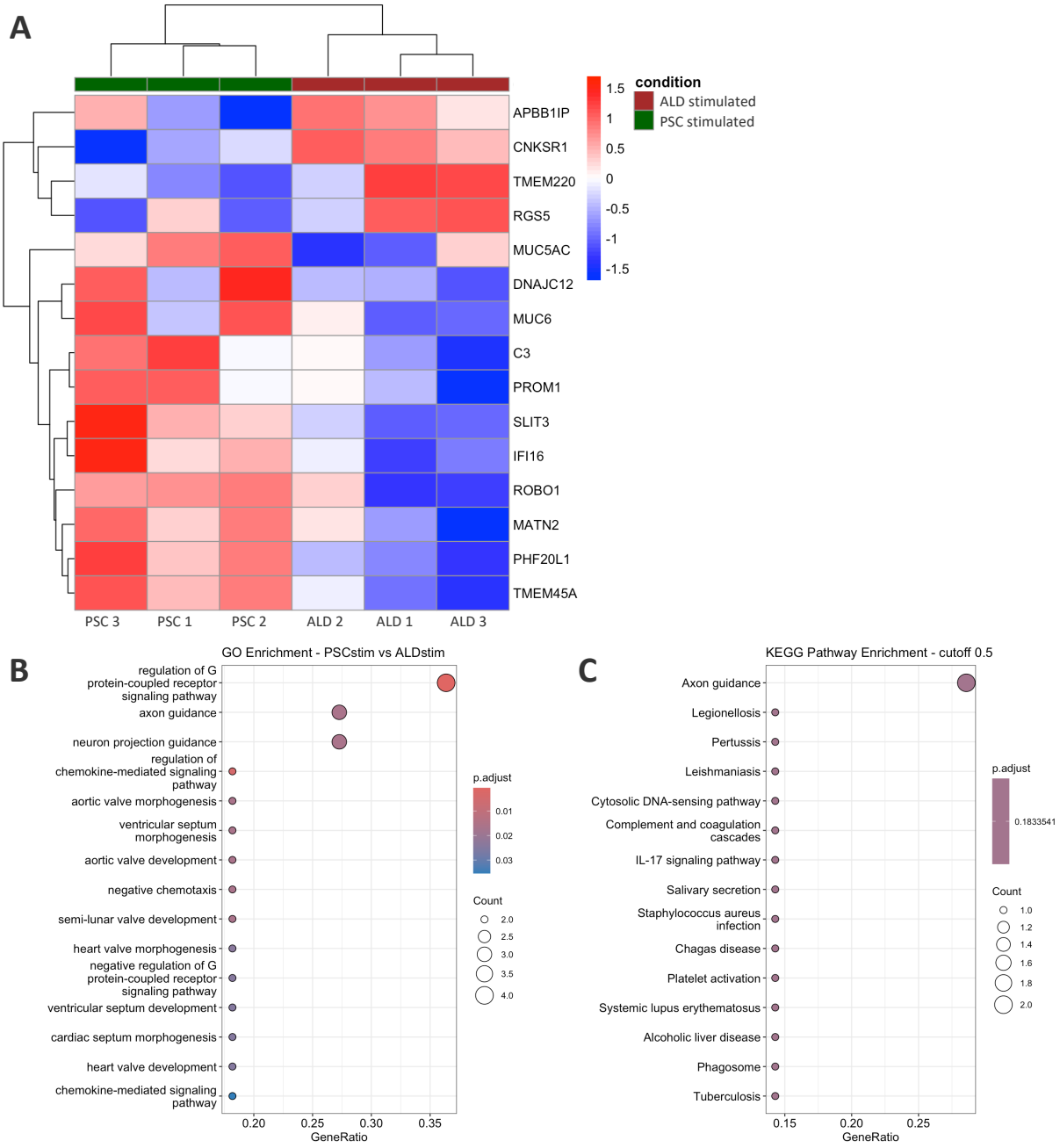

Figure 8. Transcriptomic responses of PSC- and ALD-derived cholangiocyte organoids after IL-17A stimulation.

(A) Heatmap showing the expression of 15 differentially expressed genes (DEGs) between PSC (PSC1–3) and ALD (ALD1–3) -derived cholangiocyte organoids following 24 hours of IL-17A stimulation (50 ng/ml). PSC and ALD samples cluster separately, reflecting subtle but consistent disease-specific transcriptional signatures. (B) Gene Ontology (GO) enrichment analysis of the DEGs highlights processes such as regulation of G protein-coupled receptor signalling, axon guidance, neuron projection guidance, chemokine-mediated signalling, and cardiac valve/septum development, suggesting a role in tissue

remodelling and epithelial–immune interactions. (C) KEGG pathway enrichment analysis shows axon guidance as the top pathway, alongside additional associations with immune and infection-related pathways such as Legionellosis, Pertussis, Leishmaniasis and IL-17 signalling.

The comparison between unstimulated and IL-17A–stimulated organoids revealed 50 DEGs in PSC and 58 in ALD samples. However, when comparing PSC-derived cholangiocyte organoids with ALD-derived ones under IL-17A stimulation, only 15 genes were significantly different. This is likely because IL-17A triggers a largely overlapping transcriptional programme, leading to similar inflammatory responses in both conditions. Among these 15 genes, APBB1IP, CNKSR1, TMEM220, and RGS5 were more highly expressed in IL-17A-stimulated samples derived from people with ALD. In contrast, IL-17A-stimulated PSC-derived cholangiocyte organoids showed higher expression of several genes previously associated with immune activation and epithelial remodelling, including ROBO1, SLIT3, IFI16, MUC6, C3, and TMEM45A. To better understand the biological implications of these transcriptional differences, Gene Ontology (GO) and KEGG pathway enrichment analyses were performed using genes that were upregulated in PSC versus ALD under stimulated conditions. GO enrichment revealed terms linked to axon guidance, regulation of G protein-coupled receptor signalling, and heart valve and septum morphogenesis. These results suggest a transcriptional tendency towards epithelial remodelling and guidance-related pathways in PSC-derived cholangiocyte organoids. Because the number of differentially expressed genes was relatively small, KEGG enrichment analysis was performed using a relaxed adjusted p-value threshold of 0.5. This revealed modest enrichment in axon guidance, IL-17 signalling, and cytosolic DNA sensing pathways, in line with previous observations in PSC-derived epithelial cells (Fig. 8A–C).

3. OPTIMIZING 3D CO-CULTURES FOR CHOLANGIOCYTE ORGANOIDS AND IMMUNE CELL INTERACTIONS

Primary sclerosing cholangitis (PSC) is characterised by the accumulation of immune cells around the bile ducts, where they interact with cholangiocytes and contribute to disease progression. To reproduce these interactions experimentally, we established co-culture systems combining cholangiocyte organoids with $CD4^+$ T cells. This model enabled us to examine how direct cell–cell contact and soluble factors released by immune cells influence cholangiocyte behaviour, and how such interactions may contribute to the immunopathology of PSC. Establishing co-cultures required extensive optimisation. One of the main challenges was the culture medium, which needed to maintain cholangiocyte organoid stability while also supporting $CD4^+$ T-cell activation

and survival. Extracellular matrix components, such as Matrigel, introduced additional complexity. While Matrigel is essential for preserving cholangiocyte organoid polarity and structural organisation, it can also act as a physical barrier that limits direct contact between immune cells and organoids. Maintaining epithelial polarity was particularly important, as its loss compromises barrier function and can alter the nature of interactions with immune cells. Balancing these factors highlighted the technical complexity of the model. In the following section, we describe these challenges in more detail and examine how medium composition, extracellular matrix organisation, cholangiocyte polarity and immune cell contact collectively shape the stability and functionality of 3D co-culture systems.

3.1. DEVELOPING OPTIMAL MEDIA CONDITIONS FOR CO-CULTURE SYSTEMS

T cells were efficiently activated *in vitro* by antibody-based T-cell receptor stimulation (aCD3/aCD28). For their expansion and survival, $CD4^+$ T cells were maintained in RPMI 1640 medium supplemented with 10% fetal bovine serum (FBS). In contrast, cholangiocyte organoids were cultured in expansion medium (EM) based on Advanced DMEM/F12, supplemented with growth factors required for their viability and differentiation, but without FBS, to prevent the outgrowth of non-epithelial cell types such as fibroblasts. To determine the optimal culture conditions for the co-culture system, we compared $CD4^+$ T-cell proliferation and activation in RPMI and in the classical cholangiocyte organoid EM. $CD4^+$ T-cell proliferation was monitored using CellTrace Violet (CTV), a fluorescent dye that is equally distributed between daughter cells during division, resulting in progressive dilution that can be quantified by flow cytometry. Using this approach, we measured the proportion of proliferated versus non-proliferated cells in both media. Stimulation with aCD3/aCD28 induced proliferation in only 29% of $CD4^+$ T cells cultured in cholangiocyte organoid EM, compared with markedly higher proliferation in classical RPMI medium after four days. This demonstrated that EM alone is not sufficient to support robust T-cell activation.

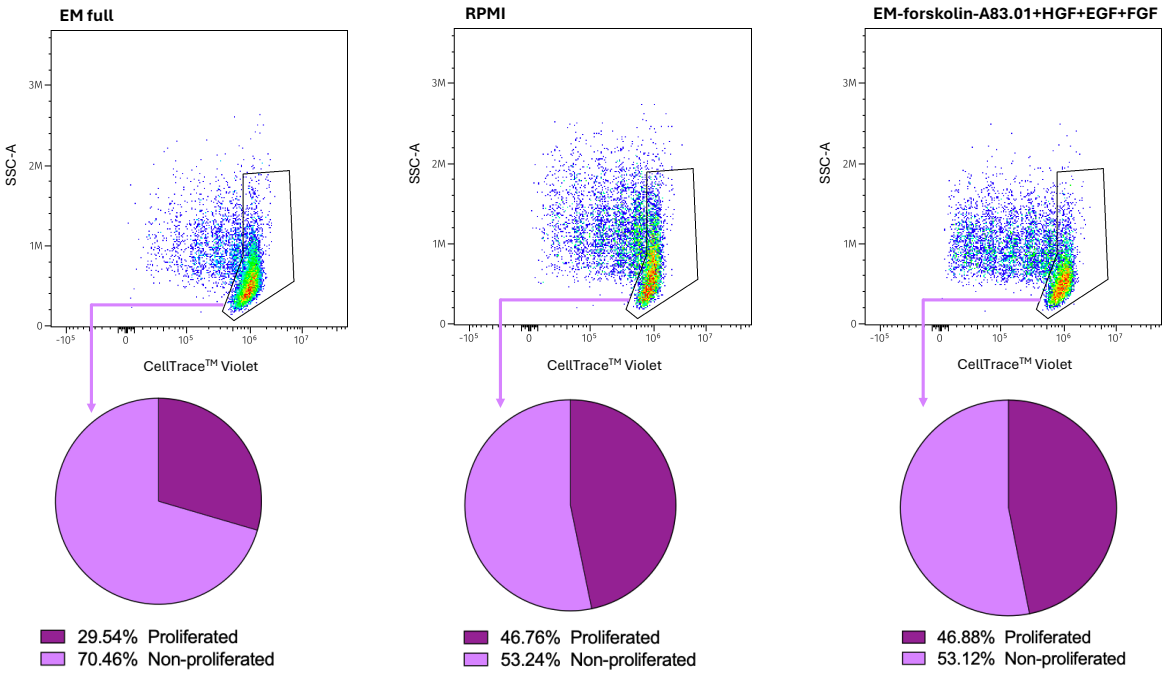

Figure 9. CD4⁺ T cell proliferation in RPMI and expansion medium (EM).
Proliferation levels were measured in response to TCR stimulation. In RPMI 1640 supplemented with FBS, 46.76% of CD4+ T cells divided, whereas in complete EM only 29.54% proliferated. The removal of forskolin and A83.01 from EM resulted in the restoration of proliferation to 46.88%, reaching levels comparable to those observed in RPMI. The results show that specific EM components impair T cell proliferation, thereby underscoring the significance of the medium composition in co-culture experiments involving organoids.

Thus, we observed that the expansion medium (EM) substantially reduced $CD4^+$ T-cell proliferation and activation. This effect was most likely linked to specific components within the EM, particularly A83-01 (a TGF-β receptor I inhibitor) and forskolin, both of which are known to interfere with signalling pathways essential for T-cell function. A83-01 is included to support cholangiocyte organoid growth by blocking inhibitory TGF-β signalling; however, it also alters cytokine production required for efficient T-cell activation. Since TGF-β plays a key role in the differentiation and maintenance of Th17 cells and regulatory T cells, its inhibition may have additional consequences on T-cell phenotype. Forskolin likewise reduced $CD4^+$ T-cell proliferation by modulating the expression of cell-cycle regulatory genes. Notably, this antiproliferative effect occurred without evidence of apoptosis, indicating an interference with proliferative signalling rather than the induction of cell death. For these reasons, we generated a modified culture medium lacking A83-01 and forskolin to assess $CD4^+$ T-cell activation in the co-culture system. Removal of these two components restored $CD4^+$ T-cell proliferation to levels comparable to those observed in classical RPMI medium, confirming that A83-01 and forskolin were responsible for the impaired proliferative capacity seen in the full EM formulation (Fig. 9).

3.1.1. ACTIVATION OF T CELLS IN CO-CULTURE EXPANSION MEDIUM

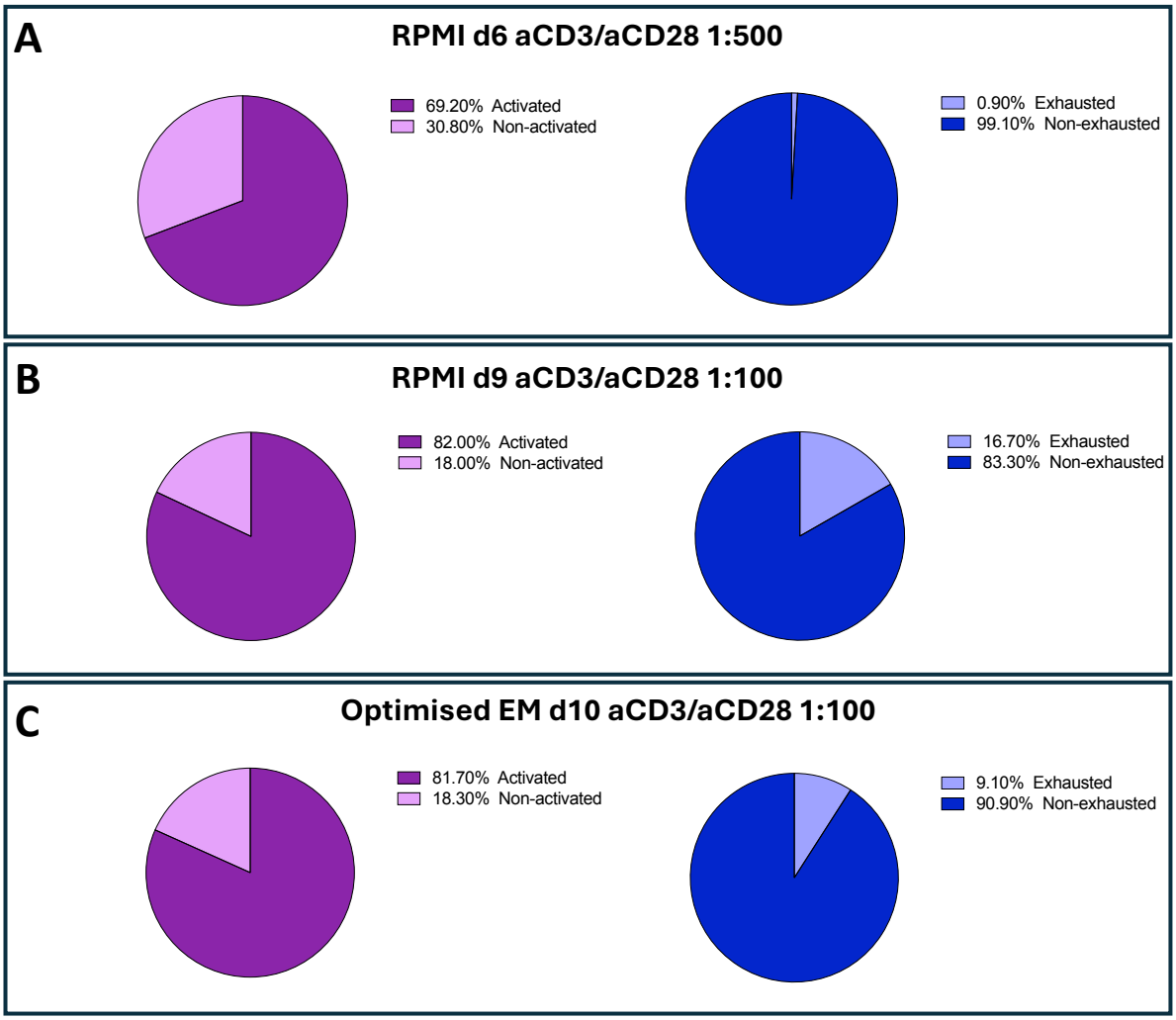

Figure 10. CD4⁺ T cell activation and exhaustion during pre-culture, expansion, and adaptation phases before co-culture setup.
(A) PBMCs after 6 days of pre-culture in RPMI medium with low aCD3/aCD28 stimulation (1:500), showing 69.2% activated (dark purple, CD25⁺) and 0.9% exhausted (light blue, PD-1⁺/LAG-3⁺) cells. (B) CD4⁺ T cells isolated by MACS on Day 6 and further expanded for 3 days in RPMI medium containing higher aCD3/aCD28 stimulation (1:100), resulting in 81.7% activation and 9.1% exhaustion. (C) CD4⁺ T cells after 24 hours in optimized expansion medium (EM) lacking forskolin and TGF-β inhibitor but supplemented with 5% Matrigel and IL-2, maintaining high activation (81.4%) and low exhaustion (5.8%).

Before establishing the optimal co-culture system, we tested different conditions to determine the CD4⁺ T-cell response in terms of activation and exhaustion. Activation was assessed by flow cytometry using CD25 expression, while LAG-3 and PD-1 served as inhibitory markers. PBMCs were thawed on day 1 and expanded for six days in a pre-culture phase in RPMI medium containing a low concentration of aCD3/aCD28 (1:500). This step allowed the cells to increase in number without inducing premature exhaustion. On day 6, CD4⁺ T cells were isolated by magnetic cell separation (MACS). At

this stage, most of the cells (69.2%) were activated, while only a small fraction (0.9%) expressed exhaustion markers. The cells were then transferred to fresh RPMI medium with a higher aCD3/aCD28 concentration (1:100) in order to maintain activation while further expanding the $CD4^+$ T-cell population. As the number of $CD4^+$ T cells obtained from patient-derived PBMCs was limited, this expansion step was necessary. After three days under these conditions (day 9), activation increased to 81.7%, while exhaustion remained relatively low (9.1%). To mirror the conditions of the co-culture environment, the cells were subsequently cultured for 24 hours in an adapted EM formulation lacking forskolin and the TGF-β inhibitor, supplemented with 5% Matrigel and IL-2. On day 10, following this period in optimised EM, activation remained high (81.4%) and exhaustion low (5.8%). This workflow therefore ensured both a sufficient number and an appropriate activation state of $CD4^+$ T cells for co-culture experiments (Fig. 10).

Of note, we also tested alternative conditions, including a 1:40 dilution of aCD3/aCD28 and variations in the duration of the activation period. However, these approaches either increased exhaustion or resulted in less efficient activation. The 1:100 dilution, followed by a 24-hour period in optimised EM, was ultimately selected as the optimal balance to maintain activation, minimise exhaustion, and ensure compatibility of $CD4^+$ T cells with cholangiocyte organoids within the co-culture system.

3.2. STABILITY OF FLOATING ORGANOIDS WITH REDUCED MATRIX SUPPORT

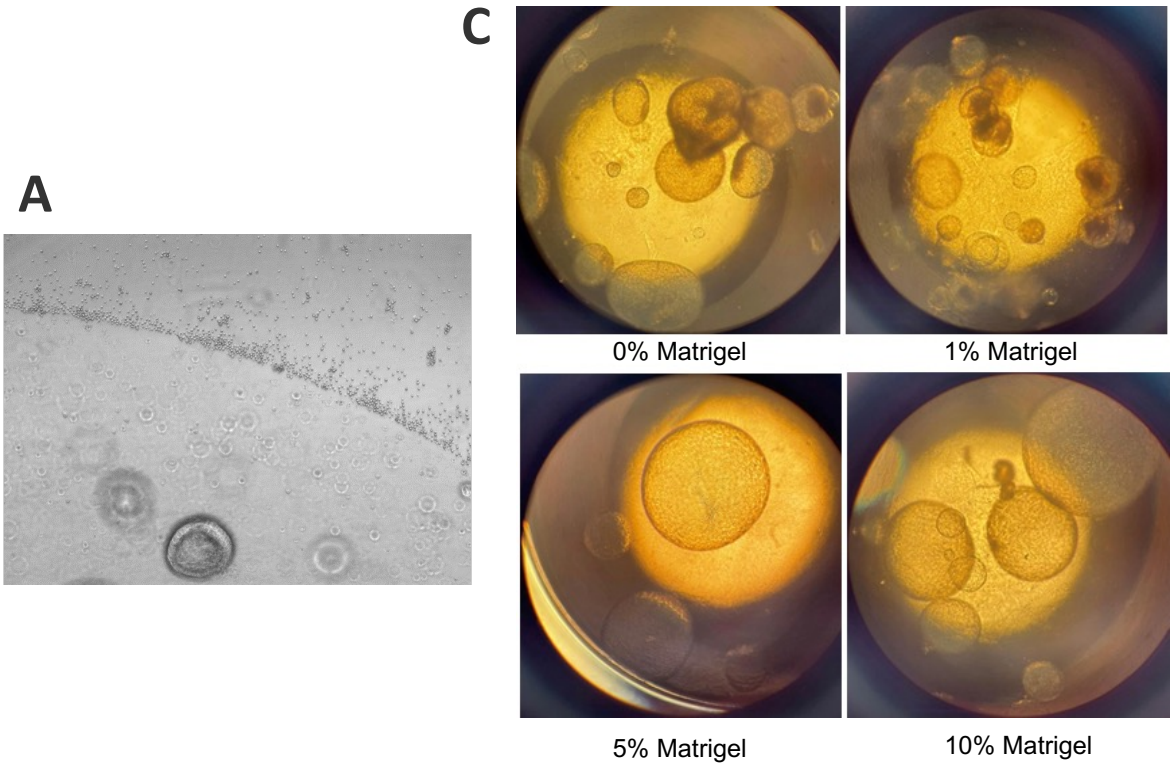

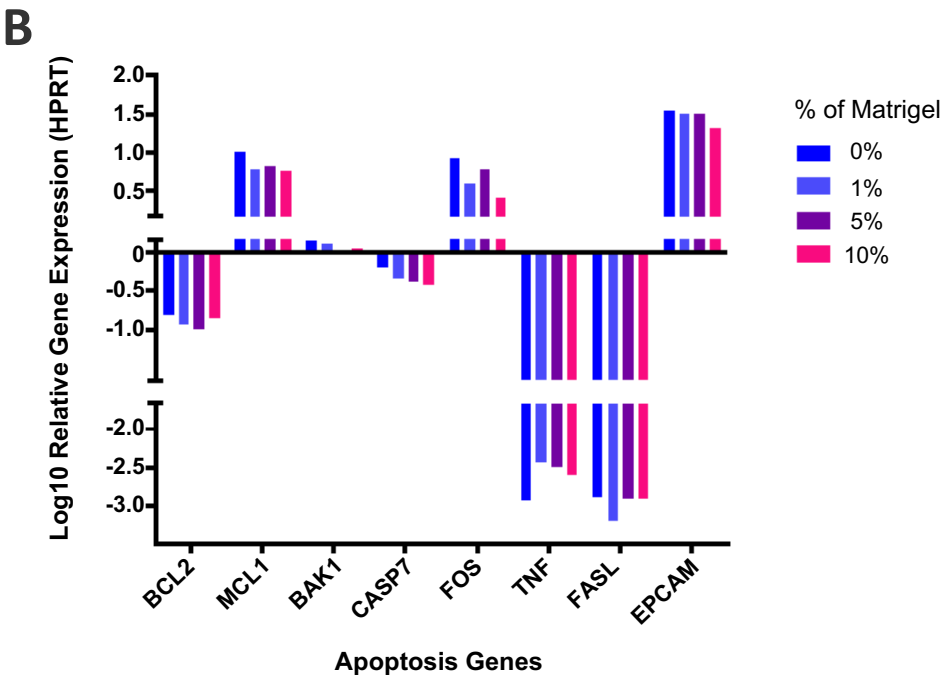

Figure 11. Matrigel matrix concentration influences cholangiocyte organoid morphology, survival, and interaction with T cells.
(A) Cholangiocyte organoids embedded in a Matrigel dome and surrounded by peripheral T cells. The lymphocytes remain viable at the periphery without penetrating the gel, illustrating the barrier properties of Matrigel in modulating organoid–immune cell interactions. (B) Relative expression of apoptosis-associated genes in cholangiocyte organoids cultured in suspension with different Matrigel concentrations (0%, 1%, 5%, 10%) for five days. Overall expression levels changed little across conditions; MCL1 remained stably expressed and may support cell survival, while TNF and FASL were consistently reduced. EPCAM expression was preserved in all groups. (C) Morphology of cholangiocyte organoids grown with increasing Matrigel concentrations. At 0% and 1%, organoids were smaller and darker, indicative of stress and loss of polarity, whereas at 5% and 10% they appeared larger, lighter, and more uniform in structure Since 10% Matrigel limited immune cell access, 5% was chosen as the optimal condition for co-culture experiments.

In 3D culture systems, the Matrigel matrix is essential because its removal affects organoid survival, architecture and function. In our co-culture system, cholangiocyte organoids embedded in Matrigel developed tissue-like morphologies, while the absence of extracellular matrix (ECM) frequently resulted in polarity reversal and an “apical-out” orientation, a condition associated with reduced proliferation and increased cell death. The Matrigel matrix also limited immune–epithelial interactions, as $CD4^+$ T cells remained positioned at the periphery of the domes rather than penetrating the matrix (Fig. 11A). To overcome this limitation, we established a floating culture condition in which cholangiocyte organoids were maintained in suspension with only a minimal amount of Matrigel. In this configuration, organoids were no longer fully embedded in a dense matrix but floated freely in the medium, which provided sufficient structural support while increasing accessibility to T cells. Different Matrigel concentrations between 1% and 10% were tested to identify the optimal balance: higher concentrations restricted T-cell movement, whereas very low concentrations compromised polarity and survival. Stress responses associated with reduced Matrigel were assessed after five days in floating culture by measuring pro- and anti-apoptotic gene expression (Fig. 11B). Organoids were grown in classical EM supplemented with 0%, 1%, 5% or 10% Matrigel. Gene expression profiles were largely comparable across conditions, with only subtle differences. FOS and CASP7 displayed minor reductions in the absence of Matrigel, while MCL1 remained stable and EPCAM expression was preserved at all concentrations tested. In this context, MCL1 rather than BCL2 supported cell survival, consistent with previous evidence that cholangiocytes rely predominantly on MCL1[146]. TNF and FASL remained suppressed across all conditions, showing no clear dependency on Matrigel concentration, suggesting that apoptotic signalling through these pathways is limited and not strongly influenced by ECM availability. Microscopy further supported these findings. Organoids grown with 0% or 1% Matrigel appeared smaller and darker, indicative of cellular stress and potential polarity disruption due to insufficient ECM support. Although 1% provided a slight improvement compared with complete absence,

it remained inadequate to maintain structural integrity. By contrast, organoids cultured with 5% or 10% Matrigel were larger, brighter and more uniform, consistent with reduced stress and preserved polarity. Since higher Matrigel content can hinder immune cell access, 5% was selected as the optimal condition for co-culture (Fig. 11C).

3.2.1. STABILITY OF CHOLANGIOCYTE ORGANOIDS IN OPTIMIZED COCULTURE EXPANSION MEDIUM

Cholangiocyte organoid stability in the optimised co-culture medium was assessed by maintaining cholangiocyte organoids in floating culture for 24, 48, and 72 hours in either standard expansion medium or co-culture medium supplemented with 5% Matrigel matrix (Fig. 12).

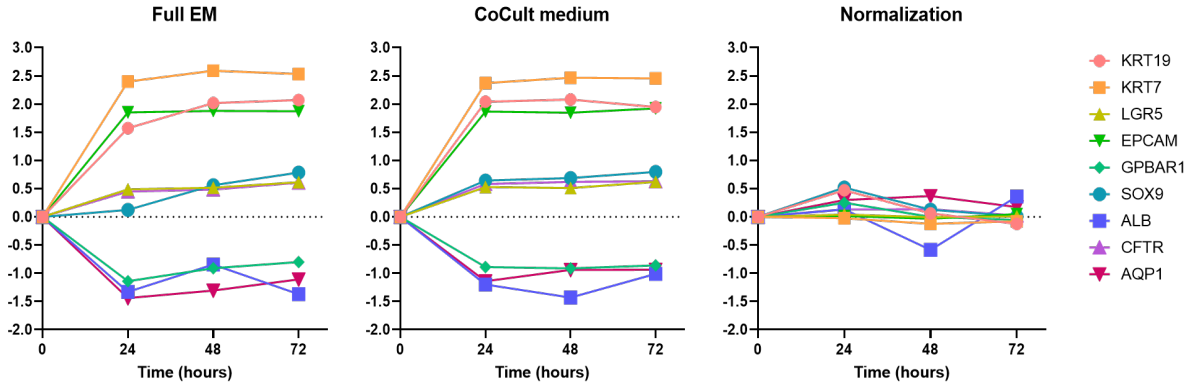

Figure 12. Analysis of cholangiocyte organoid stability and gene expression across three time points (24, 48, and 72 hours) in standard expansion medium and co-culture medium supplemented with 5% Matrigel matrix.
Normalized expression data demonstrate consistent profiles for key markers, including cholangiocyte differentiation (KRT19, KRT7), stem-like properties (LGR5), epithelial identity (EPCAM), and functional signalling (GPBAR1, SOX9). Graph A highlights overall marker expression stability in standard medium, while graphs B and C illustrate similar trends in the improved medium, confirming that the co-culture medium does not significantly alter the organoid transcriptional dynamics or stability over time.

We observed that KRT19 and KRT7 were consistently expressed at high levels in all conditions, confirming that the organoids preserved their cholangiocyte identity. Epithelial features were also maintained, as shown by stable expression of LGR5 and EPCAM. GPBAR1, linked to bile acid signalling, and SOX9, a progenitor marker typically expressed in the biliary tract, were detected at moderate levels, while ALB remained low,

in line with the absence of hepatocyte differentiation. CFTR and AQP1, associated with fluid transport and cholangiocytes functionality, showed low but steady expression. Expression profiles over time were comparable in the two media, with only minor differences, indicating that the adapted co-culture medium preserved stability without altering the main transcriptional features of the organoids.

4. UNDERSTANDING THE CROSSTALK BETWEEN RESTING CHOLANGIOCYTE ORGANOIDS AND ACTIVATED CD4+ T CELLS

Because cholangiocytes in people with disease are surrounded by reactive immune cells during inflammation, we developed a co-culture system to reproduce this *in vivo* context. This allowed us to investigate whether resting cholangiocyte organoids exhibit immunomodulatory properties at baseline and how these properties change in the presence of activated $CD4^+$ T cells. We were particularly interested in determining whether these effects depend on direct cell–cell contact, soluble mediators, or a combination of both. To address this, cholangiocyte organoids were either exposed to the supernatant of pre-activated $CD4^+$ T cells or cultured directly together to allow cell–cell contact. This approach helped us distinguish between the effects of soluble cytokines and direct cell–cell contact in shaping epithelial–immune interactions. In this way, the use of TCR-activated $CD4^+$ T cells to recreate an inflammatory environment enabled us to evaluate the potential immunomodulatory role of resting cholangiocyte organoids.

4.1. EFFECT OF $CD4^+$ T CELL–DERIVED SOLUBLE FACTORS ON CHOLANGIOCYTE ORGANOIDS

To test the role of soluble factors, $CD4^+$ T cells were stimulated via the T cell receptor for 24 hours in the co-culture optimised medium. The supernatant was collected and transferred onto cholangiocyte organoids maintained under floating conditions for another 24 hours, recreating an inflammatory milieu without direct contact. Organoids were analysed by flow cytometry and qPCR (Fig. 13).

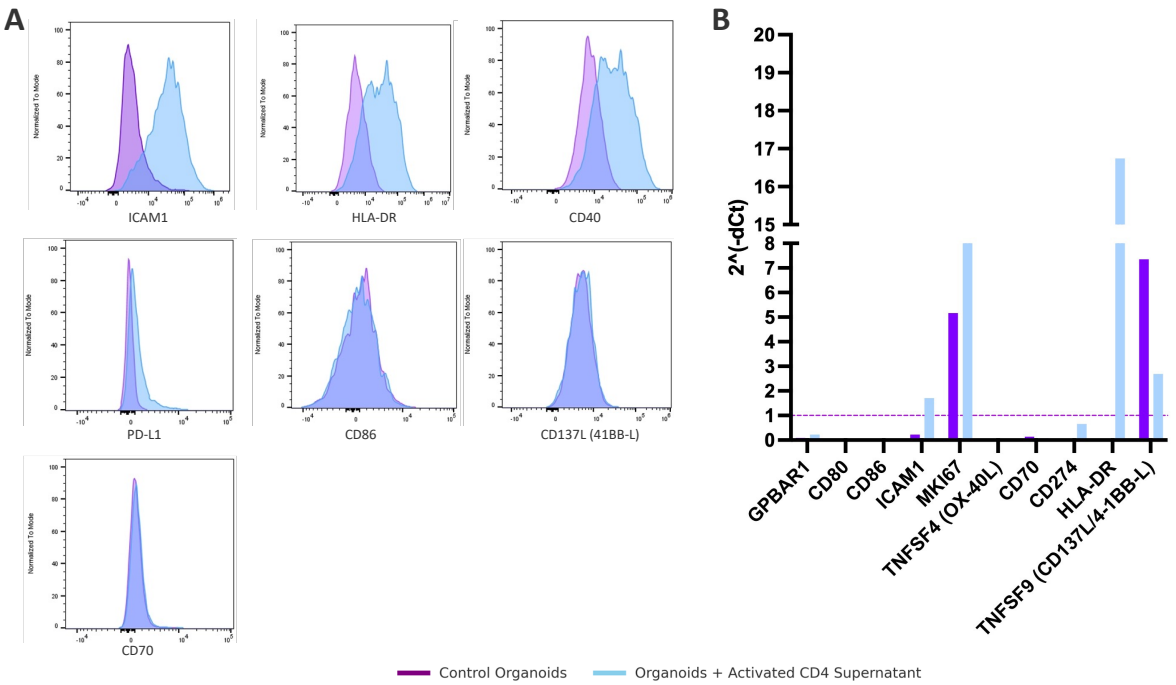

Figure 13. Immune marker expression in cholangiocyte organoids with or without CD4⁺ T cell supernatant.
(A) Flow cytometry plots of cholangiocyte organoids maintained in control medium (purple) or exposed to supernatant from activated CD4⁺ T cells (blue). ICAM1 and HLA-DR show a clear increase in the treated group, consistent with an inflammatory response. (B) Relative gene expression (2^−ΔCt) of immune-related markers in cholangiocyte organoids under the same conditions. Control samples are shown in purple, and cholangiocyte organoids exposed to CD4⁺ T cells derived supernatant are shown in grey. Consistent with the FACS data, ICAM1 and HLA-DR transcripts were strongly upregulated, supporting the notion that soluble mediators from activated CD4⁺ T cells promote pro-inflammatory activation of cholangiocyte organoids.

After exposure to T cell supernatant, cholangiocyte organoids showed higher expression of ICAM1, HLA-DR and CD40 at a protein level compared to non-stimulated organoids, as showed by FACS data. CD70 stayed unchanged as CD137L but the checkpoint molecule PD-L1 increased slightly instead. Gene expression analysis confirmed the induction of the mRNA of ICAM1 and HLA-DR. This is consistent with the flow cytometry data and hints that soluble mediators released by CD4⁺ T cells can trigger a pro-inflammatory switch in cholangiocyte organoids.

4.2. CO-CULTURE OF ORGANOIDS WITH CD4$^+$ T CELLS: COMPARING HLA-MATCHED AND MISMATCHED SETTINGS

Following the assessment of cytokine-mediated effects using supernatants from pre-activated CD4$^+$ T cells, we next explored the impact of direct cell–cell contact on cholangiocyte–T cell interactions. To this end, co-cultures of cholangiocyte organoids with pre-activated CD4$^+$ T cells were established under two conditions: HLA-matched and HLA-mismatched. In the HLA-matched setting, cholangiocyte organoids were co-cultured with autologous CD4$^+$ T cells, providing a patient-specific model to study immune responses. In the HLA-mismatched setting, cholangiocyte organoids were co-cultured with CD4$^+$ T cells from healthy donors, mimicking an alloimmune response similar to that observed in PSC. This approach was applied to both PSC- and ALD-derived cholangiocyte organoids co-cultures, enabling a direct comparison of immune dynamics in the two disease models and revealing differences in tolerance and immune activation. To prevent contamination from residual T cells during analysis, a double-gating strategy was used: after exclusion of dead cells, only EpCAM$^+$ epithelial cells derived from organoids were included. Histograms were normalised in FlowJo using mode normalisation, allowing direct comparison of fluorescence distributions across conditions.

4.2.1. CO-CULTURE SETUP: HLA-MISMATCHED AND SEX-MATCHED

For these experiments, cholangiocyte organoids derived from liver transplant patients were combined with CD4$^+$ T cells from sex-matched healthy donors. The patient cohort is listed in the table below:

Pseudonym	Age	Sex	Disease	Histopathology
ALD-04	63	female	ALD	Cirrhosis with mild steatosis, portal inflammation, local cholestasis, mild sinusoidal dilatation, chronic cholecystitis with bleeding.
ALD-06	55	male	ALD	Cirrhosis with severe hepatocellular iron accumulation, chronic cholestasis, benign bile duct cyst, and chronic cholecystitis; no tumour or dysplasia

PSC-04	33	female	PSC	Chronic sclerosing cholangitis with loss of bile ducts, fibroobliterative lesions, bile casts, ulcerative and purulent cholangitis, cholestasis, cirrhotic remodelling, and low-grade steatosis (5%).

Cholangiocyte organoids were generated from explanted liver tissue. After isolating the bile duct progenitor cells, cultures were established and expanded to obtain patient-specific organoid lines. Co-cultures were performed with cholangiocyte organoids at passages 4–5, when growth was stable. The results presented in this set-up are indicative of the findings from 3 co-culture experiments, as consistent trends were observed across all patients and disease conditions.

4.2.1.1. $CD4^+$ T CELL RESPONSES TO CO-CULTURE WITH CHOLANGIOCYTE ORGANOIDS

To assess the effect of direct epithelial contact on T cell activation, we analysed $CD4^+$ T cell surface marker expression after 24 hours of co-culture. $CD4^+$ T cells from healthy donors, pre-stimulated with aCD3/aCD28, were either cultured alone (control) or co-cultured with cholangiocyte organoids derived from people with ALD or PSC. Flow cytometry revealed distinct alterations in activation marker expression when compared with the control condition, indicating that interaction with cholangiocyte organoids affects the activation profile of $CD4^+$ T cells (Fig. 14).

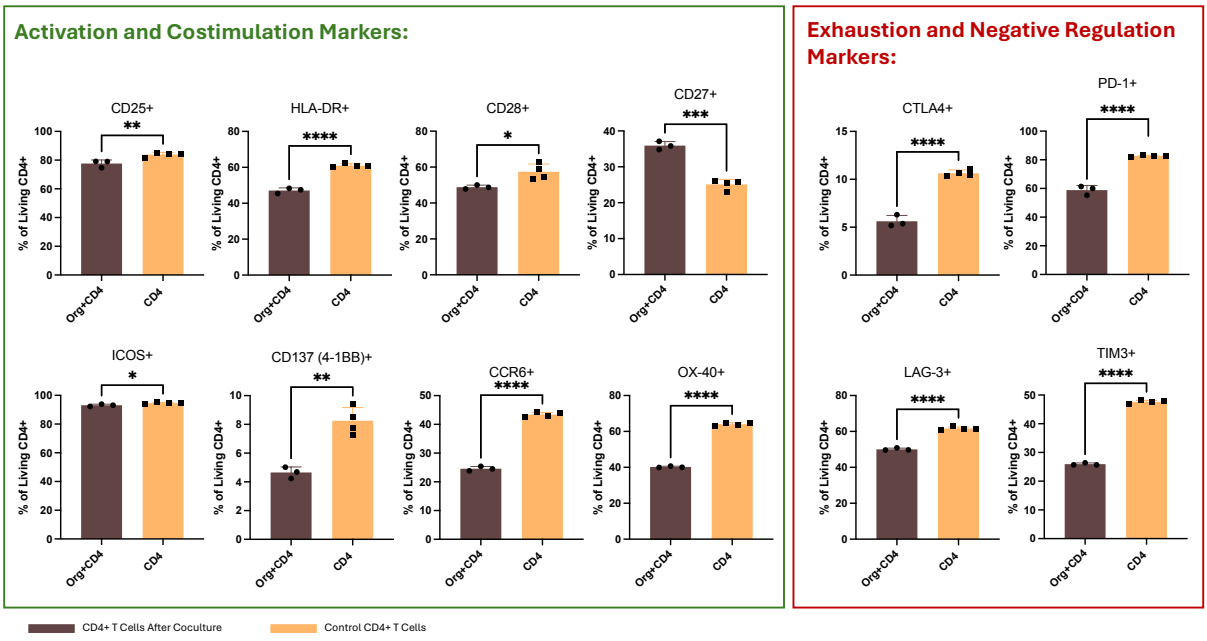

Figure 14. Impact of co-culture with cholangiocyte organoids on pre-activated CD4+ T cell marker expression.

The figure compares the expression levels of activation and costimulation markers (green box) and exhaustion/negative regulation markers (red box) in pre-activated CD4+ T cells (TCR-stimulated) after 24 hours of co-culture with cholangiocyte organoids (dark brown bars) versus CD4+ T cells cultured alone as controls (orange bars). $CD4^+$ T cells cultured together with cholangiocyte organoids (Org+CD4) showed an overall decrease in activation markers such as CD25, OX40, and CD137, as well as in regulatory or exhaustion markers including CTLA-4, PD-1, LAG-3, and TIM-3, when compared with controls. The co-culture thus reduced $CD4^+$ T cell activation and appeared to limit the risk of excessive immune activation.

In both co-culture settings, with ALD- or PSC-derived cholangiocyte organoids, $CD4^+$ T cells consistently showed reduced expression of activation and co-stimulatory markers, such as CD25, OX40, HLA-DR, ICOS, CD28, 4-1BB (CD137), and CCR6, suggesting that interaction with cholangiocyte organoids dampens T-cell activation irrespective of disease origin. CD27 expression was increased in co-cultured T cells. Although CD27 upregulation is often associated with memory differentiation, in this context it more likely reflects an early activation state while supporting short-term cell survival. At the same time, the co-cultured T cells showed decreased expression of checkpoint molecules, including CTLA-4, LAG-3 and TIM-3, with the most marked reduction observed for PD-1. These findings suggest that co-culture dampens T-cell activation without promoting exhaustion, leading to an intermediate state where $CD4^+$ T cells remain less activated but not inhibited.

4.2.1.2. IMMUNOLOGICAL MARKER EXPRESSION IN CHOLANGIOCYTE ORGANOIDS AFTER CO-CULTURE WITH CD4⁺ T CELLS

Co-culture with pre-activated CD4⁺ T cells for 24 hours induced clear changes in cholangiocyte organoids as shown by flow cytometry (Fig. 15).

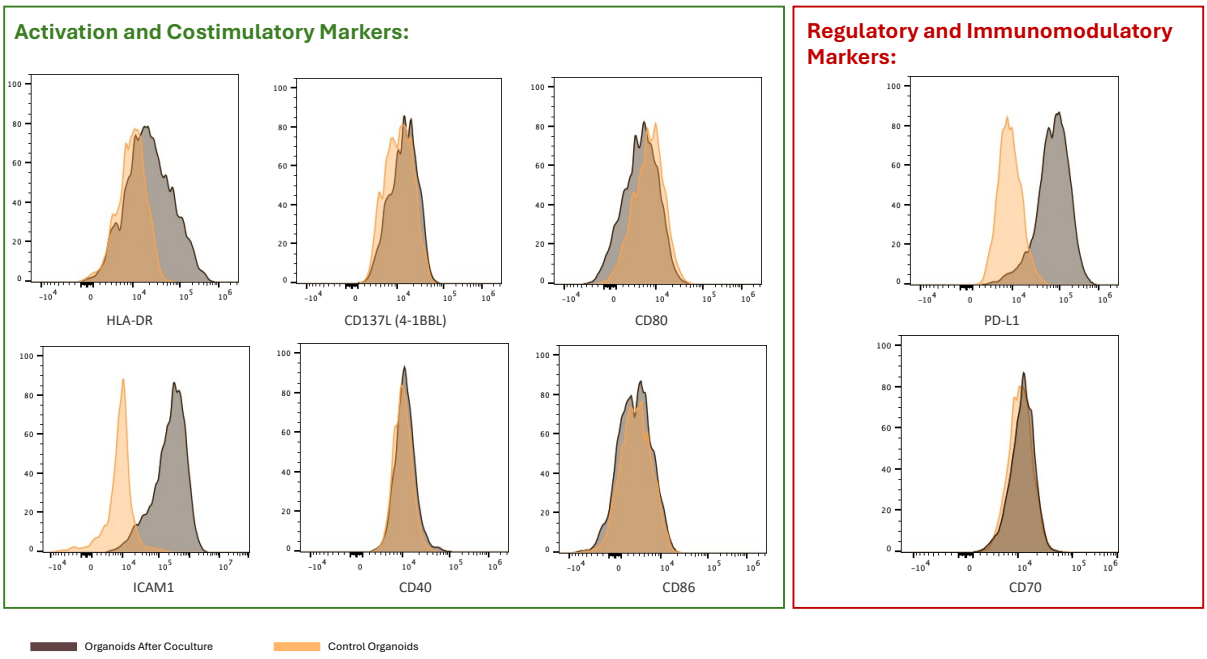

Figure 15. Expression of immunological markers on cholangiocyte organoids after 24 hours of co-culture with pre-activated CD4+ T cells.
Flow cytometry showed higher levels of HLA-DR (antigen presentation), PD-L1 (immune checkpoint), and ICAM-1 (cell adhesion) in organoids after co-culture compared with controls. In contrast, CD40, CD80, CD86, and CD70 did not show clear differences. These results suggest that cholangiocyte organoids react to activated CD4⁺ T cells by activating specific immune pathways and can be used as a model to study immune–epithelial interactions in cholangiopathies.

A marked increase in HLA-DR expression was observed, indicating an enhanced potential for antigen presentation. This effect was consistent across biological replicates and suggests that cholangiocyte organoids actively respond to the presence of activated CD4⁺ T cells by engaging immune-related pathways. PD-L1 expression was also increased, pointing to a feedback mechanism that prevents overactivation of T cells. In addition, ICAM-1 was increased, consistent with an enhanced potential of cholangiocyte organoids to engage in adhesive interactions with immune cells. In contrast, CD40, CD80, CD86 and CD70 showed minimal or no differences between co-cultured and control cholangiocyte organoids. This pattern was reproducible across three independent experiments, confirming both the stability of the co-culture system and the

ability of cholangiocyte organoids to mount a specific and coordinated response to activated CD4⁺ T cells.

4.2.1.3. GENE EXPRESSION ANALYSIS OF CHOLANGIOCYTE ORGANOIDS AFTER CO-CULTURE WITH CD4⁺ T CELLS

Gene expression analysis of cholangiocyte organoids after 24 hours of co-culture with pre-activated CD4⁺ T cells also revealed reproducible transcriptional changes across experiments. Following careful separation of cholangiocyte organoids from CD4⁺ T cells, gene expression was compared with organoids cultured alone, using HPRT as reference. Overall, these data show that cholangiocyte organoids mount a robust response to direct interaction with immune cells, characterised by a clear upregulation of several immune-related genes (Fig. 16)

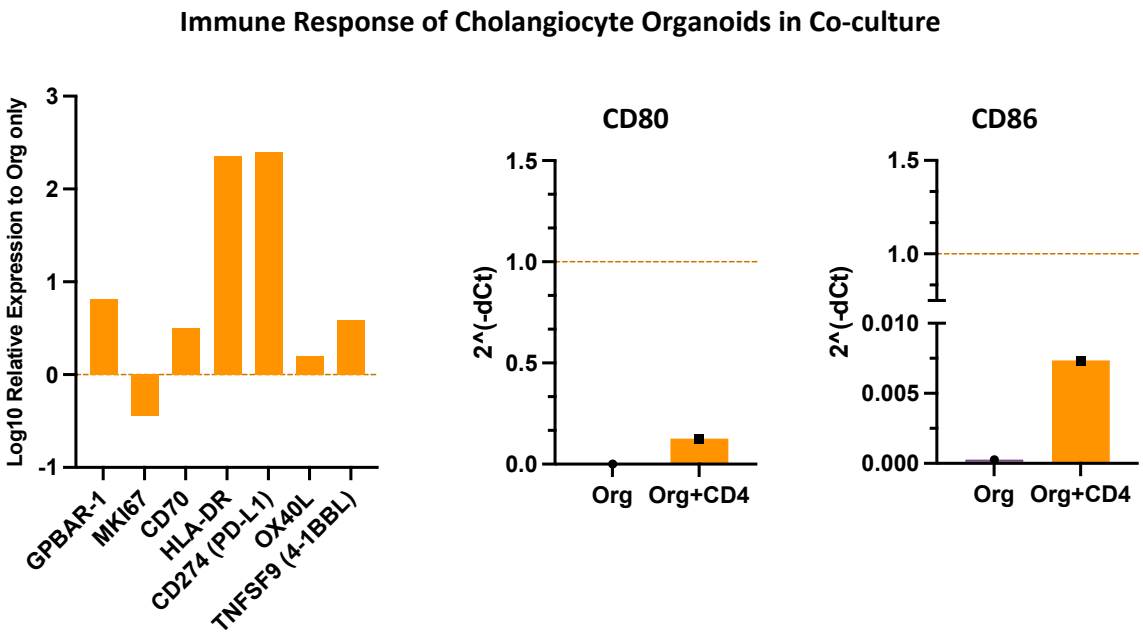

Figure 16. qPCR analysis of immune-related gene expression in cholangiocyte organoids after 24 hours of co-culture with pre-activated CD4+ T cells.
Gene expression in cholangiocyte organoids after 24 hours of co-culture with pre-activated CD4⁺ T cells. Expression was compared with organoids cultured alone, using HPRT as reference. HLA-DR and PD-L1 (CD274). CD80 and CD86 were not detected in resting organoids but showed low expression after co-culture. OX40L and 4-1BBL were detected and increased in co-cultured organoids.

HLA-DR expression was consistently increased in co-cultured cholangiocyte organoids, confirming the flow cytometry results. PD-L1 (CD274) was also upregulated compared with controls, supporting a role in restraining T-cell activity. Only small increases were

observed for CD80 and CD86. The co-stimulatory ligands OX40L and 4-1BBL also showed elevated expression, although not uniformly across all samples. Together, these findings show that cholangiocyte organoids can modulate $CD4^+$ T-cell activation. However, the specific outcome depends on the activation level and functional state of the T cells.

4.3. CO-CULTURE WITH HLA- AND SEX-MATCHED SAMPLES

In addition to experiments conducted under HLA-mismatched but sex-matched conditions, further co-cultures were performed using samples matched for both HLA and sex. This approach minimised potential allogeneic immune responses and reduced bias arising from HLA incompatibility or sex-related differences, thereby allowing a clearer evaluation of immune–epithelial interactions. Cholangiocyte organoids and $CD4^+$ T cells were isolated from liver tissue of individuals with PSC or ALD, and cultured between passages 4 and 5 prior to co-culture. The patient cohort included:

Pseudonym	Age	Sex	Disease	Histopathology
ALD-05	60	male	ALD	Cirrhosis with low-to-mid grade chronic periportal inflammation, low-grade hepatocellular siderosis, low-grade cholestasis, and chronic cholecystitis
ALD-06	55	male	ALD	Cirrhosis with severe hepatocellular iron accumulation, chronic cholestasis, benign bile duct cyst, and chronic cholecystitis; no tumour or dysplasia
ALD-07	61	male	ALD	Micronodular cirrhosis with cholestasis, hepatocellular α1-antitrypsin inclusions, siderosis, and chronic cholangitis with early cholangiopathic remodelling

PSC-05	45	female	PSC	Chronic sclerosing cholangitis with loss of intraseptal and interlobar bile ducts, fibro-obliterative lesions, biliary cirrhosis, and chronic cholecystitis.

In this case, $CD4^+$ T cells were obtained from PBMCs of the same patients, so that they matched the cholangiocyte organoids. The cells were pre-activated and then expanded, mainly to make sure we had enough and that they were ready for co-culture. The data shown here come from four separate co-cultures with consistent patterns across all the experiments.

4.3.1. RESULTS OF THE HLA MATCHED AND SEX MATCHED CO-CULTURE

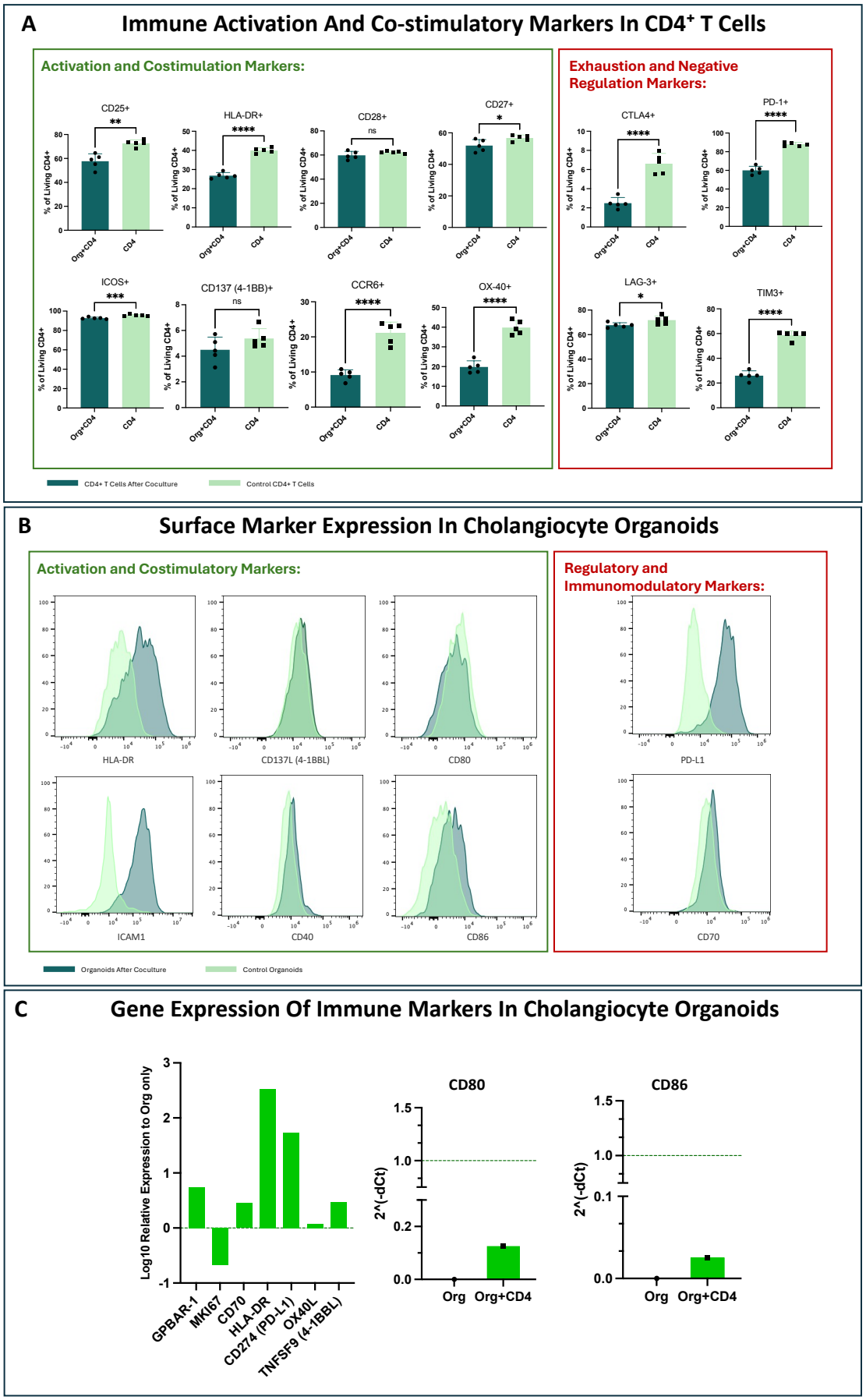

Figure 17. Analysis of immune marker expression in cholangiocyte organoids and CD4+ T cells after 24 hours of co-culture under HLA-matched and sex-matched conditions.
(A) Expression of activation and co-stimulation markers (e.g., CD25, OX40) and regulatory markers (e.g., PD-1, CTLA-4) on CD4+ T cells. The HLA-matched setup revealed a consistent balance between activation and regulation, emphasizing the compatibility of the co-culture system. (B) Upregulation of activation (e.g., CD40, CD80) and regulatory (e.g., PD-L1) markers on cholangiocyte organoids. Histogram overlays show normalized fluorescence intensity and confirm that marker levels changed in a similar way under HLA-matched conditions. (C) Gene expression analysis of cholangiocyte organoids revealed higher transcription of HLA-DR, ICAM-1, and CD274 (PD-L1), indicating that cholangiocyte organoids take an active part in immune modulation during HLA-matched co-culture.

Under HLA- and sex-matched conditions, the outcome was comparable to the mismatched set-up. In both cases, cholangiocyte organoids upregulated HLA-DR, PD-L1, CD40 and ICAM-1. Correspondingly, $CD4^+$ T cells showed increased expression of CD25, OX40, CTLA-4 and PD-1. The similarity between the two conditions indicates that the observed responses primarily arise from the intrinsic properties of cholangiocyte organoids and T cells, rather than from HLA compatibility. Overall, the co-culture model revealed a dynamic interplay in which cholangiocyte organoids stimulated immune activation yet maintained regulatory properties, and $CD4^+$ T cells reflected both activation and inhibition (Fig. 17).

DISCUSSION

1. CHOLANGIOCYTE ORGANOIDS REVEAL IMPAIRED REGENERATIVE CAPACITY IN PSC

Primary sclerosing cholangitis (PSC) is a chronic, immune-mediated cholangiopathy characterised by progressive inflammation and fibrosis of the bile ducts. The pathogenesis of PSC remains not fully understood, leaving medical treatment largely ineffective and highlighting the need for further research. In people with PSC, accumulation of immune cells around bile ducts is commonly observed, yet the nature of the interaction between cholangiocytes and infiltrating lymphocytes is still unclear. We hypothesised that cholangiocytes are not merely passive targets of immune-mediated damage, but active participants in shaping the local immune microenvironment. In particular, we focused on the crosstalk between cholangiocytes and $CD4^+$ T cells, which play a central role in mucosal and autoimmune responses. o explore this, we used cholangiocyte organoids derived from people with PSC and ALD, which reproduce key features of the human biliary epithelium, and first assessed their growth efficiency and gene expression profiles. While most ALD samples (81.2%) successfully formed cholangiocyte organoids, only about a third (34.6%) of PSC-derived cells were able to generate organoids. This difference suggests a fundamental disease-specific feature in progenitor cell behaviour. In people with ALD, hepatocytes are the primary target of injury while cholangiocytes remain relatively preserved[147]. By contrast, PSC is characterised by chronic inflammation, progressive fibrosis of the bile ducts, and bacterial colonisation, which may impair the survival and expansion of cholangiocytes even *in vitro*[64]. Understanding how disease-specific microenvironments influence epithelial regeneration is therefore a relevant area of investigation. Notably, human bile ducts can already be regenerated *in vivo* by transplanting cholangiocyte organoid–derived cells to repopulate injured tissue[121]; this regenerative capacity highlights the relevance of this system for studying how intrinsic and environmental cues influence progenitor behaviour. Finally, these findings suggest the need to adjust organoid culture conditions, such as oxidative stress or bile acid composition, when culturing cells derived from people with PSC *in vitro*.

2. BASELINE GENE EXPRESSION OF PSC AND ALD ORGANOIDS REVEAL BOTH SHARED AND DISEASE-SPECIFIC SIGNATURES

Although PSC samples showed lower efficiency in generating cholangiocyte organoids, the organoids that did grow had baseline gene expression patterns similar to those from ALD. Genes linked to epithelial identity, biliary function and some immune interactions were expressed at similar levels, indicating a notable degree of resemblance between the two conditions. A plausible explanation is that the culture system favours the survival of the most viable cholangiocyte progenitors, so that PSC-derived organoids arise from only a small fraction of the total cells isolated from the tissue. Consequently, PSC organoids become enriched in relatively "healthy" cells that do not fully reflect the complexity of disease-associated alterations present in vivo. Moreover, organoid culture media, being rich in mitogens and optimised for proliferation, can profoundly reshape cellular identity through epigenetic remodelling. As a result, cholangiocyte organoids *in vitro* tend to acquire a more uniform phenotype across samples regardless of their disease background, as the "resetting" effect of culture conditions overrides transcriptional programmes specific to each disease. For example, when adult cholangiocytes are cultured as organoids, their gene expression does not completely match the original tissue, even at early passages. These variations are not spontaneous, but rather a direct consequence of *in vitro* culture conditions[148]. A similar phenomenon occurs in hepatic organoids, which are also maintained in media rich in growth factors (EGF, R-spondin, Noggin, etc.) required to sustain viability and proliferation. Such factors not only support growth but also influence the transcriptional profile and metabolic state of hepatocytes[149]. Likewise, prolonged culture of human intestinal organoids leads to extensive changes in DNA methylation patterns, in turn masking tissue-specific epigenetic signatures[150]. In line with this, Soroka and colleagues demonstrated that bile-derived cholangiocyte organoids from people with PSC retain key immunological features of their tissue of origin, such as elevated MHC II and interferon-stimulated gene expression, yet these signatures can be modulated over time *in vitro*, suggesting that inflammatory imprinting is partially preserved but remodelled by culture conditions[151]. An unintended consequence of this cellular plasticity is that the resulting cultures become more "standardised" in phenotype, losing certain disease-specific characteristics while gaining stability in culture. To overcome this limitation, future protocols that maintain cells in conditions closer to physiological environments may help preserve tissue-specific memory in primary cholangiocytes and and enhance the physiological relevance of the model. We observed similar gene expression profiles in both PSC- and ALD-derived cholangiocyte organoid at baseline resting conditions. However, this observation does not necessarily imply functional equivalence, as a subset of differentially expressed genes suggests that disease-specific signatures

persist. We observed that genes upregulated in PSC-derived cholangiocyte organoids cluster around epithelial plasticity, progenitor-like pathways, and innate immune signalling. These include PROM1 (CD133), a membrane protein used to identify epithelial progenitor cells in both liver and hematopoietic stem cell populations[152]. INSL4, on the other hand, is a member of the insulin-like family mainly associated with proliferation and differentiation in trophoblasts. In other cellular models, INSL4 overexpression not only promotes cell growth but also influences cell fate and morphogenesis via apoptosis[153]. Since PROM1 and INSL4 are both expressed concurrently, PSC organoids may not be fully differentiated, instead adopting a regenerative-like state. It is also noteworthy that ROBO1 and SLIT3 were upregulated together. These key components of the axon-guidance pathway regulate epithelial organization, suggesting that cholangiocytes derived from individuals with PSC may activate developmental or repair processes. The SLIT3/ROBO1 axis is best known for its role in cell development and migration, but it has also more recently been associated with liver fibrosis. Its profibrotic effect primarily involves hepatic stellate cells (HSCs), which deposit extracellular matrix[154–156]. Fu et al. (2023) showed that silencing SLIT3 reduces TGF-β-induced stellate cell activation by suppressing YAP signalling. Their data indicate that SLIT3 is upregulated in response to TGF-β and, in a pro-fibrotic context, contributes to the enhancement of TGF-β-driven activation through YAP[154]. Lower SLIT3 expression therefore attenuates fibrotic tissue formation. Kong et al. (2023) further demonstrated, in a *Schistosoma japonicum* infection model, that miR-29a-3p counteracts fibrosis by targeting ROBO1[155]. By binding to ROBO1 mRNA, miR-29a-3p reduces ROBO1 protein levels and consequently attenuates hepatic stellate cell activation and extracellular matrix accumulation in the liver. Consistent with these observations, KEGG pathway analysis identified axon guidance as the only enriched signalling pathway. Finally, an increase in genes associated with immune functions has been observed in PSC samples. TXK is a tyrosine kinase belonging to the Tec family, canonically associated with the activation and polarization of T lymphocytes[157,158]. Although its role in epithelial cells has not been extensively investigated, TXK has also been implicated in the regulation of redox and inflammatory signalling pathways in immune contexts[159]. While this mechanism has not been described in cholangiocytes, the upregulation of TXK observed in PSC-derived organoids may represent an adaptive response to the oxidative and inflammatory biliary microenvironment characteristic of the disease. In this regard, other Tec-family kinases, such as BMX/ETK, are known to modulate epithelial barrier integrity and proliferative responses through PI3K/AKT, STAT3, and NF-κB signalling, and it has been described in several solid tumours where it promotes epithelial growth and survival[160,161]. By analogy, the presence of TXK in PSC cholangiocytes could indicate a shift toward a progenitor-like or regenerative phenotype driven by chronic inflammatory cues, a hypothesis that remains to be experimentally validated. IFI6 is an interferon-inducible gene involved in antiviral defence and linked to apoptosis[162,163]. From this, we can conclude that PSC cholangiocytes maintain their susceptibility to inflammatory stimuli and remain

responsive to microenvironmental cues, even at resting state. By comparison, ALD-derived cholangiocyte organoids displayed higher expression of genes associated with epithelial homeostasis, vesicle trafficking and metabolic remodelling. Under stress conditions (inflammatory or alcohol-derived), cholangiocytes from ALD appear to adapt their metabolism to mitigate damage and preserve function. Among the upregulated genes was CADPS, a calcium-dependent secretion activator that regulates calcium-mediated vesicular release and supports intercellular communication[164]. We also observed an upregulation of PTPRR, a protein tyrosine phosphatase that dampens MAPK/ERK signalling and limits proliferative activity in colorectal cancer models[165]. Furthermore, the GJC1 gene encodes Connexin-45 (Cx45), a junction protein expressed in the intestinal tract, including both small and large intestine[166], although its function in bile ducts remains unclear. Other connexins (Cx26, Cx32, Cx43 in the liver; Cx43 and Cx45 in the intestine) have well-established roles in epithelial coordination, barrier stability, proliferation and stress responses. By analogy, Cx45 may have similar relevance in cholangiocytes, though this requires direct experimental confirmation. As shown in our data, cholangiocytes *in vitro* express a broad repertoire of pattern-recognition receptors, enabling rapid responses to microbial and pro-inflammatory cues. It is well known that bile duct epithelial cells can release cytokines and chemokines to coordinate immune responses[167]. Considering cholangiocytes as central regulators of local immunity, even subtle molecular variations may influence how they interact with their microenvironment. Due to this immune-sensing capacity, small changes in gene expression can have meaningful functional consequences, potentially shaping long-term disease trajectories. Overall, our findings suggest that, despite their different tissues of origin (PSC or ALD), cholangiocytes tend to converge towards a shared basal phenotype in culture, while still retaining discrete molecular signatures that reflect their respective diseases.

3. L-17A INDUCES CONSERVED INFLAMMATORY PROGRAMS BUT UNMASKS PSC-SPECIFIC IMMUNE SIGNATURES

We next aimed to understand how inflammatory stimuli influence cholangiocyte function and responsiveness. To this end, we analysed the gene expression profiles of cholangiocyte organoids derived from people with PSC and ALD following stimulation with IL-17A. IL-17A was chosen because it is closely linked to PSC and associated with an aberrant Th17 response, particularly following microbial colonisation in the biliary tract. Peripheral $CD4^+$ T cells from people with PSC display increased IL-17A production compared to healthy controls, suggesting a bias towards the Th17 lineage[79]. Evidence

that monocytes from people with PSC enhance Th17 differentiation through abnormal cytokine release further highlights the role of innate immune cells in shaping this response[168]. Moreover, naive-like liver-resident $CD4^+$ T cells are increased in PSC, according to single-cell studies, indicating a reshaped T cell pool in the liver[169]. Th17 lymphocytes are recruited to the liver via CXCR3 and CCR6 chemokine receptors expressed on their surface. This process is largely driven by epithelial-derived chemokines that attract immune cells to inflamed sites[170]. Importantly, cholangiocytes respond to IL-17A by secreting chemokines such as CCL20, which in turn recruits additional immune cells, particularly Th17 and Tc17 lymphocytes expressing CCR6. This IL-17-dependent loop enhances communication between epithelial and immune cells and supports the ongoing recruitment of immune cells, leading to sustained inflammation in the biliary environment[171]. In line with this, we observed that despite their distinct pathogenic backgrounds (immune-mediated in PSC and toxic–metabolic in ALD) the global transcriptional response to IL-17A was remarkably similar in both groups. In particular, the coordinated upregulation of the chemokines CXCL1, CXCL3, CXCL5 and CCL20, together with the transcriptional regulator NFKBIZ (also known as IκBζ), an IL-17-responsive nuclear co-activator of NF-κB-dependent gene transcription that amplify inflammation induced by IL-17, indicates that cholangiocytes activate a conserved epithelial inflammatory programme upon stimulation. Bronchial epithelial cells and other type of cells are also susceptible to IL-17A ability to induce chemokines and inflammatory mediators. Indeed, in the lung, IL-17A induces CXCL5 and the recruitment of neutrophils, via NF-κB and MAPK. In *in vitro* models of primary human tracheobronchial epithelial cells (TBE cells), when stimulated with IL-17A, produce IL-6, which in turn acts in an autocrine/paracrine manner, amplifying the response by increasing the expression of the MUC5B/MUC5AC mucin genes[172]. It is reasonable to assume that cholangiocytes may respond in a similar way. This is in line with our findings, where PSC cholangiocyte organoids showed upregulation in the MUC5AC and MUC6 genes. However, PSC and ALD cholangiocyte organoids stimulated by IL-17A are even more similar at transcriptional level when directly compared with each other. Our data once again demonstrate the presence of the components of the axon guidance pathway genes, ROBO1 and SLIT3, in PSC cholangiocyte organoids. As previously explained, while traditionally associated with neural development[173], these genes have also been implicated in epithelial morphogenesis[174], cell migration[175], and in some context immune cell positioning[176], we can therefore confirm that PSC cholangiocytes may indeed be predisposed towards tissue remodelling and immune coordination. We found the same outcome for other PSC-specific genes. Among these, IFI16, a cytosolic DNA sensor that activates inflammasome signalling[177] , was again found to be upregulated. On the other hand, PHF20L1, a chromatin-binding protein involved in epigenetic regulation, was found to be specific to stimulated PSC cholangiocytes. PHF20L1 is a component of the NSL (Non-Specific Lethal) complex, which increases chromatin accessibility and enables rapid gene transcription through histone acetyltransferase activity[178]. Taken together,

these findings align with the concept of “transcriptional memory”. The upregulation of genes associated with innate immunity and epithelial plasticity suggests that PSC cholangiocytes may be more reactive to inflammatory clues. According to this model, previous inflammatory exposures leave stable epigenetic marks that prime cells for stronger or faster responses in the future[179]. We also identified subtle yet consistent differences between PSC and ALD cholangiocyte organoids. The immune signature of PSC organoids was defined by the coordinated activation of chemokines, cytokines and antimicrobial genes (CXCL1–3, CCL20, IL1B, IL6, DEFB4, SAA1/2), supported by key signalling pathways such as IL-17, NF-κB and TNF. ALD organoids similarly induced inflammatory genes, but with greater inter-patient variability and a narrower profile mostly limited to neutrophil-attracting chemokines (CXCL1, CXCL2, CXCL8), without the enrichment of antimicrobial or epigenetic components observed in PSC. Instead, ALD cholangiocyte organoids showed transcriptional features associated with cell adhesion, intracellular signalling and tissue homeostasis. For example, APBB1IP (amyloid beta precursor protein-binding family B member 1-interacting protein) facilitates integrin activation and promotes leukocyte adhesion to the epithelium[180]. However, APBB1IP expression alone does not indicate activation of a full inflammatory programme: we did not observe concurrent induction of HLA molecules or co-stimulatory signals such as CD40 or PD-L1. In this context, APBB1IP reflects a state of “readiness for adhesion” rather than immune activation. It is also important to emphasise that, at this stage, cholangiocytes were only stimulated *in vitro* with IL-17A. Co-culture with immune cells may therefore provide a more comprehensive view of their activation status. Similarly, CNKSR1 (connector enhancer of kinase suppressor of Ras 1) is a scaffold protein that modulates MAPK responses, but is not intrinsically pro-inflammatory; its principal role is to optimise cellular responses to cytokines, growth factors and environmental stress, preventing excessive signalling[181]. Elevated RGS5 (Regulator of G protein signalling 5) in ALD organoids may likewise reflect an adaptation aimed at dampening sustained or damaging signals, including those derived from alcohol metabolism[182]. This pattern is consistent with long-term adaptation to metabolic and oxidative stress. Cells experiencing chronic oxidative and metabolic stress in the liver often shift away from acute inflammatory responses. In ALD, alcohol and its metabolites (e.g. acetaldehyde) induce oxidative injury, while metabolic alterations (lipid composition, mitochondrial function) further modify cellular behaviour. As previously discussed, even at resting state, ALD cholangiocyte organoids show upregulation of genes such as PTPRR and GJC1 compared to unstimulated PSC organoids. Overall, our data indicate that cholangiocytes in ALD organoids prioritise the maintenance of tissue integrity over the initiation of strong immune activation. While IL-17A stimulation provides valuable insight into epithelial responsiveness, the inflammatory landscape *in vivo* is considerably more complex. Multiple cytokines (e.g. TNF-α, IFN-γ, IL-1β, IL-22) and diverse immune cell populations ($CD8^+$ T cells, NK cells, neutrophils, macrophages, dendritic cells) contribute to the biliary immune environment. Therefore, stimulation with a single cytokine *in vitro*

captures only a fraction of the inflammatory processes occurring in the livers of people with PSC or ALD.

4. DIRECT CD4$^+$ T CELL CONTACT UNVEILS THE DUAL IMMUNOMODULATORY ROLE OF CHOLANGIOCYTES

To address this limitation, we extended our co-culture experiments using cholangiocyte organoids, first with T cell–derived cytokine supernatant and then with pre-activated CD4$^+$ T cells, to better mimic the conditions of the inflamed liver in vivo, as understanding how cholangiocytes interact with CD4$^+$ T lymphocytes is key to uncovering the mechanisms that drive immune-mediated liver diseases. The importance of this interaction in PSC lies in the dual nature of cholangiocytes, which, although susceptible to inflammatory injury, also express adhesion molecules such as ICAM-1 and VCAM-1 that mediate direct interaction with T lymphocytes[183]. Recent single-cell RNA sequencing (scRNA-seq) data from our group indicate that people with sclerosing cholangitis have a higher number of naïve CD4$^+$ T cells resident in the liver. In PSC, liver-infiltrating T cells may behave differently from those in other tissues as a result of chronic inflammation. Thus, a larger reservoir of naïve cells may differentiate into pro-inflammatory subpopulations, such as Th17 cells, shaping the epithelial–immune interaction[169]. The specific effects of T cell-derived signals on cholangiocytes remain incompletely understood. In our system, cholangiocyte organoids responded to IL-17A, although the responses were limited, as expected after a single cytokine stimulus. To explore how cholangiocytes respond to immune stimuli, and to distinguish between soluble and contact-dependent signals, we first exposed cholangiocyte organoids to supernatant from pre-activated CD4$^+$ T cells, mimicking a cytokine-rich inflammatory environment, and in parallel established direct co-cultures with T cells to allow physical interaction in both PSC- and ALD-derived organoids. This approach enabled us to determine whether soluble mediators alone are sufficient for cholangiocyte activation, or whether direct contact with T cells is also required. Under stimulation with supernatant enriched in CD4$^+$ T cell mediators, we observed consistent upregulation of ICAM1 and HLA-DR at both transcriptional and protein levels, and a similar increase in CD40 protein. These molecules are involved in leukocyte adhesion and antigen presentation, reflecting a clear epithelial response to immune signals. Interestingly, CD70 and OX40L were transcriptionally upregulated, yet no corresponding increase was detected at protein level, which may reflect post-transcriptional regulation or a delayed induction pattern. This observation is consistent with previous findings in dendritic cells, where prostaglandin E_2 enhances the expression of CD70 and OX40L mRNA without immediate protein translation[184]. Additionally, the expression of co-stimulatory molecules is highly

context-dependent: the cytokine environment, such as IFN-γ, IL-17 or TNF-α, as well as whether the cells are quiescent or have been previously primed, strongly influence whether these molecules are upregulated or remain transcriptionally silent. In contrast, PD-L1, CD86, CD80 and CD137L (4-1BBL) showed no changes at either transcript or protein level. This suggests that soluble mediators released by activated $CD4^+$ cells are insufficient to fully modulate these pathways. These observations demonstrate that, although cholangiocytes clearly sense T cell-derived signals, the response remains partial in the absence of direct contact. We therefore established a co-culture system allowing direct interaction between cholangiocyte organoids and pre-activated $CD4^+$ T cells. This model was designed to capture not only the effects of soluble factors but also the spatial and physical aspects of immune–epithelial interactions that are essential for immune synapse formation and cellular crosstalk. Establishing a co-culture system that maintained the viability and functionality of both epithelial and immune cells required careful modification of culture conditions. Standard expansion medium (EM), which supports organoid growth, contains components that influence T cell behaviour. Forskolin elevates intracellular cAMP, suppressing IL-2 production and inhibiting T cell proliferation without inducing apoptosis[185]. A83-01, a selective inhibitor of the TGF-β type I receptor (ALK5), interferes with TGF-β signalling[186], a pathway crucial for Th17 and Treg differentiation[187]. Beyond its effects on $CD4^+$ T cells, TGF-β is important for maintaining epithelial homeostasis, yet can also drive fibrogenesis and epithelial–mesenchymal transition (EMT). Although stellate and immune cells are major sources of this growth factor, stressed and senescent cholangiocytes also release TGF-β. Indeed, cholangiocytes in PSC livers often exhibit a senescence-associated secretory phenotype (SASP)[75,188,189]. The TGF-β released by them promotes chronic inflammation and fibrosis, thus sustaining chronic biliary damage and progressive fibrosis[188,189]. Notably, when cholangiocytes are in contact with activated $CD4^+$ T cells, they increase the production of endogenous TGF-β, establishing regulatory feedback loops between the epithelium and immune cells. Completely blocking TGF-β signalling with A83-01 would therefore create an artificial state; cholangiocytes would no longer produce or respond to TGF-β, which would alter T cell activation in a non-physiological manner. We therefore optimised the culture conditions to preserve physiological TGF-β responsiveness. Another crucial variable was the presence of the extracellular matrix (ECM); particularly of Matrigel matrix, which is essential for maintaining organoid polarity and stability. Standard dome-embedded 3D cultures present a physical barrier that limits T cell infiltration. To address this issue, we introduced a novel floating culture system with only 5% Matrigel matrix, preserving epithelial identity and structure of cholangiocytes, while facilitating immune cell invasion. Gene expression and morphological analysis confirmed the expression of cholangiocyte markers (EPCAM, KRT7 and KRT19) without inducing stress-related apoptosis. Ultimately, the choice of 5% Matrigel matrix represented a balance between structural support and CD4+ accessibility. We also verified that higher concentrations restricted T cell mobility, while lower concentrations

(0–1%) impaired organoid polarity and survival. Careful adjustment of the culture conditions was crucial. In our optimised co-culture model, direct interaction with pre-activated $CD4^+$ T cells caused a stronger activation of cholangiocytes than exposure to T cell–derived supernatant alone. Our data indicate that robust expression of PD-L1 and a modest induction of CD80, as well as upregulation of ICAM1 and HLA-DR, occurred altogether only upon direct cell-to-cell contact. Comparable epithelial–immune interactions have also been reported in other organs, such as the lung and intestine, where epithelial cells express MHC class II and can function as non-classical antigen-presenting cells for T cells, a role typically restricted to professional APCs[190,191]. In the intestine, the epithelium shows an even more complex behaviour, being able to either stimulate or suppress T cells when needed[158,192]. Consistently, our findings indicate that cholangiocytes also require direct contact with T cells to exert the full range of their immunomodulatory functions. PD-L1 and CD80 can form cis-heterodimers on the surface of epithelial cells and send opposing signals to lymphocytes: binding of CD80 to CD28 promotes activation, whereas interaction between PD-L1 and PD-1 induces inhibitory signals leading to tolerance or functional shutdown of $CD4^+$ T cells[193]. Furthermore, our data on ICAM-1 and CD40 expression suggest that cholangiocyte interaction with $CD4^+$ T cells may also involve LFA-1 and CD40L binding, respectively. However, CD40 upregulation was less consistent across samples. ICAM-1 is known to increase in inflammatory conditions under the action of cytokines such as IFN-γ or TNF-α[53], while CD40–CD40L engagement is crucial for sustained T helper cell activation, promoting co-stimulatory molecule expression and cytokine production[194]. These interactions are not limited to transient encounters, but allow prolonged contact with sustained intracellular signalling cascades in both cells. Since these mechanisms directly contribute to the persistence of inflammation at the bile duct interface, they also represent potential therapeutic targets. Attempts have been made to block CD40–CD40L in order to reduce liver inflammation[195]. More recently, frexalimab, a next-generation anti-CD40L antibody, has entered clinical trials for the treatment of autoimmune diseases, suggesting that a similar approach could potentially be explored in PSC, where excessive T cell activation contributes to bile duct damage[196]. ICAM-1, in contrast, primarily amplifies inflammation by recruiting innate immune cells. In experimental models of hepatic ischaemia-reperfusion or cholestatic injury, ICAM-1 blockade reduced neutrophil accumulation and liver parenchymal damage[197–199]. However, the clinical translation has proven challenging: in a rat liver transplant model, ICAM-1 inhibition reduced leukocyte adhesion without improving graft function and in clinical trials, anti-ICAM-1 antibodies such as enlimomab initially showed protective effects but subsequently caused complications due to excessive immune suppression[200–201]. Interestingly, the co-culture also affected lymphocytes. $CD4^+$ T cells interacting with cholangiocyte organoids showed broad downregulation of both activation markers (CD25, OX40, ICOS) and exhaustion markers (PD-1, CTLA-4, LAG-3), which was unexpected. In the context of co-culture, cholangiocytes display a

paradoxical dual role. While they can promote immune activation by expressing adhesion or antigen-presenting molecules, they can also exert inhibitory effects through PD-L1. Clinically, this mirrors PSC, where chronic inflammation persists alongside exhausted and dysfunctional T cells. Our findings therefore highlight the role of cholangiocytes in maintaining this delicate balance within the peribiliary area. The early reduction of T-cell activation observed after 24 hours likely represents only the initial phase of a chronic phenomenon in patients. We hypothesise that, over time, exhausted T cells may lose their capacity to target altered or potentially harmful cholangiocytes. Although our data do not clarify whether these changes would persist, reverse, or evolve *in vitro*, they suggest that cholangiocytes in the liver may act both as regulators and as targets of persistent inflammatory stimuli. Cholangiocytes are constantly exposed to signals from Th17 cells, as well as to microbial products derived from the gut microbiota (the “leaky gut” hypothesis), which sustain cycles of tissue injury and repair[202]. Newly recruited T cells in the inflamed liver repeatedly encounter cholangiocyte-derived chemokines (e.g., CXCL1–3 and CXCL5), which further perpetuate local immune activation[40,41,48]. At this point, cholangiocytes would attempt to contain the aggressiveness of CD4+ cells through PD-L1, but in chronic inflammatory contexts something goes wrong. Currently, the concept of enhancing PD-L1 signalling is being explored in preclinical models of autoimmune disease to restore immune tolerance and prevent excessive tissue damage. In PSC, however, we suggest that the effect of PD-L1 is likely to be phase-dependent. Transient PD-L1 upregulation may be beneficial in the acute phase by protecting tissue from excessive immune activation. Yet, when sustained over time, PD-1/PD-L1 signalling can drive T-cell exhaustion, a state associated with loss of CD28 expression and functional impairment in intrahepatic T cells[203]. Chronic PD-1 signalling can therefore weaken immune surveillance instead of resolving inflammation. This implies that liver inflammation is not a static process, but progresses through distinct immunological phases. Consequently, the effectiveness of PD-L1-targeted therapies will depend on when they are administered. For example, short-term stabilisation of PD-L1 signalling may be protective in the early stage of inflammation. Supporting this idea, PD-1 agonists have been shown to suppress T-cell proliferation and cytokine production in mouse models of arthritis and inflammatory bowel disease[204,205]. Other strategies are being explored to increase local tolerance and stabilise PD-L1 expression. One option is to stimulate PD-L1 directly via IFN-γ or TNF-α. Another is to enhance PD-L1 transcription indirectly by increasing chromatin accessibility. In this context, drugs already under investigation in oncology, such as the histone deacetylase inhibitors entinostat and mocetinostat, or the DNA methyltransferase inhibitor decitabine, may be explored as potential strategies to boost PD-L1 expression and reduce acute biliary injury[206–208]. The situation is completely different in the chronic phase. PD-L1 remains high with T cell exhaustion. In this context, rather than increasing PD-L1, it would be more appropriate to consider partially inhibition of the PD-1/PD-L1 axis. The aim would be to reduce PD-L1 enough to restore functionality to the T cells

without triggering an uncontrolled immune response against cholangiocytes. Therefore, to determine the optimal timing of intervention, additional biological markers should be identified, for instance by monitoring exhaustion signatures (TIM-3, and CTLA-4) or IFN-γ/STAT1 activity in tissue samples. Moreover, systemic administration over a prolonged period of time could induce immune-related adverse events (irAEs) and cause severe systemic effects involving multiple organs[209,210]. An additional layer of complexity is added by cholangiocarcinoma (CCA), a major comorbidity in PSC. In cancer, PD-L1 enables tumour cells to evade immune surveillance and promotes malignant progression[211–213]. While transient PD-L1 enhancement may be advantageous in early inflammation, progression to malignancy, as observed in CCA, demands timely antineoplastic intervention. In this setting, immune checkpoint inhibitors such as nivolumab and pembrolizumab have shown efficacy in PD-L1–positive or MSI-high CCA[213–215]. Thus, tailoring treatment with intervals (intermittent dosing), and, where possible, targeted local administration (local delivery) could be conceivable[209,210]. A partial and timed strategy would also allow combination of different therapies to act simultaneously on multiple targets while blocking other pro-inflammatory cytokines or signals derived from direct cell-to-cell contact. What surprised us most was the absence of major differences between co-cultures with HLA-matched and HLA-mismatched cholangiocytes and T cells. We hypothesise that allorecognition, that is, direct recognition of the MHC complex by T cells, is not the main mechanism driving the observed interactions. A possible explanation lies in the activation state of the T cells used in our model, which had already been strongly pre-activated through the TCR, thereby reducing their dependence or sensitivity to the fine discrimination between self and non-self HLA. When a T cell is activated in vitro through TCR stimulation, for example with anti-CD3/CD28 antibodies, it undergoes strong activation, leading to global expression of activation molecules, proliferation, and cytokine release. In this state, T cells respond independently of antigen specificity, thereby masking responses to specific antigens. Consequently, the interactions we observed were likely driven by adhesion molecules and immune checkpoint engagement. Although not professional antigen-presenting cells, cholangiocytes possess the necessary molecular repertoire to actively influence immune responses in the liver, also acting on other hepatic cells, such as hepatic stellate cells, and influencing fibrogenesis. Through co-stimulatory and inhibitory signalling, cholangiocytes contribute to maintaining a state of chronic yet regulated inflammation, consistent with PSC. What remains unclear is the initial driver of this immune–epithelial imbalance, whether rooted in cholangiocytes, $CD4^+$ T cells or other cell types. More complex co-culture models that incorporate additional hepatic and immune cells, such as macrophages, MAIT cells or γδ T cells, as well as stromal components or microbial stimuli, will be required to address this question and to establish a clearer chronology of the events sustaining inflammation in the biliary tree.

5. STRENGTHS AND LIMITATIONS OF THE CHOLANGIOCYTE ORGANOID CO-CULTURE MODEL

Compared to classical 2D cell culture, organoids retain the capacity to organise themselves into structures that closely resemble the architecture and function of their tissue of origin. This allows them to better model cell–cell interactions under physiologically relevant conditions and to preserve proliferative capacity and cellular heterogeneity. Importantly, being derived directly from patient material, *in vitro* organoid cultures represent considerable value for human disease modelling and drug screening within the context of personalised medicine. In our study, cholangiocyte organoids recapitulated essential features of the biliary epithelium, including architecture, transcriptional identity, and disease-relevant phenotypes. Notably, we observed subtle yet consistent disease-associated expression signatures at baseline (e.g., PROM1/INSL4, ROBO1/SLIT3, TXK/IFI6 vs CADPS/PTPRR/GJC1), indicating the persistence of some epigenetic "priming" despite convergence during in vitro expansion. Our optimised cholangiocyte organoid culture system also proved highly adaptable to a more physiologically oriented co-culture. We successfully co-cultured organoids with $CD4^+$ T cells in a modified medium that supported the survival and function of both cell types without immunosuppression, allowing us to dissect mechanistic aspects of epithelial–immune crosstalk under controlled conditions. Furthermore, the compatibility of these organoids with CRISPR/Cas9-mediated genetic manipulation enables future functional studies of gene-specific effects, while their long-term stability supports reproducibility across experiments, making them suitable for both basic and translational research. However, several limitations should be considered when interpreting our findings. One of the main challenges relates to the incomplete tissue complexity of organoids. Being composed primarily of epithelial cells, they lack stromal and endothelial components that are essential for processes such as inflammation, neo-duct formation, and fibrosis. The absence of vascularisation further affects cholangiocyte function, as in vivo these cells are continuously exposed to bile flow and nutrient gradients. In organoid cultures, all cells experience uniform chemical and mechanical conditions, preventing the establishment of region-specific differences in transporter expression (e.g., CFTR, ABC transporters) and in flow-responsive signalling. In the native biliary tree, cholangiocytes sense bile flow and ductal pressure through Ca^{2+}-mediated mechano-responsive pathways and the Hippo–YAP/TAZ axis, which together regulate bile secretion and cholangiocyte integrity[216,217]. In organoid cultures, however, these physiological mechanical cues are absent. Instead, YAP/TAZ activity is sustained primarily by mitogen-rich medium and matrix-derived mechanical tension rather than flow-dependent mechanotransduction, so these pathways are not fully engaged as they are in vivo, resulting in a more homogeneous and less physiologically

patterned epithelial state. Additionally, the use of growth factor-rich culture conditions may induce epigenetic reprogramming and partial phenotypic convergence, potentially masking some disease-specific signals. Another limitation of our study concerns the short co-culture window (24 h), which may have prevented us from capturing the temporal dynamics of activation and the emergence of dysfunction/exhaustion phenotypes in both cholangiocyte organoids and $CD4^+$ T cells. Gene and protein expression changes involved in epithelial–immune crosstalk often develop over longer periods (48–96 h), and may therefore not be fully represented in our dataset. Finally, the use of pre-activated T cells likely bypasses HLA-dependent activation, limiting conclusions regarding antigen presentation and allorecognition. To address this, future work should aim to introduce naïve autologous $CD4^+$ T cells, which strictly require MHC-II engagement for activation. This would allow us to determine whether cholangiocytes can function as non-professional antigen-presenting cells and to distinguish antigen-dependent from contact- or cytokine-mediated immune modulation.

CONCLUSIONS

Our research established a co-culture system combining ALD- and PSC-derived cholangiocyte organoids with activated $CD4^+$ T cells to investigate immune modulation within the biliary niche. This model revealed a fundamental duality: cholangiocytes are not merely passive targets of immune attack, but active contributors to the regulation of local immune microenvironment. Although PSC- and ALD-derived organoids converged transcriptionally under basal culture conditions, they retained few distinct disease-related features. PSC organoids exhibited gene expression patterns consistent with epithelial plasticity and heightened immune readiness, indicating a greater propensity to sustain inflammatory responses and initiate tissue regeneration. In contrast, ALD organoids preferentially expressed genes associated with metabolic regulation, vesicular trafficking, and epithelial homeostasis, suggesting a tendency to prioritise tissue integrity and functional stability over immune activation. These persistent transcriptional signatures imply that cholangiocytes keep a memory of their pathological environment, which may influence how they respond to subsequent immune-derived stimuli. Building on these observations, we demonstrated that direct contact with pre-activated T lymphocytes induces resting cholangiocyte organoids to express regulatory molecules capable of shaping immune response. Notably, this effect extends to the T cells themselves: $CD4^+$ T cells co-cultured with cholangiocyte organoids showed a consistent reduction in both activation and exhaustion markers. In this way cholangiocytes exert a dual regulatory influence, able to promote immune engagement via adhesion molecules and MHC-II, while simultaneously suppressing excessive immune activation through PD-L1. These findings reflect the clinical paradox observed in PSC, where persistent inflammation coexists with dysfunctional and partially exhausted T cells. Under sustained inflammatory pressure, cholangiocytes may become senescent and adopt a SASP phenotype, releasing pro-inflammatory mediators and proteases. Over time, this cycle contributes to ductal damage and the progressive fibrosis characteristic of PSC. While the co-culture system developed here provides a valuable platform for dissecting epithelial–immune crosstalk, several refinements will be required to more accurately recapitulate *in vivo* complexity. The current model lacks stromal and endothelial components and does not reproduce the mechanical and metabolic cues coming from bile flow and vascularisation. These factors are fundamental for full cholangiocyte differentiation, and their absence may mask disease-specific signatures. In this regard, microfluidic organoid-on-a-chip platforms represent a promising advancement. These systems integrate 3D organoid structures within perfused chambers, enabling controlled nutrient flow, shear stress, and compartmentalised co-culture[218]. Microchannels can be co-seeded with liver sinusoidal endothelial cells or Kupffer-like macrophages to more closely resemble the biliary

tissue. Moreover, immune cells, such as $CD4^+$ or $CD8^+$ T cells, can be introduced via perfusion in a time-resolved manner, allowing the progression from early activation to chronic dysfunction to be monitored experimentally. Beyond reproducing tissue architecture, our model can be applied to test mechanistic hypotheses arising from our findings. Among these, PD-L1 blockade experiments would allow us to determine whether the reduction in T-cell activation that we observed is primarily driven by PD-L1/PD-1 checkpoint signalling, or whether cholangiocytes also employ additional contact-dependent inhibitory mechanisms. This could be addressed either by co-culturing cholangiocyte organoids and $CD4^+$ T cells in the presence of blocking antibodies against PD-L1/PD-1, or by selectively reducing PD-L1 expression in cholangiocytes using CRISPR-based approaches. For example, CRISPR-interference (CRISPRi) can be used to selectively suppress CD274 transcription in cholangiocytes, producing organoids in which PD-L1 is stably reduced while the cells remain otherwise genetically identical to their parental counterparts. Overall, our findings highlight the value of organoid-based system as translational platform capable of linking basic immunology with clinically relevant questions, with the expectation that this model will support the identification of novel therapeutic targets aimed at improving both the quality of life and life expectancy of people affected with cholangiopathies.

MATHERIALS

Tab.1 List of consumables used in this study

Article	**Catalog number**	**Company**	**County**
Cell Culture Multiwell plate, 24 well	662160	Greiner Bio-One	Germany
Corning® 96-well Clear Flat Bottom Ultra-Low Attachment Microplate	3474	Corning	USA
Costar® 6-well Clear Flat Bottom Ultra-Low Attachment Multiple Well Plates	3471	Corning	USA
Cryotubes 1.8 ml	379	Sarstedt AG	Germany
FACS Tubes	551579	Sarstedt AG	Germany
gentleMACS C Tubes	130-093-237	Miltenyi Biotec	Germany
Pasteur Pipette	4522.1	Roth Selection	Germany
Pipette tips 0.01 ml	1130100	Sarstedt AG	Germany
Pipette tips 0.2 ml	760012	Sarstedt AG	Germany
Pipette tips 1 ml	762	Sarstedt AG	Germany
Pipettes 10 ml	1688010	Sarstedt AG	Germany
Pipettes 25 ml	1685020	Sarstedt AG	Germany
Pipettes 5 ml	1687010	Sarstedt AG	Germany
Strainer 100 µm	542000	Roth Selection	Germany
Strainer 30 µm	130-098-458	Miltenyi Biotec	Germany
Tubes 1.8 ml	379	Sarstedt AG	Germany
Tubes 10 ml	62515006	Sarstedt AG	Germany
Tubes 15 ml	188271	Greiner Bio-One	Germany
Tubes 2 ml	72691	Sarstedt AG	Germany
Tubes 5 ml	72701	Sarstedt AG	Germany
Tubes 5 ml, for FACS	551579	Sarstedt AG	Germany

Tubes 50 ml	227261	Greiner Bio-One	Germany

Tab.2 List of devices used in this study

Article	**Catalog number**	**Company**	**County**
Cytek Aurora 5 Lasers flow cytometer		Cytek	USA
Eppendorf 5427R	5409000010	Eppendorf	Germany
Eppendorf 5810R	5810000010	Eppendorf	Germany
Eppendorf 5920R	5948000010	Eppendorf	Germany
Eppendorf Research® plus 0.1 – 2 µl	3123000012	Eppendorf	Germany
Eppendorf Research® plus 0.5 – 10 µl	3124000016	Eppendorf	Germany
Eppendorf Research® plus 10 – 200 µl	3124000083	Eppendorf	Germany
Eppendorf Research® plus 100 – 1000 µl	3124000121	Eppendorf	Germany
Eppendorf ThermoMixer® Comfort	5382000015	Eppendorf	Germany
gentleMACS Octo Dissociator with Heaters	130-096-427	Miltenyi Biotec	Germany
GFL 1083 water bath	1083	GFL GmbH	Germany
Leica DM IRB		Leica Microsystems	Germany
Nanodrop 2000	ND-2000	Thermofisher Scientific	USA
Pipetboy Acu 2	155000	Integra Biosciences	Germany
T100 Thermal Cycler Bio-Rad, USA	1861096	Bio-rad	USA
ViiA 7 Real-Time PCR System		Thermofisher Scientific	USA
Vortex-Genie 2	SI-0236	Scientific industries	USA

Tab. 3 List of media used in this study

Article	Catalog number	Company	County
Advanced DMEM/F12	12634010	Gibco	USA
DMEM GlutaMAX	11965092	Gibco	USA
EBSS (Ca2+/Mg2+)	24010043	Gibco	USA
RPMI 1640	11875085	ThermoFisher	USA

Tab. 4 List of commercially available solutions used in this study

Article	Catalog number	Company	County
Cell Recovery Solution	354253	Corning	USA
CellTrace™ Violet Cell Proliferation Kit	C34557	ThermoFisher	USA
Collagenase D	1108866001	Roche	Switzerland
Ficoll-Paque PLUS		Cytiva	UK
Matrigel-Culturex RGF BME Type2	3533-005-02	R&D Systems	USA
RBC Lysis/Fixation Solution (10X)	422401	Biolegend	USA
Recovery CellCulture freezing medium	12648-010	Gibco	USA
Sodium pyruvate	11360070	Gibco	USA
Trypan blue solution (0.4 %)	15250 - 061	Thermofisher Scientific	USA
Trypan blue solution (0.4%)	15250 - 061	Thermofisher Scientific	USA
TrypLE™ Express Enzym (1x), Phenolred	10043382	Gibco	USA
UltraComp eBeads™	01-2222-42	Thermofisher Scientific	USA

β-Mercaptoethanol	444203-250ML	Sigma-Aldrich	Germany
Sodium Pyruvate	11360070	Gibco	USA

Tab. 5 List of cell culture supplements used in this study

Article	**Catalog number**	**Company**	**County**
[Leu] Gastrin	G9145	Sigma-Aldrich	Germany
A83-01	2939	Tocris	UK
B27	12587-010	Life Technologies	USA
EGF	AF-100-15	PeproTech	USA
FCS	P40-37500	PAN - Biotech	Germany
FGF10	AF 100-26	PeproTech	USA
Forskolin	1099	Tocris	UK
HGF	100-39	PeproTech	USA
Human IL-17A Recombinant Protein	200-17-25UG	PeproTech	USA
IL-2 (cell culture)	202-IL-010	R&D Systems	USA
ImmunoCult™™ Human CD3/CD28 T Cell Activator	100-0784	STEMCELL Technologies	Canada
L-Glutamin	25030-024	Gibco	USA
N-acetylcysteine	A0737	Sigma-Aldrich	Germany
N2	17502-048	Life Technologies	USA
Nicotinamide	N0636	Sigma-Aldrich	Germany
Penicillin / Streptomycin	15140122	Thermofisher Scientific	USA

Tab. 6 List of commercially available Kits used in this study

Article	Catalog number	Company	County
CellTrace™ Violet Cell Proliferation Kit	C34557	ThermoFisher	USA
Clariom™ S Assay, Human	902927	Applied Biosystems	USA
High-capacity cDNA reverse transcription kit	4368814	Applied Biosystems	USA
Human CD4+ T Cell Isolation Kit	130-096-533	Miltenyi Biotec	Germany
NucleoSpin® RNA	740955.50	Macherey-Nagel	Germany
TaqMan™ Fast Advanced Master Mix	11380912	Applied Biosystems	USA
Zombie NIR™ Fixable Viability Kit	423105	Biolegend	USA
Zombie Aqua™ Fixable Viability Kit	423101	Biolegend	USA

Tab. 7 List of softwares used in this study

Article	Company	County
Biorender	Biorender	Canada
FlowJo™ v10	BD	USA
Graphpad prism (v10)	Graphpad	USA
Nanodrop 2000/2000c Software (v1.6.198)	Thermofisher Scientific	USA
R (v 4.4.2)	The R Project for Statistical Computing	Austria
Spectroflo (v3.3.0)	Cytek Biosciences	USA
Viia 7 software (v1.2.4)	Thermofisher Scientific	USA

Tab. 8 List of buffers and solutions used in this study

Article	**Concentration**	**Composition**	**County**
PBS, pH 7,4	1,5 mM	KH2PO4	
	6,5 mM	Na2HPO4	
	2,7 mM	KCl	
	137 mM	NaCl	
		in Distilled water	
FACS-Buffer	EDTA	2 mM	Carl Roth, Germany
	FCS	2 %	Carl Roth, Germany
	NaN3	0.01 %	Merck, Germany
		in PBS	
MACS-Buffer	EDTA	2 mM	Carl Roth, Germany
	BSA	1 %	Carl Roth, Germany
		in PBS	
Differentiation Medium	Rspo1	10 %	
	Wnt	30 %	
	P/S	1 %	
	L-Glutamin	1 %	Gibco, USA
	B27	2 %	Life Technologies, USA
	N2	1 %	Life Technologies, USA
	N-acetylcysteine	1 mM	Sigma-Aldrich, Germany
	Nicotinamide	10 mM	Sigma-Aldrich, Germany

	[Leu] Gastrin	10 nM	Sigma-Aldrich, Germany
	EGF	50 ng/ml	PeproTech, USA
	HGF	25 ng/ml	PeproTech, USA
	FGF10	100 ng/ml	PeproTech, USA
	Forskolin	10 uM	Tocris, UK
	A83-01	5 uM	Tocris, UK
		In Advanced DMEM/F12	
Expansion Medium	Rspo1	10 %	
	P/S	1 %	
	L-Glutamin	1 %	Gibco, USA
	B27	2 %	Life Technologies, USA
	N2	1 %	Life Technologies, USA
	N-acetylcysteine	1 mM	Sigma-Aldrich, Germany
	Nicotinamide	10 mM	Sigma-Aldrich, Germany
	Gastrin	10 nM	Sigma-Aldrich, Germany
	EGF	50 ng/ml	PeproTech, USA
	HGF	25 ng/ml	PeproTech, USA
	FGF10	100 ng/ml	PeproTech, USA

	Forskolin	10 uM	Tocris, UK
	A83-01	5 uM	Tocris, UK
		In Advanced DMEM/F12	
Optimized Expansion Medium			
Basal Medium	P/S	1 %	
	L-Glutamin	1 %	GIBCO
		In Advanced DMEM	
Wash Medium	FBS	1 %	
	P/S	1 %	
	Sodium Pyruvate	1 %	
		In DMEM	
Digestion Solution	Collagenase D	2,5 mg/mL	Roche, Switzerland
	DNase I	1 U/ml	Roche, Switzerland
		in EBSS	

METHODS

1. PATIENT SELECTION

A total of 11 livers from patients who attended the specialized outpatient clinic of the I. Department of Medicine, University Medical Centre Hamburg-Eppendorf (UKE), were included in this study. Diseases were diagnosed and treated following the guidelines of the European Association for the Study of the Liver (EASL)[219]. Patient characteristics are summarised in the Results section. This was a single-centre, cross-sectional study conducted in adult patients (>18 years of age) undergoing liver transplantation (LTX) for PSC (n = 5) or ALD (n = 6) at the University Medical Centre Hamburg-Eppendorf (UKE, Hamburg, Germany). Liver tissue and whole blood samples were obtained from each patient at the time of surgery, and clinical parameters were recorded immediately beforehand. The age of participants ranged from 33 to 66 years. Where possible, patients of similar age and with comparable histopathological and pharmacological backgrounds were matched in order to minimise inter-individual variability. All patients participating in this study provided written informed consent in accordance with the ethical guidelines of the Institutional Review Board of the Medical Faculty of the University of Hamburg (PV4081).

2. ISOLATION OF MONONUCLEAR CELLS FROM WHOLE BLOOD

PBMCs were isolated from whole blood collected in EDTA tubes using Ficoll density-gradient separation. Briefly, 15 mL of blood were diluted 1:2 in 1× PBS and gently layered onto 15 mL of 33/77% Ficoll in a 50 mL tube. Samples were centrifuged at 600 g for 20 minutes at room temperature, using low acceleration and no brake. The PBMC layer was then collected using a Pasteur pipette and washed twice with 1× PBS. Cells were counted immediately after the final wash.

3. THAWING OF LYMPHOCYTES

Frozen mononuclear cells were taken from long-term storage (LN_2) and directly put into a water bath of 37 °C until they were completely thawed. After washing twice in RPMI 1640 medium, cells were counted and their viability was assessed with Trypan Blue (Sigma-Aldrich, Germany).

4. MAGNETIC-ACTIVATED CELL SORTING (MACS)

$CD4^+$ T cells were enriched from freshly isolated PBMCs using the Human $CD4^+$ T Cell Isolation Kit (Miltenyi Biotec, Germany). All steps were carried out in accordance with the manufacturer's instructions.

5. IN VITRO PROLIFERATION ASSAY OF CD4+ T CELLS

Freshly isolated $CD4^+$ T cells were resuspended at a density of 5×10^6 cells/mL in RPMI 1640 medium and incubated with 5 µM CellTrace Violet (CTV; ThermoFisher Scientific, USA) for 20 minutes at 37 °C. The staining reaction was stopped by adding culture medium containing 10% fetal calf serum (FCS). For optimal proliferation, cells were subsequently cultured in RPMI 1640 supplemented with 10% FCS, 1% penicillin/streptomycin, and IL-2, in the presence of ImmunoCult™ Human CD3/CD28 T Cell Activator (STEMCELL Technologies, Canada). Half of the culture medium was replaced with fresh medium with IL-2, every three days. On day 6, dilution of CTV in viable cells was assessed by flow cytometry.

6. IN VITRO ACTIVATION AND EXPANSION OF CD4+ T CELLS FOR CO-CULTURE

PBMCs were thawed on day 1 and cultured in RPMI medium supplemented with ImmunoCult™ diluted 1:500 and with 50 U/mL IL-2 to prevent premature cell exhaustion. Every three days, 50% of the medium was then refreshed with new IL-2. After six days, CD4+ T cells were isolated from the cultured PBMCs using MACS separation (see XX) and

transferred to fresh RPMI medium containing a 1:100 dilution of ImmunoCult™ and 50 U/mL IL-2 for further expansion. Cells were maintained in culture for another three days and then on day 10, were transferred to our optimized culture medium (EM) supplemented with 5% Matrigel and 50 U/mL IL-2 for 24 h before starting co-culture experiments.

7. HUMAN INTRAHEPATIC CHOLANGIOCYTE ORGANOIDS (ICOs) ESTABLISHMENT AND EXPANSION

Tissue samples from people undergoing liver transplantation at the University Medical Centre Hamburg-Eppendorf (UKE) were collected with approval from the local Medical Ethics Board (PV4081). Liver-derived intrahepatic cholangiocyte organoids (ICOs) were isolated and cultured following an adapted version of the protocol described by Broutier et al. (2016). No more than 48 hours were allowed to elapse between liver explant and tissue processing. Liver pieces were weighed and washed in cold wash medium prior to digestion. Reagents were pre-cooled, sterile equipment was used throughout, and all possible steps were carried out on ice; centrifugation was performed at 4°C. Liver tissue was transferred to a sterile 10 cm Petri dish and finely minced using a scalpel and forceps into pieces of approximately 0.5 mm. The minced tissue was placed into gentleMACS C Tubes™ (Miltenyi Biotec, Germany) containing 5 mL of digestion solution per gram of tissue. The digestion solution consisted of Earle's Balanced Salt Solution (EBSS), collagenase D (2.5 mg/mL) and DNase I (1 U/mL). Mechanical dissociation was performed using the gentleMACS Octo Dissociator™ (Miltenyi Biotec, Germany) at 37°C for 36 minutes. Following digestion, 5 mL of pre-cooled wash medium was added to stop further enzymatic activity. The suspension was passed through a 100 µm sterile cell strainer to remove undigested debris and centrifuged at 500 g for 5 minutes at 4°C in cold basal medium. To isolate hepatoblasts, a discontinuous Percoll gradient (77%/33%) was prepared by layering 3.5 mL of 77% Percoll beneath 3.5 mL of 33% Percoll in a 15 mL tube. The cell pellet was resuspended in 3 mL of ice-cold PBS and carefully layered on top of the gradient. Samples were centrifuged at 500 g for 30 minutes at 4°C with minimal acceleration and no brake. Hepatoblasts were collected from the yellow-brown interface (~6 mL mark), transferred into a new tube and centrifuged again at 400 g for 5 minutes at 4°C in basal medium. The resulting viscous cell pellet was resuspended in Cultrex Basement Membrane Extract (BME), Type 2, at a ratio of 5 µL per 600 µL BME, thereby providing the extracellular matrix (R&D Systems, USA) required for cholangiocyte organoid formation. Domes of 60 µL were plated in 24-well plates (Corning, USA) and incubated at 37°C for 30 minutes to polymerise. Wells were then overlaid with 500 µL of differentiation medium (DM), and any remaining pellet was frozen in Recovery Cell

Culture Freezing Medium (Gibco, USA) for future use. Differentiation medium consisted of Advanced DMEM/F12 (Gibco, USA) supplemented with 1% penicillin/streptomycin, 1% GlutaMAX, 1% N2, 2% B27 (Thermo Fisher Scientific, USA), 1 mM N-acetylcysteine, 10 nM gastrin I, 10 mM nicotinamide (Sigma-Aldrich, Germany), 10% R-spondin1–conditioned medium and 30% Wnt3a–conditioned medium (home-produced from cell lines kindly provided by Prof. C.J. Kuo, Stanford University), together with 50 ng/mL EGF, 100 ng/mL FGF10, 25 ng/mL HGF (PeproTech, USA), 5 µM A83-01 and 10 µM forskolin (both Tocris Bioscience, UK). After three days, DM was replaced with Expansion Medium (EM), identical to DM but lacking Wnt3a-conditioned medium, to promote organoid maturation. Organoids were passaged at a ratio of 1:3–1:4 every week once they reached approximately 80% confluence (typically after six days), and medium was refreshed every three days to maintain optimal growth conditions

8. ORGANOID PASSAGING AND EMBEDDING IN MATRIGEL

Matrigel/Cultrex RGF BME Type 2 was thawed on ice, and basal medium was kept cold throughout the procedure. Organoid domes were split as required, typically at a ratio of 1:3. After removing the old culture medium, 500 µL of ice-cold basal medium was added to each well, and the organoids were gently resuspended and transferred to a 15 mL tube. No more than three to four domes were processed per tube. The volume was brought to 8 mL with additional ice-cold basal medium and centrifuged at 400 g for 5 minutes at 4°C. Following centrifugation, approximately 2 mL of medium was retained, and organoids were mechanically dissociated by pipetting up and down 4–5 times using a 2 mL serological pipette fitted with a 100 µL filter tip. The volume was then refilled to 8 mL with ice-cold basal medium and centrifuged again under the same conditions. After the second centrifugation, the supernatant was removed and the pellet was resuspended in Cultrex BME Type 2. For reseeding, organoids from one well were resuspended in 180–240 µL of fresh BME; when pooling three wells, up to 750 µL was used. A 60 µL droplet of the organoid–BME mixture was plated per well in 24-well flat-bottom plates (Greiner Bio-One, Germany) to form domes. Domes were allowed to settle briefly and polymerised at 37°C for 15–30 minutes. Once polymerisation was complete, 500 µL of differentiation medium was added to each well. After three days, the medium was replaced with 500 µL of expansion medium lacking Wnt but containing all other growth factors necessary to sustain organoid proliferation.

9. ORGANOID FREEZING AND LONG-TERM STORAGE

Organoids were handled as described in the splitting protocol, including thawing Matrigel/Cultrex RGF BME Type 2 on ice, keeping basal medium at 4°C, removing the supernatant, resuspending organoids in ice-cold basal medium and centrifuging at 400 g for 5 minutes at 4°C. At this stage, instead of proceeding with Matrigel embedding, the supernatant was removed and the cell pellet (corresponding to up to four domes) was resuspended in 1 mL of freezing medium (Life Technologies, USA). Organoids were then frozen at −80°C in an insulated (cotton) freezing box and transferred to liquid nitrogen after 24 hours for long-term storage.

10. ORGANOIDS STIMULATION WITH IL-17A OR SUPERNATANT OF PRE-ACTIVATED CD4+ T CELLS

Organoids were first maintained for three days in differentiation medium to allow growth and adaptation, followed by one day in expansion medium to support further development. Cultures were then stimulated for 24 h at 37°C either with recombinant human IL-17A (50 ng/mL in expansion medium; 500 µL per well) or with supernatant collected from pre-activated $CD4^+$ T cells cultured in our optimised co-culture medium. Following stimulation, the medium was removed and organoids were harvested for downstream analyses.

11. DISSOCIATION OF ORGANOIDS INTO SINGLE CELLS

The supernatant was removed, and 1 mL of cold Cell Recovery Solution (Corning, USA) was added to each well, followed by incubation on ice for up to 15 minutes. Matrigel domes were gently broken by repeated pipetting and scraping, and the suspension was transferred to a 15 mL tube. Wells were rinsed with an additional 300 µL of Cell Recovery Solution to maximise recovery, and the suspension was combined. Tubes were incubated on ice for 15 minutes, diluted to a final volume of 10 mL with cold basal medium, and centrifuged at 400 g for 5 minutes at 4°C. The supernatant was removed, leaving approximately 2 mL, and organoids were further dissociated according to the splitting protocol. The volume was again adjusted to 10 mL with basal medium and centrifuged under the same conditions. After centrifugation, the pellet was resuspended

in pre-warmed TrypLE supplemented with DNase I (200 U/mL) and incubated at 37°C. To assist dissociation, the suspension was vortexed briefly at intervals, each step followed by a 5-minute incubation at 37°C. Dissociation status was monitored microscopically by examining 10 µL aliquots as required. Optimal dissociation into single cells was typically achieved within 25–30 minutes. The reaction was stopped by diluting to 10 mL with MACS buffer (PBS 1×, 2 mM EDTA, 0.5–1% BSA), followed by centrifugation at 500 g for 5 minutes at 4°C. The pellet was resuspended in MACS buffer and used immediately for downstream applications, including flow cytometry.

12. FLOATING ORGANOID HANDLING AND SEEDING FOR CO-CULTURE

Organoids were cultured for at least three days in differentiation medium, followed by one day in expansion medium in Matrigel domes. It is important that organoids do not grow excessively large, as this may lead to collapse and loss of structure. To release organoids from the matrix, 1 mL of cold Cell Recovery Solution (Corning, USA) was added per dome and incubated for 15–30 minutes on ice. The solution was then removed and replaced with 1 mL of cold basal medium (or other medium of interest). Using cut 1000 µL pipette tips, organoids were gently resuspended and transferred into 50 mL tubes, with no more than four domes processed per tube. Tubes were left on ice for up to 1 hour to allow organoids to settle by gravity; no centrifugation was required. The supernatant was carefully removed and organoids were resuspended in the desired culture medium supplemented with 2–5% Matrigel. Organoids were then seeded into 96-well ultra-low attachment plates (Corning, USA) for co-culture. If organoids appeared collapsed or dark under the microscope, they were instead resuspended in 2–3 mL of expansion medium and transferred to 6-well ultra-low attachment plates, allowing them to recover their spherical morphology over 1–2 days. After recovery, organoids were again resuspended in cold basal medium, transferred to 50 mL tubes, allowed to settle on ice, and processed as described above.

13. CO-CULTURE OF CD4+ T CELLS WITH FLOATING ORGANOIDS

Organoids were kept in suspension according to the procedure described above, and $CD4^+$ T cells were isolated and pre-activated prior to co-culture. Typically, the yield from one Matrigel dome was sufficient to seed approximately four wells in a 96-well ultra-low attachment plate, with organoids reaching about 80% confluence. For each co-culture, organoids and $CD4^+$ T cells were resuspended together in the optimised co-culture medium, and a total of 250 µL of this suspension was added per well, corresponding to a final concentration of 2.5×10^5 $CD4^+$ T cells per well. The medium was supplemented with 50 U/mL IL-2, a 1:100 dilution of ImmunoCult™, and 2–5% Matrigel in order to sustain cell viability and activation throughout the co-culture period. Control conditions were established in parallel using the same co-culture medium. Organoid-only cultures received 50 U/mL IL-2 and 2–5% Matrigel, while $CD4^+$ T cell-only wells were maintained with 50 U/mL IL-2, a 1:100 dilution of ImmunoCult™, and 2–5% Matrigel. All conditions were kept under identical incubation and handling procedures. Organoids were always manipulated using cut P1000 filter tips to preserve their morphology and prevent physical damage. Co-cultures were maintained for 24 hours before proceeding to downstream analyses.

14. ISOLATION OF CD4+ T CELLS AND CHOLANGIOCYTE ORGANOIDS AFTER CO-CULTURE

Following co-culture, $CD4^+$ T cells and cholangiocyte organoids were isolated while maintaining all solutions and equipment on ice to preserve cell integrity and reduce matrix interference. The contents of each well were gently resuspended using a cut P1000 pipette tip, and the entire suspension from one well of a 96-well plate was passed through a 30 µm strainer placed over a FACS tube. Wells were then rinsed with 200 µL of cold basal medium, and the rinse was passed again through the same strainer to maximise recovery of $CD4^+$ T cells. To retrieve organoids, the strainer was washed with 1–2 mL of basal medium using firm pipetting with a cut tip, allowing organoids retained on the filter to be transferred into a separate 15 mL tube. Organoids were washed in basal medium and dissociated into single cells immediately prior to downstream applications, including RNA extraction or flow cytometry. In parallel, PBMCs collected in FACS tubes were centrifuged at 400 g for 5 minutes at 4°C, and pellets were resuspended in ice-cold PBS (1×) and prepared for flow cytometric staining.

15. IMMUNOFLUORESCENT SURFACE STAINING AND FLOW CYTOMETRY ANALYSIS OF CD4+ T CELLS AND ORGANOIDS

Surface staining was performed on $CD4^+$ T cells and dissociated organoid-derived cells using fluorochrome-conjugated antibodies (see Tables X and Y). $CD4^+$ T cells were incubated with the antibody panel for 15 minutes at 37°C, followed by an additional 15 minutes at room temperature. Organoid samples were incubated for 30 minutes at room temperature. Dead cells were identified and excluded using Zombie NIR or Zombie Aqua viability dyes. A multicolour spectral panel was established to assess activation and inhibitory markers on $CD4^+$ T cells, including CD4, HLA-DR, CD25, CD27, CD28, CD134/OX-40, CD137/4-1BB, CD152/CTLA-4, CD196/CCR6, CD223/LAG-3, CD278/ICOS, CD279/PD-1 and CD366/TIM-3. Organoid-derived cells were analysed for immune and adhesion-related surface markers, targeting CD40, CD54/ICAM-1, CD70, CD80, CD86, CD274/PD-L1, CD326/EpCAM and HLA-DR. An anti-CD4 antibody was included to exclude immune cell contamination by double-gating on $EpCAM^+/CD4^-$ cells. Flow cytometry was performed using a Cytek Aurora spectral cytometer (five-laser configuration). Data acquisition and spectral unmixing were carried out in SpectroFlo™ (v3.3.0). Subsequent gating and population analysis were performed in FlowJo™ (v10), and statistical analyses and visualisations were generated in GraphPad Prism (v10).

Tab. 9: CD4+ T Cell Surface Marker Panel for Flow Cytometry

Antigen	Conjugate	Clone	Company
CD4	FITC	OKT4	Biolegend, USA
HLA-DR	PE-Cy5	L243	Biolegend, USA
CD25	BUV563	M-A251	BD Biosciences, USA
CD27	BUV805	L128	BD Biosciences, USA
CD28	PE-Cy7	CD28.2	Biolegend, USA
CD134 (OX-40)	BV711	Ber-ACT35 (ACT35)	Biolegend, USA
CD137 (4-1BB)	AF594	145501	R&D Systems, USA
CD152 (CTLA-4)	PE-Dazzle594	L3D10	Biolegend, USA
	APC-Fire750	L3D10	Biolegend, USA
CD196 (CCR6)	BUV737	11A9	BD Biosciences, USA
CD223 (LAG-3)	PE	11C3C65	Biolegend, USA
	AF647	11C3C65	Biolegend, USA
CD278 (ICOS)	AF700	C398.4.A	Biolegend, USA
CD279 (PD-1)	BV785	EH12.2H7	Biolegend, USA
CD366 (TIM-3)	BV605	F38-2E2	Biolegend, USA
Live/Dead	Zombie NIR		
	Zombie Aqua		

Table 10: Organoid Surface Marker Panel for Flow Cytometry

Antigen	Conjugate	Clone	Company
CD4	V500	L200	BD Biosciences, USA
	AF700	OKT4	Biolegend, USA
CD40	BV750	5C3	BD Biosciences, USA
CD54 (ICAM-1)	Pacific Blue	HCD54	Biolegend, USA
CD70	BUV737	Ki-24	BD Biosciences, USA
CD80	PE	QA18A16	Biolegend, USA
CD86	AF594	37301	R&D Systems, USA
CD274 (PD-L1)	PE-Cy7	29E.2A3	Biolegend, USA
CD326 (EPCAM)	APC	9C4	Biolegend, USA
HLA-DR	FITC	L243	Biolegend, USA
Live/Dead	Zombie NIR		
	Zombie Aqua		

16. GENE EXPRESSION ANALYSIS IN ORGANOIDS

Total RNA was isolated from corganoids, after breaking them into single cells, using the NucleoSpin RNA Kit, and cDNA was then prepared using the High-Capacity cDNA Reverse Transcription Kit. All kits were used according to the manufacturers' protocols. For quantitative real-time PCR, the mRNA expression of the genes was analysed using TaqMan™ Fast Advanced Master Mix and TaqMan™ Gene Expression Assays tool. The primer sequences and genes are listed in Table 11. Target gene expression were normalised to HPRT mRNA expression, and relative fold changes were calculated using the ΔΔCt method, as in the following equations:

$$\Delta Ct = Ct_{HPRT} - Ct_{target\ gene}$$

$$\Delta\Delta Ct = \Delta Ct_{sample} - \Delta Ct_{control\ group}$$

$$\text{x-fold expression} = 2^{-\Delta\Delta Ct}$$

Table 11: TaqMan Gene Expression Assays

Symbol	***Gene Name***	***Chromosome Location on Build GRCh38***	***Assay-ID***	***Company***
BCL2	B-cell lymphoma 2	Chr.18: 63123346 - 63319778	Hs00608023_m1	Thermo Fisher, USA
MCL1	Myeloid cell leukemia 1	Chr.1: 150574551 - 150579738	Hs01050896_m1	Thermo Fisher, USA
BAK1	BCL2 antagonist/killer 1	Chr.6: 33572552 - 33580276	Hs00940249_m1	Thermo Fisher, USA
CASP7	Caspase 7	Chr.10: 113679162 - 113730909	Hs00169152_m1	Thermo Fisher, USA
FOS	FBJ murine osteosarcoma viral oncogene homolog	Chr.14: 75278778 - 75282234	Hs00170630_m1	Thermo Fisher, USA

TNF	Tumor necrosis factor	Chr.6: 31575567 - 31578336	Hs00174128_m1	Thermo Fisher, USA
FASL	Fas ligand	Chr.1: 172659008 - 172666873	Hs00181225_m1	Thermo Fisher, USA
EPCAM	Epithelial cell adhesion molecule	Chr.2: 47369148 - 47387028	Hs00158980_m1	Thermo Fisher, USA
KRT19	Keratin 19	Chr.17: 41523617 - 41528389	Hs00761767_s1	Thermo Fisher, USA
KRT7	Keratin 7	Chr.12: 52233170 - 52252667	Hs00559840_m1	Thermo Fisher, USA
LGR5	Leucine-rich repeat-containing G-protein coupled receptor 5	Chr.12: 71439770 - 71586310	Hs00969422_m1	Thermo Fisher, USA
GPBAR1	G protein-coupled bile acid receptor 1	Chr.2: 218259496 - 218263861	Hs00544894_m1	Thermo Fisher, USA
SOX9	SRY-box transcription factor 9	Chr.17: 72121020 - 72126420	Hs00165814_m1	Thermo Fisher, USA
ALB	Albumin	Chr.4: 73404255 - 73421412	Hs00910225_m1	Thermo Fisher, USA
CFTR	Cystic fibrosis transmembrane conductance regulator	Chr.7: 117478367 - 117668665	Hs00357011_m1	Thermo Fisher, USA

AQP1	Aquaporin 1	Chr.7: 30911800 - 30925516	Hs01028916_m1	Thermo Fisher, USA
HPRT1	Hypoxanthine phosphoribosyltransferase 1	Chr.X: 134460145 - 134500668	Hs02800695_m1	Thermo Fisher, USA
CD80	CD80 molecule	Chr.3: 119523909 - 119559709	Hs01045161_m1	Thermo Fisher, USA
CD86	CD86 molecule	Chr.3: 122055362 - 122121143	Hs01567026_m1	Thermo Fisher, USA
HLA-DR	Major histocompatibility complex, class II, DR	Chr.6: 32439842 - 32445046	Hs00219575_m1	Thermo Fisher, USA
CD274	CD274 molecule (PD-L1)	Chr.9: 5450503 - 5470567	Hs00204257_m1	Thermo Fisher, USA
ICAM-1	Intercellular adhesion molecule 1	Chr.19: 10270841 - 10286615	Hs00164932_m1	Thermo Fisher, USA
MKI67	Marker of proliferation Ki-67	Chr.10: 128096659 - 128126405	Hs00606991_m1	Thermo Fisher, USA
TNFSF4	Tumor necrosis factor superfamily member 4	Chr.1: 173183729 - 173462208	Hs00967195_m1	Thermo Fisher, USA
CD70	CD70 molecule	Chr.19: 6581646 - 6591152	Hs00174297_m1	Thermo Fisher, USA

TNFSF9	Tumor necrosis factor superfamily member 9	Chr.19: 6530999 - 6535928	Hs00169409_m1	Thermo Fisher, USA

17. STATISTICAL ANALYSES

Statistical analyses were performed using GraphPad Prism (v10). Differences between 2 groups were calculated using the Mann-Whitney U test after calculation of p values, by setting error α to the conventional 0.05, for all analyses. Significant differences were marked as follows: ****: $p < 0.0001$; ***: $p < 0.001$; **: $p < 0.01$; *: $p < 0.05$.

18. TRANSCRIPTOMIC ANALYSIS OF IL-17A-STIMULATED AND NON-STIMULATED ORGANOIDS USING MICROARRAY TECHNOLOGY

Organoids were stimulated with IL-17A for 24 hours, dissociated into single cells, and total RNA was extracted for transcriptomic profiling. RNA samples were analysed by ATLAS Biolabs GmbH (Berlin, Germany) using the Clariom™ S Human Assay (Applied Biosystems™), a high-throughput microarray platform that provides broad transcriptome coverage and allows sensitive detection of both coding and non-coding RNA species. Raw .CEL files were processed in R (version 4.4.2). Data preprocessing was performed using the *oligo* package and included background correction, $\log_2$ transformation and Robust Multi-array Average (RMA) normalisation to standardise expression values across samples. Differential expression analysis was conducted with *limma*, fitting linear models to each transcript cluster and applying empirical Bayes moderation to stabilise variance estimates. Experimental groups were defined according to stimulation conditions, and statistical contrasts were generated to identify differentially expressed genes. Genes were considered significantly regulated when displaying $p < 0.05$ and an absolute $\log_2$ fold change greater than one. Annotation was carried out using the Clariom_S_Human.r1.na36.hg38.a1.transcript.csv reference file, mapping transcript cluster IDs to gene symbols and retaining only valid annotated entries. Expression patterns were visualised using the *pheatmap* package, enabling hierarchical clustering of differentially expressed genes and comparison between experimental conditions.

Functional enrichment analysis was performed with *clusterProfiler*. Gene symbols were converted to Entrez Gene IDs using *org.Hs.eg.db*, and over-representation analyses were conducted against KEGG pathways and Gene Ontology (GO) categories to identify biological processes and signalling pathways significantly enriched among the differentially expressed genes.

SAFETY

All experiments in this study were conducted following biosafety level 1 and 2 guidelines, ensuring proper handling of cell cultures, reagents, and laboratory materials. Processing of explanted liver tissue was performed in laboratories with biosafety level 3 (BSL-3), following strict containment measures to prevent contamination and exposure to potentially infectious materials. The use of chemical reagents and biological samples was performed under controlled laboratory conditions to minimize exposure risks. Several reagents used in this study pose potential health hazards and require proper precautions during handling. The Globally Harmonized System (GHS) classification, CAS numbers, hazard (H) statements, and precautionary (P) statements for the most critical chemicals are summarized in table below:

Article	***GHS Classification***	***CAS Number***	***H-Statements***	***P-Statements***
CellTrace™ Violet Cell Proliferation Kit	Warning	67-68-5	227	210-280
Collagenase D	Warning	2593923	H315, H319, H334	P261, P280, P305 + P351 + P338
DMEM/F12 (with Phenol Red)	Warning	143-74-8	H341, H351	P201, P281
DMSO	Warning	67-68-5	227	210-280
Forskolin	Warning	66575-29-9	H302, H315, H319	P264, P270, P280, P301+P312
L-Glutamine	Warning	56-85-9	H319	P264, P280, P305+P351+ P338

N-acetylcysteine	Warning	616-91-1	H315, H319	P280, P302+P352, P305+P351+ P338
NaN_3	Danger	26628-22-8	H300, H310, H330, H373	P260, P264, P280, P301+P310
Nicotinamide	Warning	98-92-0	H315, H319	P264, P280, P305+P351+ P338
Penicillin/Streptomycin	Warning	69-57-8 (Pen), 3810-74-0 (Strep)	H317	P261, P272, P280, P302+P352
RBC Lysis/Fixation Solution (10X)	Danger	111-46-6, 50-00-0	H331, H302, H319, H315, H317, H350, H341, H335, H373	P201, P202, P280, P271, P260, P270, P264, P272
Sodium Pyruvate	Warning	113-24-6	H315, H319	P280, P305 + P351 + P338
Trypan Blue Solution (0.4%)	Warning	72-57-1	H341, H350	P201, P281
TrypLE™ Express Enzyme (1x), Phenol Red	Warning	143-74-8	H341, H351	P201, P281
Zombie Aqua™ Fixable Viability Kit	Danger	50-00-0	H350, H341, H317, H314	P201, P280, P305+P351+ P338
Zombie NIR™ Fixable Viability Kit	Danger	50-00-0	H350, H341, H317, H314	P201, P280, P305+P351+ P338
β-Mercaptoethanol	Danger	60-24-2	H301, H312, H331, H373	P261, P280, P301 + P310

BIBLIOGRAFY

1. Invernizzi P. Liver auto-immunology: The paradox of autoimmunity in a tolerogenic organ. J Autoimmun. 2013;46:1-6. doi:10.1016/j.jaut.2013.08.006
2. Gao B, Jeong WI, Tian Z. Liver: An organ with predominant innate immunity. Hepatology. 2008;47(2):729-736. doi:10.1002/hep.22034
3. Parker GA, Picut CA. Immune Functioning in Non lymphoid Organs: The Liver. Toxicol Pathol. 2012;40(2):237-247. doi:10.1177/0192623311428475
4. Racanelli V, Rehermann B. The Liver as an Immunological Organ. Hepatology. 2006;43(Supplement 1):S54-S62. doi:10.1002/hep.21060
5. Elvevold K, Smedsrød B, Martinez I. The liver sinusoidal endothelial cell: a cell type of controversial and confusing identity. Am J Physiol-Gastrointest Liver Physiol. 2008;294(2):G391-G400. doi:10.1152/ajpgi.00167.2007
6. Ludwig J, Ritman EL, LaRusso NF, Sheedy PF, Zumpe G. Anatomy of the human biliary system studied by quantitative computer-aided three-dimensional imaging techniques. Hepatology. 1998;27(4):893-899. doi:10.1002/hep.510270401
7. Kanno N, LeSage G, Glaser S, Alvaro D, Alpini G. Functional heterogeneity of the intrahepatic biliary epithelium. Hepatology. 2000;31(3):555-561. doi:10.1002/hep.510310302
8. Alpini G, McGill JM, LaRusso NF. The pathobiology of biliary epithelia. Hepatology. 2002;35(5):1256-1268. doi:10.1053/jhep.2002.33541
9. Ludwig J. New Concepts in Biliary Cirrhosis. Semin Liver Dis. 1987;7(04):293-301. doi:10.1055/s-2008-1040584
10. Benedetti A, Bassotti C, Rapino K, Marucci L, Jezequel AM. A morphometric study of the epithelium lining the rat intrahepatic biliary tree. J Hepatol. 1996;24(3):335-342. doi:10.1016/S0168-8278(96)80014-6
11. Maroni L, Haibo B, Ray D, et al. Functional and structural features of cholangiocytes in health and disease. Cell Mol Gastroenterol Hepatol. 2015;1(4):368-380. doi:10.1016/j.jcmgh.2015.05.005
12. LaRusso NF, Ishii M, Vroman BT. The ins and outs of membrane movement in biliary epithelia. Trans Am Clin Climatol Assoc. 1991;102:245-258; discussion 258-259.
13. Masyuk AI, Masyuk TV, LaRusso NF. Cholangiocyte primary cilia in liver health and disease. Dev Dyn. 2008;237(8):2007-2012. doi:10.1002/dvdy.21530
14. Sasaki H, Schaffner F, Popper H. Bile ductules in cholestasis: morphologic evidence for secretion and absorption in man. Lab Investig J Tech Methods Pathol. 1967;16(1):84-95.
15. Francis H, Glaser S, DeMorrow S, et al. Small mouse cholangiocytes proliferate in response to H1 histamine receptor stimulation by activation of the IP3 /CaMK I/CREB pathway. Am J Physiol-Cell Physiol. 2008;295(2):C499-C513. doi:10.1152/ajpcell.00369.2007
16. Schaffner F, Popper H. Electron microscopic studies of normal and proliferated bile ductules. Am J Pathol. 1961;38(4):393-410.
17. Glaser SS, Gaudio E, Rao A, et al. Morphological and functional heterogeneity of the mouse intrahepatic biliary epithelium. Lab Invest. 2009;89(4):456-469. doi:10.1038/labinvest.2009.6

18. Alpini G, Glaser S, Robertson W, et al. Large but not small intrahepatic bile ducts are involved in secretin-regulated ductal bile secretion. Am J Physiol-Gastrointest Liver Physiol. 1997;272(5):G1064-G1074. doi:10.1152/ajpgi.1997.272.5.G1064
19. Antoniou A, Raynaud P, Cordi S, et al. Intrahepatic Bile Ducts Develop According to a New Mode of Tubulogenesis Regulated by the Transcription Factor SOX9. Gastroenterology. 2009;136(7):2325-2333. doi:10.1053/j.gastro.2009.02.051
20. Zong Y, Panikkar A, Xu J, et al. Notch signaling controls liver development by regulating biliary differentiation. Dev Camb Engl. 2009;136(10):1727-1739. doi:10.1242/dev.029140
21. Alpini G, Roberts S, Kuntz S, et al. Morphological, molecular, and functional heterogeneity of cholangiocytes from normal rat liver. Gastroenterology. 1996;110(5):1636-1643. doi:10.1053/gast.1996.v110.pm8613073
22. Afroze S, Meng F, Jensen K, et al. The physiological roles of secretin and its receptor. Ann Transl Med. 2013;1(3):29. doi:10.3978/j.issn.2305-5839.2012.12.01
23. Hohenester S, Wenniger LM de B, Paulusma CC, et al. A biliary HCO3- umbrella constitutes a protective mechanism against bile acid-induced injury in human cholangiocytes. Hepatol Baltim Md. 2012;55(1):173-183. doi:10.1002/hep.24691
24. Boyer JL. Bile Formation and Secretion. In: Terjung R, ed. Comprehensive Physiology. 1st ed. Wiley; 2013:1035-1078. doi:10.1002/cphy.c120027
25. Tabibian JH, Masyuk AI, Masyuk TV, O'Hara SP, LaRusso NF. Physiology of Cholangiocytes. In: Prakash YS, ed. Comprehensive Physiology. 1st ed. Wiley; 2013:541-565. doi:10.1002/cphy.c120019
26. Trauner M, Boyer JL. Bile Salt Transporters: Molecular Characterization, Function, and Regulation. Physiol Rev. 2003;83(2):633-671. doi:10.1152/physrev.00027.2002
27. Syal G, Fausther M, Dranoff JA. Advances in cholangiocyte immunobiology. Am J Physiol Gastrointest Liver Physiol. 2012;303(10):G1077-1086. doi:10.1152/ajpgi.00227.2012
28. Woo K, Sathe M, Kresge C, et al. Adenosine Triphosphate Release and Purinergic (P2) Receptor–Mediated Secretion in Small and Large Mouse Cholangiocytes. Hepatology. 2010;52(5):1819-1828. doi:10.1002/hep.23883
29. Dutta AK, Khimji A karim, Kresge C, et al. Identification and Functional Characterization of TMEM16A, a Ca2+-activated Cl− Channel Activated by Extracellular Nucleotides, in Biliary Epithelium. J Biol Chem. 2011;286(1):766-776. doi:10.1074/jbc.M110.164970
30. Guerrier M, Attili F, Alpini G, Glaser S. Prolonged administration of secretin to normal rats increases biliary proliferation and secretin-induced ductal secretory activity. Hepatobiliary Surg Nutr. 2014;3(3):118-125. doi:10.3978/j.issn.2304-3881.2014.04.04
31. Sato K, Meng F, Venter J, Giang T, Glaser S, Alpini G. The role of the secretin/secretin receptor axis in inflammatory cholangiocyte communication via extracellular vesicles. Sci Rep. 2017;7(1):11183. doi:10.1038/s41598-017-10694-3
32. Cardinale V, Wang Y, Carpino G, et al. Multipotent stem/progenitor cells in human biliary tree give rise to hepatocytes, cholangiocytes, and pancreatic islets. Hepatology. 2010;54(6):2159-2172. doi:10.1002/hep.24590
33. Turner R, Lozoya O, Wang Y, et al. Human Hepatic Stem Cell and Maturational Liver Lineage Biology Δ. Hepatology. 2011;53(3):1035-1045. doi:10.1002/hep.24157

34. Carpentier R, Suñer RE, van Hul N, et al. Embryonic ductal plate cells give rise to cholangiocytes, periportal hepatocytes, and adult liver progenitor cells. Gastroenterology. 2011;141(4):1432-1438, 1438.e1-4. doi:10.1053/j.gastro.2011.06.049
35. Fickert P, Stöger U, Fuchsbichler A, et al. A new xenobiotic-induced mouse model of sclerosing cholangitis and biliary fibrosis. Am J Pathol. 2007;171(2):525-536. doi:10.2353/ajpath.2007.061133
36. Alpini G, Glaser SS, Ueno Y, et al. Heterogeneity of the proliferative capacity of rat cholangiocytes after bile duct ligation. Am J Physiol. 1998;274(4):G767-775. doi:10.1152/ajpgi.1998.274.4.G767
37. Sato K, Marzioni M, Meng F, Francis H, Glaser S, Alpini G. Ductular Reaction in Liver Diseases: Pathological Mechanisms and Translational Significances. Hepatology. 2019;69(1):420-430. doi:10.1002/hep.30150
38. Banales JM, Huebert RC, Karlsen T, Strazzabosco M, LaRusso NF, Gores GJ. Cholangiocyte pathobiology. Nat Rev Gastroenterol Hepatol. 2019;16(5):269-281. doi:10.1038/s41575-019-0125-y
39. Chen XM, O'Hara SP, LaRusso NF. The immunobiology of cholangiocytes. Immunol Cell Biol. 2008;86(6):497-505. doi:10.1038/icb.2008.37
40. Yokoyama T, Komori A, Nakamura M, et al. Human intrahepatic biliary epithelial cells function in innate immunity by producing IL-6 and IL-8 via the TLR4-NF-kappaB and -MAPK signaling pathways. Liver Int Off J Int Assoc Study Liver. 2006;26(4):467-476. doi:10.1111/j.1478-3231.2006.01254.x
41. Mueller T, Beutler C, Picó AH, et al. Enhanced innate immune responsiveness and intolerance to intestinal endotoxins in human biliary epithelial cells contributes to chronic cholangitis. Liver Int Off J Int Assoc Study Liver. 2011;31(10):1574-1588. doi:10.1111/j.1478-3231.2011.02635.x
42. Chen XM, O'Hara SP, Nelson JB, et al. Multiple TLRs are expressed in human cholangiocytes and mediate host epithelial defense responses to Cryptosporidium parvum via activation of NF-kappaB. J Immunol Baltim Md 1950. 2005;175(11):7447-7456. doi:10.4049/jimmunol.175.11.7447
43. Matsushita H, Miyake Y, Takaki A, et al. TLR4, TLR9, and NLRP3 in biliary epithelial cells of primary sclerosing cholangitis: relationship with clinical characteristics. J Gastroenterol Hepatol. 2015;30(3):600-608. doi:10.1111/jgh.12711
44. Harada K, Nakanuma Y. Biliary innate immunity and cholangiopathy. Hepatol Res Off J Jpn Soc Hepatol. 2007;37 Suppl 3:S430-437. doi:10.1111/j.1872-034X.2007.00247.x
45. Tian J, Yang G, Chen HY, et al. Galectin-3 regulates inflammasome activation in cholestatic liver injury. FASEB J Off Publ Fed Am Soc Exp Biol. 2016;30(12):4202-4213. doi:10.1096/fj.201600392RR
46. Maroni L, Agostinelli L, Saccomanno S, et al. Nlrp3 Activation Induces Il-18 Synthesis and Affects the Epithelial Barrier Function in Reactive Cholangiocytes. Am J Pathol. 2017;187(2):366-376. doi:10.1016/j.ajpath.2016.10.010
47. Hu G, Gong AY, Liu J, Zhou R, Deng C, Chen XM. miR-221 suppresses ICAM-1 translation and regulates interferon-gamma-induced ICAM-1 expression in human cholangiocytes. Am J Physiol Gastrointest Liver Physiol. 2010;298(4):G542-550. doi:10.1152/ajpgi.00490.2009
48. Heydtmann M, Lalor PF, Eksteen JA, Hübscher SG, Briskin M, Adams DH. CXC chemokine ligand 16 promotes integrin-mediated adhesion of liver-infiltrating

lymphocytes to cholangiocytes and hepatocytes within the inflamed human liver. J Immunol Baltim Md 1950. 2005;174(2):1055-1062. doi:10.4049/jimmunol.174.2.1055
49. Afford SC, Humphreys EH, Reid DT, et al. Vascular cell adhesion molecule 1 expression by biliary epithelium promotes persistence of inflammation by inhibiting effector T-cell apoptosis. Hepatol Baltim Md. 2014;59(5):1932-1943. doi:10.1002/hep.26965
50. Leon MP, Bassendine MF, Gibbs P, Thick M, Kirby JA. Immunogenicity of biliary epithelium: study of the adhesive interaction with lymphocytes. Gastroenterology. 1997;112(3):968-977. doi:10.1053/gast.1997.v112.pm9041260
51. Fava G, Glaser S, Francis H, Alpini G. The immunophysiology of biliary epithelium. Semin Liver Dis. 2005;25(3):251-264. doi:10.1055/s-2005-916318
52. Cruickshank SM, Southgate J, Selby PJ, Trejdosiewicz LK. Expression and cytokine regulation of immune recognition elements by normal human biliary epithelial and established liver cell lines in vitro. J Hepatol. 1998;29(4):550-558. doi:10.1016/s0168-8278(98)80149-9
53. Ayres RC, Neuberger JM, Shaw J, Joplin R, Adams DH. Intercellular adhesion molecule-1 and MHC antigens on human intrahepatic bile duct cells: effect of pro-inflammatory cytokines. Gut. 1993;34(9):1245-1249. doi:10.1136/gut.34.9.1245
54. Broomé U, Scheynius A, Hultcrantz R. Induced expression of heat-shock protein on biliary epithelium in patients with primary sclerosing cholangitis and primary biliary cirrhosis. Hepatol Baltim Md. 1993;18(2):298-303. doi:10.1002/hep.1840180212
55. Godfrey DI, Uldrich AP, McCluskey J, Rossjohn J, Moody DB. The burgeoning family of unconventional T cells. Nat Immunol. 2015;16(11):1114-1123. doi:10.1038/ni.3298
56. Jeffery HC, Van Wilgenburg B, Kurioka A, et al. Biliary epithelium and liver B cells exposed to bacteria activate intrahepatic MAIT cells through MR1. J Hepatol. 2016;64(5):1118-1127. doi:10.1016/j.jhep.2015.12.017
57. Schrumpf E, Tan C, Karlsen TH, et al. The biliary epithelium presents antigens to and activates natural killer T cells. Hepatol Baltim Md. 2015;62(4):1249-1259. doi:10.1002/hep.27840
58. Kamihira T, Shimoda S, Nakamura M, et al. Biliary epithelial cells regulate autoreactive T cells: implications for biliary-specific diseases. Hepatol Baltim Md. 2005;41(1):151-159. doi:10.1002/hep.20494
59. Iwai Y, Terawaki S, Ikegawa M, Okazaki T, Honjo T. PD-1 inhibits antiviral immunity at the effector phase in the liver. J Exp Med. 2003;198(1):39-50. doi:10.1084/jem.20022235
60. Stein S, Henze L, Poch T, et al. IL-17A/F enable cholangiocytes to restrict T cell-driven experimental cholangitis by upregulating PD-L1 expression. J Hepatol. 2021;74(4):919-930. doi:10.1016/j.jhep.2020.10.035
61. Lazaridis KN, Strazzabosco M, Larusso NF. The cholangiopathies: disorders of biliary epithelia. Gastroenterology. 2004;127(5):1565-1577. doi:10.1053/j.gastro.2004.08.006
62. European Association for the Study of the Liver. EASL Clinical Practice Guidelines: Management of cholestatic liver diseases. J Hepatol. 2009;51(2):237-267. doi:10.1016/j.jhep.2009.04.009
63. Rajapaksha IG, Angus PW, Herath CB. Current therapies and novel approaches for biliary diseases. World J Gastrointest Pathophysiol. 2019;10(1):1-10. doi:10.4291/wjgp.v10.i1.1

64. Karlsen TH, Folseraas T, Thorburn D, Vesterhus M. Primary sclerosing cholangitis - a comprehensive review. J Hepatol. 2017;67(6):1298-1323. doi:10.1016/j.jhep.2017.07.022
65. Aron JH, Bowlus CL. The immunobiology of primary sclerosing cholangitis. Semin Immunopathol. 2009;31(3):383-397. doi:10.1007/s00281-009-0154-7
66. Grant AJ, Lalor PF, Salmi M, Jalkanen S, Adams DH. Homing of mucosal lymphocytes to the liver in the pathogenesis of hepatic complications of inflammatory bowel disease. Lancet Lond Engl. 2002;359(9301):150-157. doi:10.1016/S0140-6736(02)07374-9
67. Tabibian JH, O'Hara SP, Splinter PL, Trussoni CE, LaRusso NF. Cholangiocyte senescence by way of N-ras activation is a characteristic of primary sclerosing cholangitis. Hepatology. 2014;59(6):2263-2275. doi:10.1002/hep.26993
68. Lemoinne S, Cadoret A, Rautou P, et al. Portal myofibroblasts promote vascular remodeling underlying cirrhosis formation through the release of microparticles. Hepatology. 2015;61(3):1041-1055. doi:10.1002/hep.27318
69. Mederacke I, Hsu CC, Troeger JS, et al. Fate tracing reveals hepatic stellate cells as dominant contributors to liver fibrosis independent of its aetiology. Nat Commun. 2013;4(1):2823. doi:10.1038/ncomms3823
70. Penz-Österreicher M, Österreicher CH, Trauner M. Fibrosis in Autoimmune and Cholestatic Liver Disease. Best Pract Res Clin Gastroenterol. 2011;25(2):245-258. doi:10.1016/j.bpg.2011.02.001
71. Rupp C, Bode KA, Chahoud F, et al. Risk factors and outcome in patients with primary sclerosing cholangitis with persistent biliary candidiasis. BMC Infect Dis. 2014;14(1):562. doi:10.1186/s12879-014-0562-8
72. Boonstra K, Beuers U, Ponsioen CY. Epidemiology of primary sclerosing cholangitis and primary biliary cirrhosis: A systematic review. J Hepatol. 2012;56(5):1181-1188. doi:10.1016/j.jhep.2011.10.025
73. Chapman MH, Thorburn D, Hirschfield GM, et al. British Society of Gastroenterology and UK-PSC guidelines for the diagnosis and management of primary sclerosing cholangitis. Gut. 2019;68(8):1356-1378. doi:10.1136/gutjnl-2018-317993
74. Loftus EV. PSC-IBD: a unique form of inflammatory bowel disease associated with primary sclerosing cholangitis. Gut. 2005;54(1):91-96. doi:10.1136/gut.2004.046615
75. Tabibian JH, Trussoni CE, O'Hara SP, Splinter PL, Heimbach JK, LaRusso NF. Characterization of cultured cholangiocytes isolated from livers of patients with primary sclerosing cholangitis. Lab Invest. 2014;94(10):1126-1133. doi:10.1038/labinvest.2014.94
76. Borchers AT, Shimoda S, Bowlus C, Keen CL, Gershwin ME. Lymphocyte recruitment and homing to the liver in primary biliary cirrhosis and primary sclerosing cholangitis. Semin Immunopathol. 2009;31(3):309-322. doi:10.1007/s00281-009-0167-2
77. Bo X. Tumour necrosis factor alpha impairs function of liver derived T lymphocytes and natural killer cells in patients with primary sclerosing cholangitis. Gut. 2001;49(1):131-141. doi:10.1136/gut.49.1.131
78. Sebode M, Peiseler M, Franke B, et al. Reduced FOXP3+ regulatory T cells in patients with primary sclerosing cholangitis are associated with IL2RA gene polymorphisms. J Hepatol. 2014;60(5):1010-1016. doi:10.1016/j.jhep.2013.12.027

79. Katt J, Schwinge D, Schoknecht T, et al. Increased T Helper Type 17 Response To Pathogen Stimulation in Patients With Primary Sclerosing Cholangitis. Hepatology. 2013;58(3):1084-1093. doi:10.1002/hep.26447
80. Hirschfield GM, Heathcote EJ, Gershwin ME. Pathogenesis of Cholestatic Liver Disease and Therapeutic Approaches. Gastroenterology. 2010;139(5):1481-1496. doi:10.1053/j.gastro.2010.09.004
81. Martins EB, Graham AK, Chapman RW, Fleming KA. Elevation of γδ T lymphocytes in peripheral blood and livers of patients with primary sclerosing cholangitis and other autoimmune liver diseases. Hepatology. 1996;23(5):988-993. doi:10.1002/hep.510230508
82. Von Seth E, Zimmer CL, Reuterwall-Hansson M, et al. Primary sclerosing cholangitis leads to dysfunction and loss of MAIT cells. Eur J Immunol. 2018;48(12):1997-2004. doi:10.1002/eji.201847608
83. Burak K, Angulo P, Pasha TM, Egan K, Petz J, Lindor KD. Incidence and Risk Factors for Cholangiocarcinoma in Primary Sclerosing Cholangitis. Am J Gastroenterol. 2004;99(3):523-526. doi:10.1111/j.1572-0241.2004.04067.x
84. Aune D, Sen A, Norat T, Riboli E, Folseraas T. Primary sclerosing cholangitis and the risk of cancer, cardiovascular disease, and all-cause mortality: a systematic review and meta-analysis of cohort studies. Sci Rep. 2021;11(1):10646. doi:10.1038/s41598-021-90175-w
85. Liang H, Manne S, Shick J, Lissoos T, Dolin P. Incidence, prevalence, and natural history of primary sclerosing cholangitis in the United Kingdom. Medicine (Baltimore). 2017;96(24):e7116. doi:10.1097/MD.0000000000007116
86. Lindor KD, Bowlus CL, Boyer J, Levy C, Mayo M. Primary Biliary Cholangitis: 2018 Practice Guidance from the American Association for the Study of Liver Diseases. Hepatology. 2019;69(1):394-419. doi:10.1002/hep.30145
87. Fosby B. Recurrence and rejection in liver transplantation for primary sclerosing cholangitis. World J Gastroenterol. 2012;18(1):1. doi:10.3748/wjg.v18.i1.1
88. Vos T, Lim SS, Abbafati C, et al. Global burden of 369 diseases and injuries in 204 countries and territories, 1990–2019: a systematic analysis for the Global Burden of Disease Study 2019. The Lancet. 2020;396(10258):1204-1222. doi:10.1016/S0140-6736(20)30925-9
89. Wang W, Wang C, Xu H, Gao Y. Aldehyde Dehydrogenase, Liver Disease and Cancer. Int J Biol Sci. 2020;16(6):921-934. doi:10.7150/ijbs.42300
90. Charatcharoenwitthaya P, Liangpunsakul S, Piratvisuth T. Alcohol-Associated Liver Disease: East Versus West. Clin Liver Dis. 2020;16(6):231-235. doi:10.1002/cld.920
91. Huang DQ, Mathurin P, Cortez-Pinto H, Loomba R. Global epidemiology of alcohol-associated cirrhosis and HCC: trends, projections and risk factors. Nat Rev Gastroenterol Hepatol. 2023;20(1):37-49. doi:10.1038/s41575-022-00688-6
92. Ilyas F, Ali H, Patel P, et al. Increasing nonalcoholic fatty liver disease–related mortality rates in the United States from 1999 to 2022. Hepatol Commun. 2023;7(7). doi:10.1097/HC9.0000000000000207
93. Anouti A, Mellinger JL. The Changing Epidemiology of Alcohol-Associated Liver Disease: Gender, Race, and Risk Factors. Semin Liver Dis. 2023;43(01):050-059. doi:10.1055/a-2000-6680
94. Rehm J, Samokhvalov AV, Shield KD. Global burden of alcoholic liver diseases. J Hepatol. 2013;59(1):160-168. doi:10.1016/j.jhep.2013.03.007

95. Gao B, Ahmad MF, Nagy LE, Tsukamoto H. Inflammatory pathways in alcoholic steatohepatitis. J Hepatol. 2019;70(2):249-259. doi:10.1016/j.jhep.2018.10.023
96. Huang DQ, Singal AG, Kono Y, Tan DJH, El-Serag HB, Loomba R. Changing global epidemiology of liver cancer from 2010 to 2019: NASH is the fastest growing cause of liver cancer. Cell Metab. 2022;34(7):969-977.e2. doi:10.1016/j.cmet.2022.05.003
97. Szabo G, Mandrekar P. A Recent Perspective on Alcohol, Immunity, and Host Defense. Alcohol Clin Exp Res. 2009;33(2):220-232. doi:10.1111/j.1530-0277.2008.00842.x
98. Maccioni L, Fu Y, Horsmans Y, et al. Alcohol-associated bowel disease: new insights into pathogenesis. eGastroenterology. 2023;1(1):e100013. doi:10.1136/egastro-2023-100013
99. Tripathi A, Debelius J, Brenner DA, et al. The gut–liver axis and the intersection with the microbiome. Nat Rev Gastroenterol Hepatol. 2018;15(7):397-411. doi:10.1038/s41575-018-0011-z
100. Cassard AM, Ciocan D. Microbiota, a key player in alcoholic liver disease. Clin Mol Hepatol. 2018;24(2):100-107. doi:10.3350/cmh.2017.0067
101. Khan RS, Lalor PF, Thursz M, Newsome PN. The role of neutrophils in alcohol-related hepatitis. J Hepatol. 2023;79(4):1037-1048. doi:10.1016/j.jhep.2023.05.017
102. Cho Y, Bukong TN, Tornai D, et al. Neutrophil extracellular traps contribute to liver damage and increase defective low-density neutrophils in alcohol-associated hepatitis. J Hepatol. 2023;78(1):28-44. doi:10.1016/j.jhep.2022.08.029
103. Wu X, Fan X, Miyata T, et al. Recent Advances in Understanding of Pathogenesis of Alcohol-Associated Liver Disease. Annu Rev Pathol Mech Dis. 2023;18(1):411-438. doi:10.1146/annurev-pathmechdis-031521-030435
104. Ahmadi AR, Song G, Gao T, et al. Discovery and characterization of cross-reactive intrahepatic antibodies in severe alcoholic hepatitis. eLife. 2023;12:RP86678. doi:10.7554/eLife.86678.2
105. Ariño S, Aguilar-Bravo B, Coll M, et al. Ductular reaction-associated neutrophils promote biliary epithelium proliferation in chronic liver disease. J Hepatol. 2023;79(4):1025-1036. doi:10.1016/j.jhep.2023.05.045
106. Chao X, Wang S, Ma X, et al. Persistent mTORC1 activation due to loss of liver tuberous sclerosis complex 1 promotes liver injury in alcoholic hepatitis. Hepatology. 2023;78(2):503-517. doi:10.1097/HEP.0000000000000373
107. Mackowiak B, Gao B. Activation of cholangiocyte mTORC1 drives alcohol-induced ductular reaction. Hepatology. 2023;78(2):378-381. doi:10.1097/HEP.0000000000000416
108. Elßner C, Goeppert B, Longerich T, et al. Nuclear Translocation of RELB Is Increased in Diseased Human Liver and Promotes Ductular Reaction and Biliary Fibrosis in Mice. Gastroenterology. 2019;156(4):1190-1205.e14. doi:10.1053/j.gastro.2018.11.018
109. Zhang Z, Zhong X, Shen H, et al. Biliary NIK promotes ductular reaction and liver injury and fibrosis in mice. Nat Commun. 2022;13(1):5111. doi:10.1038/s41467-022-32575-8
110. Buch S, Stickel F, Trépo E, et al. A genome-wide association study confirms PNPLA3 and identifies TM6SF2 and MBOAT7 as risk loci for alcohol-related cirrhosis. Nat Genet. 2015;47(12):1443-1448. doi:10.1038/ng.3417

111. Stickel F, Buch S, Nischalke HD, et al. Genetic variants in PNPLA3 and TM6SF2 predispose to the development of hepatocellular carcinoma in individuals with alcohol-related cirrhosis. Am J Gastroenterol. 2018;113(10):1475-1483. doi:10.1038/s41395-018-0041-8
112. Innes H, Buch S, Hutchinson S, et al. Genome-Wide Association Study for Alcohol-Related Cirrhosis Identifies Risk Loci in MARC1 and HNRNPUL1. Gastroenterology. 2020;159(4):1276-1289.e7. doi:10.1053/j.gastro.2020.06.014
113. Buch S, Innes H, Lutz PL, et al. Genetic variation in TERT modifies the risk of hepatocellular carcinoma in alcohol-related cirrhosis: results from a genome-wide case-control study. Gut. 2023;72(2):381-391. doi:10.1136/gutjnl-2022-327196
114. Mancina RM, Dongiovanni P, Petta S, et al. The MBOAT7-TMC4 Variant rs641738 Increases Risk of Nonalcoholic Fatty Liver Disease in Individuals of European Descent. Gastroenterology. 2016;150(5):1219-1230.e6. doi:10.1053/j.gastro.2016.01.032
115. Speliotes EK, Yerges-Armstrong LM, Wu J, et al. Genome-Wide Association Analysis Identifies Variants Associated with Nonalcoholic Fatty Liver Disease That Have Distinct Effects on Metabolic Traits. McCarthy MI, ed. PLoS Genet. 2011;7(3):e1001324. doi:10.1371/journal.pgen.1001324
116. Trépo E, Caruso S, Yang J, et al. Common genetic variation in alcohol-related hepatocellular carcinoma: a case-control genome-wide association study. Lancet Oncol. 2022;23(1):161-171. doi:10.1016/S1470-2045(21)00603-3
117. Bataller R, Arab JP, Shah VH. Alcohol-Associated Hepatitis. Hardin CC, ed. N Engl J Med. 2022;387(26):2436-2448. doi:10.1056/NEJMra2207599
118. Ambade A, Lowe P, Kodys K, et al. Pharmacological Inhibition of CCR2/5 Signaling Prevents and Reverses Alcohol-Induced Liver Damage, Steatosis, and Inflammation in Mice. Hepatology. 2019;69(3):1105-1121. doi:10.1002/hep.30249
119. Forbes SJ, Gupta S, Dhawan A. Cell therapy for liver disease: From liver transplantation to cell factory. J Hepatol. 2015;62(1):S157-S169. doi:10.1016/j.jhep.2015.02.040
120. Asrani SK, Devarbhavi H, Eaton J, Kamath PS. Burden of liver diseases in the world. J Hepatol. 2019;70(1):151-171. doi:10.1016/j.jhep.2018.09.014
121. Sampaziotis F, Muraro D, Tysoe OC, et al. Cholangiocyte organoids can repair bile ducts after transplantation in the human liver. Science. 2021;371(6531):839-846. doi:10.1126/science.aaz6964
122. Takebe T, Sekine K, Enomura M, et al. Vascularized and functional human liver from an iPSC-derived organ bud transplant. Nature. 2013;499(7459):481-484. doi:10.1038/nature12271
123. Huch M, Koo BK. Modeling mouse and human development using organoid cultures. Development. 2015;142(18):3113-3125. doi:10.1242/dev.118570
124. Zhao Z, Chen X, Dowbaj AM, et al. Organoids. Nat Rev Methods Primer. 2022;2(1):94. doi:10.1038/s43586-022-00174-y
125. Broutier L, Andersson-Rolf A, Hindley CJ, et al. Culture and establishment of self-renewing human and mouse adult liver and pancreas 3D organoids and their genetic manipulation. Nat Protoc. 2016;11(9):1724-1743. doi:10.1038/nprot.2016.097
126. Sampaziotis F, Cardoso De Brito M, Madrigal P, et al. Cholangiocytes derived from human induced pluripotent stem cells for disease modeling and drug validation. Nat Biotechnol. 2015;33(8):845-852. doi:10.1038/nbt.3275

127. Ogawa M, Ogawa S, Bear CE, et al. Directed differentiation of cholangiocytes from human pluripotent stem cells. Nat Biotechnol. 2015;33(8):853-861. doi:10.1038/nbt.3294
128. Roos FJM, Verstegen MMA, Muñoz Albarinos L, et al. Human Bile Contains Cholangiocyte Organoid-Initiating Cells Which Expand as Functional Cholangiocytes in Non-canonical Wnt Stimulating Conditions. Front Cell Dev Biol. 2021;8:630492. doi:10.3389/fcell.2020.630492
129. Gjorevski N, Sachs N, Manfrin A, et al. Designer matrices for intestinal stem cell and organoid culture. Nature. 2016;539(7630):560-564. doi:10.1038/nature20168
130. Broguiere N, Isenmann L, Hirt C, et al. Growth of Epithelial Organoids in a Defined Hydrogel. Adv Mater. 2018;30(43):1801621. doi:10.1002/adma.201801621
131. Sorrentino G, Rezakhani S, Yildiz E, et al. Mechano-modulatory synthetic niches for liver organoid derivation. Nat Commun. 2020;11(1):3416. doi:10.1038/s41467-020-17161-0
132. Hughes CS, Postovit LM, Lajoie GA. Matrigel: A complex protein mixture required for optimal growth of cell culture. PROTEOMICS. 2010;10(9):1886-1890. doi:10.1002/pmic.200900758
133. Fiorotto R, Mariotti V, Taleb SA, et al. Cell-matrix interactions control biliary organoid polarity, architecture, and differentiation. Hepatol Commun. 2023;7(4). doi:10.1097/HC9.0000000000000094
134. Francis H, Glaser S, Ueno Y, et al. cAMP stimulates the secretory and proliferative capacity of the rat intrahepatic biliary epithelium through changes in the PKA/Src/MEK/ERK1/2 pathway. J Hepatol. 2004;41(4):528-537. doi:10.1016/j.jhep.2004.06.009
135. Budi NYP, Lai WY, Huang YH, Ho HN. 3D organoid cultivation improves the maturation and functional differentiation of cholangiocytes from human pluripotent stem cells. Front Cell Dev Biol. 2024;12:1361084. doi:10.3389/fcell.2024.1361084
136. Dutta A, Chowdhury N, Chandra S, Guha P, Saha V, GuhaSarkar D. Gallbladder cholangiocyte organoids. Biol Cell. 2025;117(2):e2400132. doi:10.1111/boc.202400132
137. Nusse R, Clevers H. Wnt/β-Catenin Signaling, Disease, and Emerging Therapeutic Modalities. Cell. 2017;169(6):985-999. doi:10.1016/j.cell.2017.05.016
138. Addante A, Roncero C, Lazcanoiturburu N, et al. A Signaling Crosstalk between BMP9 and HGF/c-Met Regulates Mouse Adult Liver Progenitor Cell Survival. Cells. 2020;9(3):752. doi:10.3390/cells9030752
139. Meng Y, Ren Z, Xu F, et al. Nicotinamide Promotes Cell Survival and Differentiation as Kinase Inhibitor in Human Pluripotent Stem Cells. Stem Cell Rep. 2018;11(6):1347-1356. doi:10.1016/j.stemcr.2018.10.023
140. Gurung S, Werkmeister JA, Gargett CE. Inhibition of Transforming Growth Factor-β Receptor signaling promotes culture expansion of undifferentiated human Endometrial Mesenchymal Stem/stromal Cells. Sci Rep. 2015;5(1):15042. doi:10.1038/srep15042
141. Tanimizu N, Ichinohe N, Sasaki Y, et al. Generation of functional liver organoids on combining hepatocytes and cholangiocytes with hepatobiliary connections ex vivo. Nat Commun. 2021;12(1):3390. doi:10.1038/s41467-021-23575-1
142. Lu W, Rettenmeier E, Paszek M, et al. Crypt Organoid Culture as an In Vitro Model in Drug Metabolism and Cytotoxicity Studies. Drug Metab Dispos. 2017;45(7):748-754. doi:10.1124/dmd.117.075945

143. Wang H, Luo X, Yao L, Lehman DM, Wang P. Improvement of Cell Survival During Human Pluripotent Stem Cell Definitive Endoderm Differentiation. Stem Cells Dev. 2015;24(21):2536-2546. doi:10.1089/scd.2015.0018
144. Rauth S, Karmakar S, Batra SK, Ponnusamy MP. Recent advances in organoid development and applications in disease modeling. Biochim Biophys Acta BBA - Rev Cancer. 2021;1875(2):188527. doi:10.1016/j.bbcan.2021.188527
145. Verstegen MMA, Roos FJM, Burka K, et al. Human extrahepatic and intrahepatic cholangiocyte organoids show region-specific differentiation potential and model cystic fibrosis-related bile duct disease. Sci Rep. 2020;10(1):21900. doi:10.1038/s41598-020-79082-8
146. Minagawa N, Kruglov EA, Dranoff JA, Robert ME, Gores GJ, Nathanson MH. The Anti-apoptotic Protein Mcl-1 Inhibits Mitochondrial Ca2+ Signals. J Biol Chem. 2005;280(39):33637-33644. doi:10.1074/jbc.M503210200
147. Gao B, Bataller R. Alcoholic Liver Disease: Pathogenesis and New Therapeutic Targets. Gastroenterology. 2011;141(5):1572-1585. doi:10.1053/j.gastro.2011.09.002
148. Aloia L, McKie MA, Vernaz G, et al. Epigenetic remodelling licences adult cholangiocytes for organoid formation and liver regeneration. Nat Cell Biol. 2019;21(11):1321-1333. doi:10.1038/s41556-019-0402-6
149. Hendriks D, Artegiani B, Margaritis T, Zoutendijk I, Chuva De Sousa Lopes S, Clevers H. Mapping of mitogen and metabolic sensitivity in organoids defines requirements for human hepatocyte growth. Nat Commun. 2024;15(1):4034. doi:10.1038/s41467-024-48550-4
150. Edgar RD, Perrone F, Foster AR, et al. Culture-Associated DNA Methylation Changes Impact on Cellular Function of Human Intestinal Organoids. Cell Mol Gastroenterol Hepatol. 2022;14(6):1295-1310. doi:10.1016/j.jcmgh.2022.08.008
151. Soroka CJ, Assis DN, Alrabadi LS, et al. Bile-Derived Organoids From Patients With Primary Sclerosing Cholangitis Recapitulate Their Inflammatory Immune Profile. Hepatology. 2019;70(3):871-882. doi:10.1002/hep.30470
152. Wu R, Pan S, Chen Y, et al. Fate and functional roles of Prominin 1+ cells in liver injury and cancer. Sci Rep. 2020;10(1):19412. doi:10.1038/s41598-020-76458-8
153. Scopetti D, Piobbico D, Brunacci C, et al. INSL4 as prognostic marker for proliferation and invasiveness in Non-Small-Cell Lung Cancer. J Cancer. 2021;12(13):3781-3795. doi:10.7150/jca.51332
154. Fu X, Chang J, Jiao D, Zhu M, Ma Y. SLIT3 knockdown inhibited TGF-β-induced hepatic stellate cells activation by down-regulating YAP signal. Mol Cell Toxicol. Published online February 9, 2023. doi:10.1007/s13273-023-00336-3
155. Kong H, Song Q, Hu W, et al. MicroRNA-29a-3p prevents Schistosoma japonicum-induced liver fibrosis by targeting Roundabout homolog 1 in hepatic stellate cells. Parasit Vectors. 2023;16(1):184. doi:10.1186/s13071-023-05791-4
156. Basha S, Jin-Smith B, Sun C, Pi L. The SLIT/ROBO Pathway in Liver Fibrosis and Cancer. Biomolecules. 2023;13(5):785. doi:10.3390/biom13050785
157. Kashiwakura J ichi, Suzuki N, Nagafuchi H, et al. Txk, a Nonreceptor Tyrosine Kinase of the Tec Family, Is Expressed in T Helper Type 1 Cells and Regulates Interferon γ Production in Human T Lymphocytes. J Exp Med. 1999;190(8):1147-1154. doi:10.1084/jem.190.8.1147

158. Olivares-Villagómez D, Algood HMS, Singh K, et al. Intestinal Epithelial Cells Modulate CD4 T Cell Responses via the Thymus Leukemia Antigen. J Immunol. 2011;187(8):4051-4060. doi:10.4049/jimmunol.1101052
159. Xu QL, Wu J. Effects of Txk-mediated activation of NF-κB signaling pathway on neurological deficit and oxidative stress after ischemia-reperfusion in rats. Mol Med Rep. 2021;24(1):524. doi:10.3892/mmr.2021.12163
160. Dai B, Kim O, Xie Y, et al. Tyrosine Kinase Etk/BMX Is Up-regulated in Human Prostate Cancer and Its Overexpression Induces Prostate Intraepithelial Neoplasia in Mouse. Cancer Res. 2006;66(16):8058-8064. doi:10.1158/0008-5472.CAN-06-1364
161. Li Y, Cui N, Zheng PS, Yang WT. BMX/Etk promotes cell proliferation and tumorigenicity of cervical cancer cells through PI3K/AKT/mTOR and STAT3 pathways. Oncotarget. 2017;8(30):49238-49252. doi:10.18632/oncotarget.17493
162. Qi Y, Li Y, Zhang Y, et al. IFI6 Inhibits Apoptosis via Mitochondrial-Dependent Pathway in Dengue Virus 2 Infected Vascular Endothelial Cells. Jin X, ed. PLOS ONE. 2015;10(8):e0132743. doi:10.1371/journal.pone.0132743
163. Sajid M, Ullah H, Yan K, et al. The Functional and Antiviral Activity of Interferon Alpha-Inducible IFI6 Against Hepatitis B Virus Replication and Gene Expression. Front Immunol. 2021;12:634937. doi:10.3389/fimmu.2021.634937
164. Sadakata T, Sekine Y, Oka M, Itakura M, Takahashi M, Furuichi T. Calcium-dependent activator protein for secretion 2 interacts with the class II ARF small GTPases and regulates dense-core vesicle trafficking. FEBS J. 2012;279(3):384-394. doi:10.1111/j.1742-4658.2011.08431.x
165. Menigatti M, Cattaneo E, Sabates-Bellver J, et al. The protein tyrosine phosphatase receptor type R gene is an early and frequent target of silencing in human colorectal tumorigenesis. Mol Cancer. 2009;8(1):124. doi:10.1186/1476-4598-8-124
166. Maes M, Crespo Yanguas S, Willebrords J, Cogliati B, Vinken M. Connexin and pannexin signaling in gastrointestinal and liver disease. Transl Res. 2015;166(4):332-343. doi:10.1016/j.trsl.2015.05.005
167. Harada K, Nakanuma Y. Biliary Innate Immunity in the Pathogenesis of Biliary Diseases. Inflamm Allergy - Drug Targets. 2010;9(2):83-90. doi:10.2174/187152810791292809
168. Kunzmann LK, Schoknecht T, Poch T, et al. Monocytes as Potential Mediators of Pathogen-Induced T-Helper 17 Differentiation in Patients With Primary Sclerosing Cholangitis (PSC). Hepatology. 2020;72(4):1310-1326. doi:10.1002/hep.31140
169. Poch T, Krause J, Casar C, et al. Single-cell atlas of hepatic T cells reveals expansion of liver-resident naive-like CD4+ T cells in primary sclerosing cholangitis. J Hepatol. 2021;75(2):414-423. doi:10.1016/j.jhep.2021.03.016
170. Oo YH, Banz V, Kavanagh D, et al. CXCR3-dependent recruitment and CCR6-mediated positioning of Th-17 cells in the inflamed liver. J Hepatol. 2012;57(5):1044-1051. doi:10.1016/j.jhep.2012.07.008
171. Harada K, Shimoda S, Sato Y, Isse K, Ikeda H, Nakanuma Y. Periductal interleukin-17 production in association with biliary innate immunity contributes to the pathogenesis of cholangiopathy in primary biliary cirrhosis. Clin Exp Immunol. 2009;157(2):261-270. doi:10.1111/j.1365-2249.2009.03947.x
172. Chen Y, Thai P, Zhao YH, Ho YS, DeSouza MM, Wu R. Stimulation of Airway Mucin Gene Expression by Interleukin (IL)-17 through IL-6 Paracrine/Autocrine Loop. J Biol Chem. 2003;278(19):17036-17043. doi:10.1074/jbc.M210429200

173. Borrell V, Cárdenas A, Ciceri G, et al. Slit/Robo Signaling Modulates the Proliferation of Central Nervous System Progenitors. Neuron. 2012;76(2):338-352. doi:10.1016/j.neuron.2012.08.003
174. Macias H, Moran A, Samara Y, et al. SLIT/ROBO1 Signaling Suppresses Mammary Branching Morphogenesis by Limiting Basal Cell Number. Dev Cell. 2011;20(6):827-840. doi:10.1016/j.devcel.2011.05.012
175. Dou C, Wang H, Zhou G, Zhu H, Wen H, Xu S. Slit3 regulates migration of endothelial progenitor cells by activation of the RhoA/Rho kinase pathway. Int J Clin Exp Pathol. 2018;11(7):3398-3404.
176. Ye BQ, Geng ZH, Ma L, Geng JG. Slit2 Regulates Attractive Eosinophil and Repulsive Neutrophil Chemotaxis through Differential srGAP1 Expression during Lung Inflammation. J Immunol. 2010;185(10):6294-6305. doi:10.4049/jimmunol.1001648
177. Diner BA, Lum KK, Javitt A, Cristea IM. Interactions of the Antiviral Factor Interferon Gamma-Inducible Protein 16 (IFI16) Mediate Immune Signaling and Herpes Simplex Virus-1 Immunosuppression. Mol Cell Proteomics. 2015;14(9):2341-2356. doi:10.1074/mcp.M114.047068
178. Van HT, Harkins PR, Patel A, et al. Methyl-lysine readers PHF20 and PHF20L1 define two distinct gene expression–regulating NSL complexes. J Biol Chem. 2022;298(3):101588. doi:10.1016/j.jbc.2022.101588
179. D'Urso A, Takahashi Y hei, Xiong B, et al. Set1/COMPASS and Mediator are repurposed to promote epigenetic transcriptional memory. eLife. 2016;5:e16691. doi:10.7554/eLife.16691
180. Lafuente EM, Van Puijenbroek AAFL, Krause M, et al. RIAM, an Ena/VASP and Profilin Ligand, Interacts with Rap1-GTP and Mediates Rap1-Induced Adhesion. Dev Cell. 2004;7(4):585-595. doi:10.1016/j.devcel.2004.07.021
181. Therrien M, Wong AM, Rubin GM. CNK, a RAF-Binding Multidomain Protein Required for RAS Signaling. Cell. 1998;95(3):343-353. doi:10.1016/S0092-8674(00)81766-3
182. Zhou J, Moroi K, Nishiyama M, et al. Characterization of RGS5 in regulation of G protein-coupled receptor signaling. Life Sci. 2001;68(13):1457-1469. doi:10.1016/S0024-3205(01)00939-0
183. Jeffery HC, Hunter S, Humphreys EH, et al. Bidirectional Cross-Talk between Biliary Epithelium and Th17 Cells Promotes Local Th17 Expansion and Bile Duct Proliferation in Biliary Liver Diseases. J Immunol. 2019;203(5):1151-1159. doi:10.4049/jimmunol.1800455
184. Krause P, Bruckner M, Uermösi C, Singer E, Groettrup M, Legler DF. Prostaglandin E2 enhances T-cell proliferation by inducing the costimulatory molecules OX40L, CD70, and 4-1BBL on dendritic cells. Blood. 2009;113(11):2451-2460. doi:10.1182/blood-2008-05-157123
185. Rodriguez G, Ross JA, Nagy ZS, Kirken RA. Forskolin-inducible cAMP Pathway Negatively Regulates T-cell Proliferation by Uncoupling the Interleukin-2 Receptor Complex. J Biol Chem. 2013;288(10):7137-7146. doi:10.1074/jbc.M112.408765
186. Tojo M, Hamashima Y, Hanyu A, et al. The ALK-5 inhibitor A-83-01 inhibits Smad signaling and epithelial-to-mesenchymal transition by transforming growth factor-β. Cancer Sci. 2005;96(11):791-800. doi:10.1111/j.1349-7006.2005.00103.x

187. Zhou L, Lopes JE, Chong MMW, et al. TGF-β-induced Foxp3 inhibits TH17 cell differentiation by antagonizing RORγt function. Nature. 2008;453(7192):236-240. doi:10.1038/nature06878
188. Ferreira-Gonzalez S, Lu WY, Raven A, et al. Paracrine cellular senescence exacerbates biliary injury and impairs regeneration. Nat Commun. 2018;9(1):1020. doi:10.1038/s41467-018-03299-5
189. Jalan-Sakrikar N, Anwar A, Yaqoob U, et al. Telomere dysfunction promotes cholangiocyte senescence and biliary fibrosis in primary sclerosing cholangitis. JCI Insight. 2023;8(20):e170320. doi:10.1172/jci.insight.170320
190. Shenoy AT, Lyon De Ana C, Arafa EI, et al. Antigen presentation by lung epithelial cells directs CD4+ TRM cell function and regulates barrier immunity. Nat Commun. 2021;12(1):5834. doi:10.1038/s41467-021-26045-w
191. Heuberger CE, Janney A, Ilott N, et al. MHC class II antigen presentation by intestinal epithelial cells fine-tunes bacteria-reactive CD4 T-cell responses. Mucosal Immunol. 2024;17(3):416-430. doi:10.1016/j.mucimm.2023.05.001
192. Cruickshank SM. Colonic epithelial cell mediated suppression of CD4 T cell activation. Gut. 2004;53(5):678-684. doi:10.1136/gut.2003.029967
193. Zhao Y, Lee CK, Lin CH, et al. PD-L1:CD80 Cis-Heterodimer Triggers the Co-stimulatory Receptor CD28 While Repressing the Inhibitory PD-1 and CTLA-4 Pathways. Immunity. 2019;51(6):1059-1073.e9. doi:10.1016/j.immuni.2019.11.003
194. Schoenberger SP, Toes REM, Van Der Voort EIH, Offringa R, Melief CJM. T-cell help for cytotoxic T lymphocytes is mediated by CD40–CD40L interactions. Nature. 1998;393(6684):480-483. doi:10.1038/31002
195. Datta SK, Kalled SL. CD40-CD40 ligand interaction in autoimmune disease. Arthritis Rheum. 1997;40(10):1735-1745. doi:10.1002/art.1780401002
196. Vermersch P, Granziera C, Mao-Draayer Y, et al. Inhibition of CD40L with Frexalimab in Multiple Sclerosis. N Engl J Med. 2024;390(7):589-600. doi:10.1056/NEJMoa2309439
197. Farhood A, McGuire GM, Manning AM, Miyasaka M, Smith CW, Jaeschke H. Intercellular adhesion molecule 1 (ICAM-1) expression and its role in neutrophil-induced ischemia-reperfusion injury in rat liver. J Leukoc Biol. 1995;57(3):368-374.
198. Gujral JS, Liu J, Farhood A, Hinson JA, Jaeschke H. Functional importance of ICAM-1 in the mechanism of neutrophil-induced liver injury in bile duct-ligated mice. Am J Physiol-Gastrointest Liver Physiol. 2004;286(3):G499-G507. doi:10.1152/ajpgi.00318.2003
199. Monson KM, Dowlatshahi S, Crockett ET. CXC-chemokine regulation and neutrophil trafficking in hepatic ischemia-reperfusion injury in P-selectin/ICAM-1 deficient mice. J Inflamm. 2007;4(1):11. doi:10.1186/1476-9255-4-11
200. Rentsch M, Post S, Palma P, Lang G, Menger MD, Messmer K. Anti-ICAM-1 blockade reduces postsinusoidal WBC adherence following cold ischemia and reperfusion, but does not improve early graft function in rat liver transplantation. J Hepatol. 2000;32(5):821-828. doi:10.1016/S0168-8278(00)80252-4
201. Enlimomab Acute Stroke Trial Investigators. Use of anti-ICAM-1 therapy in ischemic stroke: Results of the Enlimomab Acute Stroke Trial. Neurology. 2001;57(8):1428-1434. doi:10.1212/WNL.57.8.1428

202. Nakamoto N, Sasaki N, Aoki R, et al. Gut pathobionts underlie intestinal barrier dysfunction and liver T helper 17 cell immune response in primary sclerosing cholangitis. Nat Microbiol. 2019;4(3):492-503. doi:10.1038/s41564-018-0333-1
203. Liaskou E, Jeffery LE, Trivedi PJ, et al. Loss of CD28 Expression by Liver-Infiltrating T Cells Contributes to Pathogenesis of Primary Sclerosing Cholangitis. Gastroenterology. 2014;147(1):221-232.e7. doi:10.1053/j.gastro.2014.04.003
204. Curnock AP, Bossi G, Kumaran J, et al. Cell-targeted PD-1 agonists that mimic PD-L1 are potent T cell inhibitors. JCI Insight. 2021;6(20):e152468. doi:10.1172/jci.insight.152468
205. Suzuki K, Tajima M, Tokumaru Y, et al. Anti–PD-1 antibodies recognizing the membrane-proximal region are PD-1 agonists that can down-regulate inflammatory diseases. Sci Immunol. 2023;8(79):eadd4947. doi:10.1126/sciimmunol.add4947
206. Woods DM, Sodré AL, Villagra A, Sarnaik A, Sotomayor EM, Weber J. HDAC Inhibition Upregulates PD-1 Ligands in Melanoma and Augments Immunotherapy with PD-1 Blockade. Cancer Immunol Res. 2015;3(12):1375-1385. doi:10.1158/2326-6066.CIR-15-0077-T
207. Gameiro SR, Malamas AS, Tsang KY, Ferrone S, Hodge JW. Inhibitors of histone deacetylase 1 reverse the immune evasion phenotype to enhance T-cell mediated lysis of prostate and breast carcinoma cells. Oncotarget. 2016;7(7):7390-7402. doi:10.18632/oncotarget.7180
208. Huang KCY, Chiang SF, Chen WTL, et al. Decitabine Augments Chemotherapy-Induced PD-L1 Upregulation for PD-L1 Blockade in Colorectal Cancer. Cancers. 2020;12(2):462. doi:10.3390/cancers12020462
209. Postow MA, Sidlow R, Hellmann MD. Immune-Related Adverse Events Associated with Immune Checkpoint Blockade. Longo DL, ed. N Engl J Med. 2018;378(2):158-168. doi:10.1056/NEJMra1703481
210. Haanen J, Obeid M, Spain L, et al. Management of toxicities from immunotherapy: ESMO Clinical Practice Guideline for diagnosis, treatment and follow-up. Ann Oncol. 2022;33(12):1217-1238. doi:10.1016/j.annonc.2022.10.001
211. Chung BK, Karlsen TH, Folseraas T. Cholangiocytes in the pathogenesis of primary sclerosing cholangitis and development of cholangiocarcinoma. Biochim Biophys Acta BBA - Mol Basis Dis. 2018;1864(4):1390-1400. doi:10.1016/j.bbadis.2017.08.020
212. Grimsrud MM, Folseraas T. Pathogenesis, diagnosis and treatment of premalignant and malignant stages of cholangiocarcinoma in primary sclerosing cholangitis. Melum E, ed. Liver Int. 2019;39(12):2230-2237. doi:10.1111/liv.14180
213. Villard C, Jorns C, Bergquist A. Treatment of cholangiocarcinoma in patients with primary sclerosing cholangitis: a comprehensive review. eGastroenterology. 2024;2(1):e100045. doi:10.1136/egastro-2023-100045
214. Kim RD, Chung V, Alese OB, et al. A Phase 2 Multi-institutional Study of Nivolumab for Patients With Advanced Refractory Biliary Tract Cancer. JAMA Oncol. 2020;6(6):888. doi:10.1001/jamaoncol.2020.0930
215. Manthopoulou E, Ramai D, Dhar J, et al. Cholangiocarcinoma in the Era of Immunotherapy. Vaccines. 2023;11(6):1062. doi:10.3390/vaccines11061062
216. Rodrigues MA, Gomes DA, Nathanson MH. Calcium Signaling in Cholangiocytes: Methods, Mechanisms, and Effects. Int J Mol Sci. 2018;19(12):3913. doi:10.3390/ijms19123913

217. Verboven E, Moya IM, Sansores-Garcia L, et al. Regeneration Defects in Yap and Taz Mutant Mouse Livers Are Caused by Bile Duct Disruption and Cholestasis. Gastroenterology. 2021;160(3):847-862. doi:10.1053/j.gastro.2020.10.035
218. Liu J, Du Y, Xiao X, Tan D, He Y, Qin L. Construction of in vitro liver-on-a-chip models and application progress. Biomed Eng OnLine. 2024;23(1):33. doi:10.1186/s12938-024-01226-y
219. European Association for the Study of the Liver. EASL Clinical Practice Guidelines: Management of cholestatic liver diseases. J Hepatol. 2009;51(2):237-267. doi:10.1016/j.jhep.2009.04.009